Chemical Vapor Deposition

of

Interstitial Carbides

Hideaki Itoh

瞐 ・ 本 驀

Chemical   Vapor   Deposition

of.

Interstitial   Carbides

Hideaki   Itoh

Department of Applied Chemistry

Faculty of Engineering

Nagoya University

1972

A   Dissertation

for

The   Degree   of   Doctor   of   Engineering

at

Department   of   Applied   Chemistry

Faculty   of   Engineering

Nagoya   University

February,   1972

Preface

The present dissertation involves a series of studies on the chemical vapor deposition of interstitial carbides, which have been investigated at Faculty of Engineering, Nagoya University under the direction of Professor Takehiko Takahashi during 1967-1972.

It is aimed in the present thesis to prepare one dimensional deposit of interstitial carbides by chemical vapor deposition. Informations on syntheses of various morphologies of the carbide crystals are presented together with some properties of the products.

The author wishes to express his most grateful acknowledgment to Professor Takehiko Takahashi for his kind guidance and encouragement for this work, and sincere thanks to Dr. Kozoh Sugiyama (Professor of Gifu University) for his instructive suggestions and discussions.

The author is also greatly indebted to Dr. Osamu Yamamoto, Dr. Hiroyasu Iwahara, Mr. Yutaka Suzuki and Dr. Katsumi Kuwabara for their interests and valuable advices for this study, and extends his gratitude to all other members in his laboratory. He is sincerely grateful to his parents and many friends for their continual encouragement and understanding.

Finally, the author hopes that this work will contribute to the development of today's material science.

<div align="right">Hideaki Itoh</div>

Department of Applied Chemistry
Faculty of Engineering
Nagoya University
February, 1972

Contents

CHAPTER   1

Introduction to Chemical Vapor Deposition

of Interstitial Carbides

1.1   Structures and Properties of the Interstitial Compounds

Crystal structures   It is well known that the transition metals (M) in lVa, Va and Vla groups combine with nonmetallic elements (X) such as carbon, nitrogen, boron, etc. to form so called "interstitial compounds". Typical examples of these compounds are listed in Table 1.1 together with the crystal systems and their properties. It is noticeable that they have MX, MX_2 and M_2X type structutes with the best thermodynamical stabilities. In this case, the light nonmetallic atoms are considered to be located at the interstitial sites of the close packed sub-lattice of metals. Many of them are crystallized in face centered cubic system of the NaCl type, but sometimes in hexagonal closest packed system, as seen in TiB_2, WC, $\alpha\text{-}Mo_2C$, etc. At the stoichiometric composition, it is expected that they exhibit the char-

acteristic properties based on metallic M-M bond and covalent M-X bond. In fact, these materials show metallic luster, high electrical conductivity, high melting point and super-hardness (see Table 1.1).
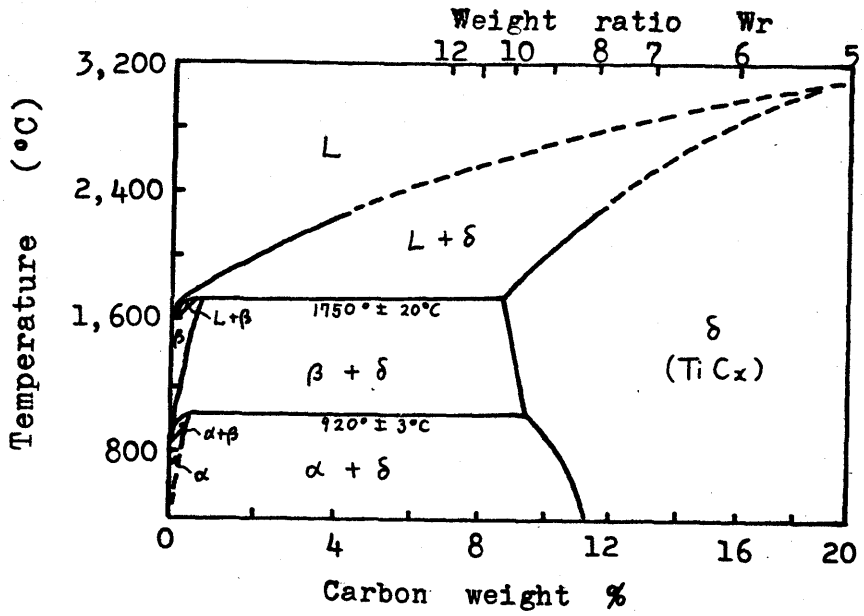
The covalent M-X bond in the NaCl type compound was explained by Rundle in the following way (2): From a viewpoint that the hybrid orbitals of nonmetallic atoms result in the formation of strong M-X bond, the resonance structure of "1/2 bonds" (by three 2p-electrons) or "2/3 bonds" (by two sp-hybrid orbitals and two 2p-electrons) should be considered in interstitial compounds, as given by Pauling's rule, since nonmetallic atom such as C or N is regarded as having an electron-defifient structure in octahedral bonds. In the case of TiN or VC, one electron may remain to contribute to M-M bond. Carbon atoms in hexagonal α-Mo_2C or W_2C, will occupy the interstitial sites of the octahedral configurations.

Another structural characteristic of the interstitial compounds consists in the wide range of the solid solubilities of nonmetallic atoms. The phase diagrams of the Ti-C and W-C systems are showm in Fig.1.1. A homogeneous stable phase with nonstoichiometric composition can be confirmed between $TiC_{0.45}$ and $TiC_{1.0}$ in the system Ti-C. If the carbon concentration is decreased, free electrons at the defects will increase in number and they will contribute to the metallic character of the bonding. But it should be noted that the titanium carbide differs in character from the solid solutions like metallic alloys, since the solubilities of carbon atoms are limited.
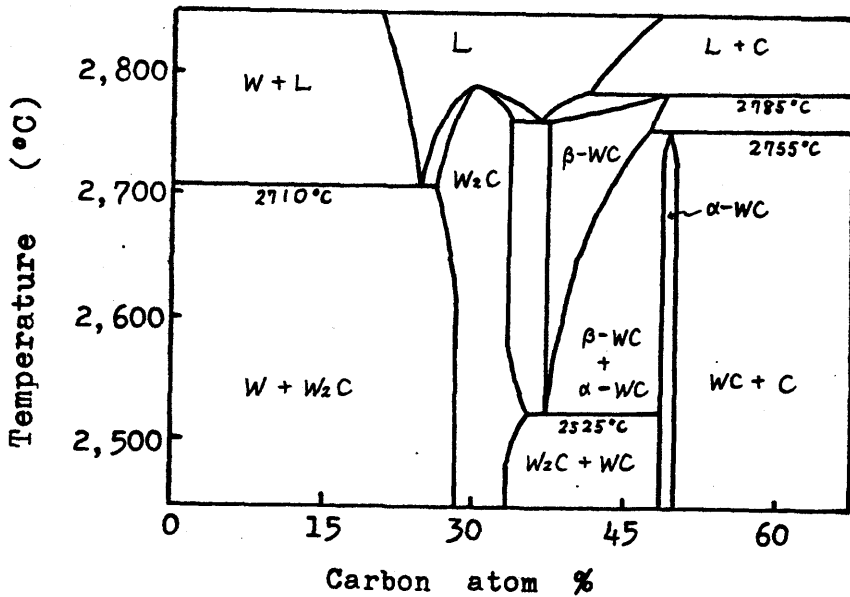
Chemical properties   In general, interstitial compounds have high melting points, as shown in Table 1.1,

Table 1.1 Properties of interstitial compounds.(1)

Compound	Crystal system	M.p. (°C)	Micro-hardness (kg/mm²)	Resistivity (μ ohm·cm)
TiC	fcc	3,250	3,200	59
TiN	fcc	2,950	1,700	21
TiB₂	hcp	2,900	3,480	9
ZrC	fcc	3,535	2,560	42
ZrN	fcc	2,980	1,520	21
ZrB₂	hcp	3,040	2,200	10
HfC	fcc	3,535	2,700	37
NbC	fcc	2,490	2,400	35
NbN	fcc	2,300	1,400	78
TaC	fcc	3,880	2,400	35
α-Mo₂C	hcp	2,400	1,950	133
WC	hcp	2,600	2,080	22

(a)

Weight ratio Wr

12 10 8 7 6 5

3,200

Temperature (°C)

L

2,400

L + δ

1,600

L+β

1750° ± 20°C

β + δ

δ (Ti Cₓ)

α+β

920° ± 3°C

800

α

α + δ

0   4   8   12   16   20

Carbon weight %

(a) System Ti-C

(b)

2,800

W + L

L

L + C

2785°C

β-WC

2755°C

2,700

2710°C

W₂C

α-WC

Temperature (°C)

2,600

β-WC + α-WC

WC + C

W + W₂ C

2,500

2525°C

W₂C + WC

0   15   30   45   60

Carbon atom %

(b) System W-C

Fig.1.1   Phase diagrams of the Ti-C (a) and W-C (b)
systems, (3 & 4)

- 4 -

which are comparable with other refractory oxides (m.p., ThO_2: 3,050°C, MgO: 2,800°C, β-Al_2O_3: 2,050°C) or metals (m.p., W: 3,370°C, Re: 3,167°C) (5). Especially, the hafnium and tantalum carbides show the highest class of melting point in all the materials which is above 3,500° C. But, the inert or reducing atmosphere is required when they are used at the elevated temperature, for they are not protective enough from the oxidation of the surface layer. Webb et al. (6) studied the rate of oxidation of WC in comparison to that of tungsten. They suggested that the oxidation of WC obeyed the linear rate law in the temperature range of 700° to 1,000°C and its higher rate was facilitated by the rupture of the oxide film due to the formation of CO or CO_2. The effect of the temperature on the oxidation of titanium carbide has been investigated by Nikolaiski (7) and Stewart et al. (8). The data obtained for the oxidation of powdered titanium carbide, were found to correlate well with the parabolic rate law in the temperature range of 600° to 850°C.

Sugiyama and Takahashi examined the corrosion resistivity of titanium carbide obtained by C.V.D. (9). They did not observed any corrosion by hydrogen chloride and sulfide up to 1,000°C. But the remarkable decrease in weight was found for chlorine gas in the temperature range of 460° to 500°C, which would be due to the direct chlorination of titanium carbide and substrate alloys. The stability of the carbide surface against sulfur oxide was decreased above 700°C by the formation of rutile type oxide. Above 1,000°C, therefore, the practical use in the corrosive gases should be avoided except the case when the etching effect of the surface layer is applied

positively as can be used in I.C. techniques of the semi-conductors (10-12).

The greater part of the interstitial compounds show relatively strong erosion resistivities against hydro-chloric, nitric and sulfuric acids at ambient temperatures. But, some of them (Mo_2C, TiC, etc.) can be dissolved in hot concentrated nitric acid, aqua regia or fluoric acid.

Mechanical properties   One of the superior merits of the interstitial compound is its super-hardness. Above all, the carbides of metals in lVa group have the micro-hardness between 2,800 and 3,200 kg/mm^2 (Mohs hardness: 9-10), which is slightly smaller value than that of sili-con carbide (3,340 kg/mm^2) or boron carbide (5,000 kg/mm^2). The peculiarity of the hardness may be attributed to the diamond-like covalent bond between carbon and lVa metals as has been explained previously. But the strong toughness for bending can not be expected because the hardness and brittleness are often consistent properties of the materials. Many fibrous compounds of borides and boron carbide are found empirically in the author's la-boratory to have higher bending strength than other car-bides or nitrides. Higgins et al. (13) measured the bending strength of boron carbide filaments which were prepared by C.V.D. on tungsten substrate, and obtained the maximum value of about 18×10^5 psi (1,260 kg/mm^2). The curvature tests of vapor-deposited silicon carbide are interesting, which was attempted by Beau and Gleim (14) on silicon slice.

The plastic behaviors (shear stress, creep stress, etc.) of single crystal carbides of titanium (15) and zirconium (16) were studied in relation to their disloca-

tion structures, slip systems and nonstoichiometries.
The slip system of {111}⟨110⟩ type was identified in the
case of single crystal titanium carbide by several in-
vestigators (17 & 18).   The tensile strength of whiskers
of interstitial compounds has rarely been reported be-
cause of their synthetic difficulties, notwithstanding
the tensile strength measurements (19) having been de-
veloped for the as-grown metallic or ceramic whiskers
(Fe, Cu, W, SiC, Al_2O_3, MgO, etc.). Gatti and Mehan
found the linear relations between the ultimate stress
and the cross sectional area of boron carbide whisker
(20) and aluminum oxide whisker (21), as shown in Fig.
1.2.   Recently, comparatively high strength (200-300
kg/mm^2 at 10 μm) of fibrous interstitial borides which
were obtained by discharge method were measured by Taka-
hashi et al. (22 & 23).

Electrical properties   It is apparent from Table 1.1
that the resistivities of the interstitial compounds are
the order of 10^{-6} ohm·cm at room temperature. They be-
long to the electronic conductors due to metallic M-M
bond. Electrical properties of the interstitial com-
pounds in 1Va group have been investigated mainly by
chemists in U.S.S.R. Айвазов et al. (24) studied the
effects of nonstoichiometry of TiN_x on the electrical
conductivity, temperature coefficient of resistance (T.
C.R.) and thermo-electromotive force (T.E.M.F.), and
found a tendency to increase the resistivities with de-
creasing the concentration of nitrogen. Some character-
istics of electrical behaviors were studied by Нешпор on
the pyrolytic carbides or nitrides of 1Va metals (25).
They obtained the contradictory results to those by
Айвазов, and suggested that the nitrogen vacancies which
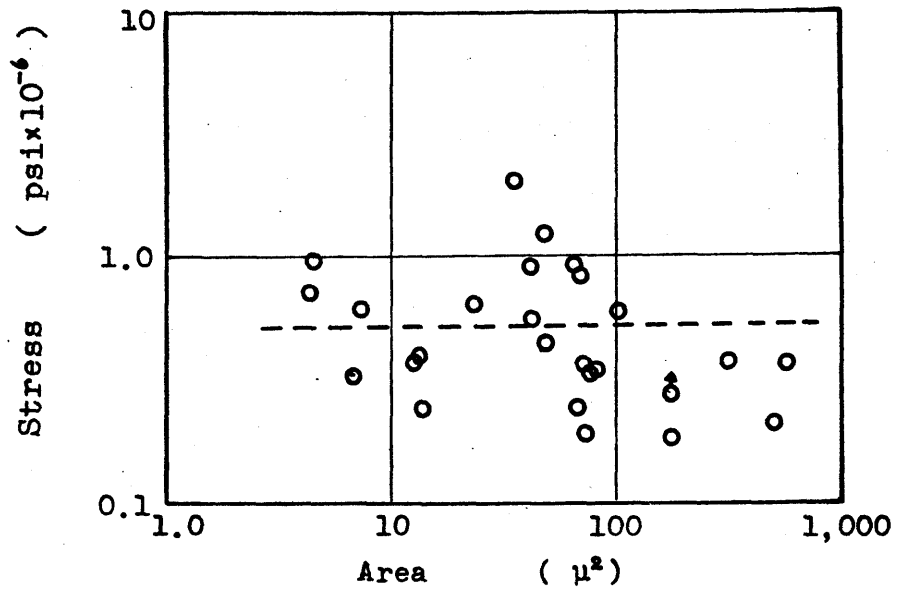
(a) Ultimate stress vs. cross-sectional area of B_4C.
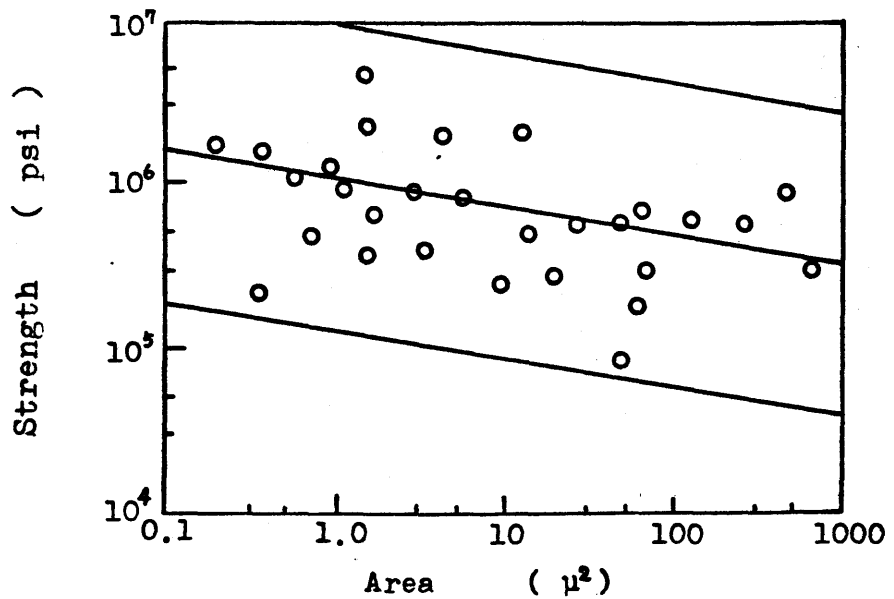
(b) Strength vs. cross-sectional area of Al_2O_3.

Fig.1.2 Tensile strength of B_4C (a) and α-Al_2O_3 (b) whiskers. (20 & 21).

reduced the screen effects of M-M bond made the concentration of free electron increase. The comparison of the data concerning T.E.M.F. (1.8-8.2 μV/°C) and T.C.R. with those of Айвазов was made also by them. Требенкина and Деньобецкая (26) measured T.C.R. of interstitial carbides, silicides or their solid solutions, and concluded that the smaller value of T.C.R. which was obtained by ZrC or TaC was due to the stability of the covalent bond.

Nitrides and carbides of Va group metals show the interesting electrical properties (27). Particularly, niobium compounds are expected as the super-conductors. The critical temperature Tc (°C) of the materials which are known to show good super-conduction are as follows (28); NbN: 16, NbC: 10.1-10.5, TaC: 9.3-9.6, MoN: 12.0, NbSn: 18.05, Nb$_3$Al: 17.5, etc. The super-conductivities of NbC, NbN and NbC-NbN were studied in detail by Darnell (29) and Pessall (30).


1.2　Historical Survey on the Syntheses of Interstitial Carbides by C.V.D.

<u>Starting materials</u>　It is an important problem in the preparation of interstitial carbides what starting materials should be supplied to the preparation zone. A general way is to provide separately the sources for carbon and metals in the gaseous or solid state, except when the pyrolytic decomposition of the organo-metallic compound is employed for the formation of carbide. As the supplying sources for carbon, various kinds of hydrocarbons or solid carbons (graphite and amorphous carbon) are utilized. Takahashi and Sugiyama (31) plated tita-

nium carbide on iron by C.V.D. and found that the avail-
ability of the constituent hydrocarbons for the synthetic
reaction was arranged in the following order: i-C_5H_{12} >
C_2H_6 > C_3H_8 > C_3H_6 > C_2H_4 > CO > CH_4. This is obviously con-
nected with the facility for the production of carbon
radicals (pyrocarbon), which may serve to the catalytic
reaction at the substrate surface. On the other hand,
metal halides and sometimes hydrides are used as the
transport reagents for metallic species. Instead of de-
composable halides of VIa group like WCl_6 and $MoCl_5$,
foils or filaments of tungsten and molybdenum are often
supplied as the metallic sources.

IVa group (TiC, ZrC and HfC)   The chemical vapor de-
position of interstitial carbides was initiated in 1925
by van Arkel and de Boer (32). While they were studying
to prepare pure metals of IVa group by hydrogen reduc-
tion of corresponding halides, they found it possible to
obtain the deposits of carbides on the heated tungsten
wire by introducing hydrocarbon or carbon monoxide sim-
ultaneously with halides and hydrogen, for example;

$$ZrCl_4 + 3H + CO \longrightarrow ZrC + 4HCl + H_2O.$$
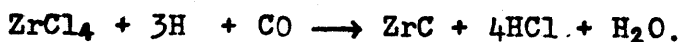
This was followed by the detailed study by Moers (1931),
who obtained the monocrystalline carbides of titanium,
zirconium and hafnium on the substrates, the temperatures
of which were 1,300° - 1,700°C, 1,700° - 2,400°C, and 2,400°
-2,800°C, respectively (33). The atmosphere employed
was composed of a mixture of the purified hydrogen satu-
rated with toluen vapor at -15°C and metal chloride.
Burgers and Besart (34) prepared titanium and zirconium
carbides in the chloride vapor on carbon filament (about
100 μm in diameter) which was used as the heater of re-
action tube. The uniform and bright coatings of zirco-

nium and titanium carbides on graphite could be obtained
by Blocher and Campbell (35), in the halide atmosphere
in the temperature and pressure ranges which were un-
favorable for the deposition of metals, but still favor-
able for the carbide formation in thermodynamical mean-
ings. The adherent platings of titanium and zirconium
carbides on iron were succeeded recently in the author's
laboratory (36 & 37).

Va group (NbC and TaC)　　Preparation of tantalum car-
bide was tried also by Moers (33) using a mixture of
$TaCl_5 + H_2 + C_7H_8$, but it was unsuccessful because of
the rapid formation of free metal at the temperature in-
vestigated (700°-1,000°C). Becker et al. (38) found it
possible in 1930 to prepare the carbide layer by carbu-
rization of a tantalum wire at 2,000° to 3,000°C in a
hydrocarbon-hydrogen mixture. The formation of two kinds
of carbides, TaC and Ta_2C was observed by Burgers and
Besart (34), when they heated the carbon filament in the
atmosphere of $TaCl_5$. In vapor-solid reactions as des-
cribed above, the temperatures above 2,000°C are required.
The limiting-pressure technique was applied by Blocher
et al. (35) to the uniform coating of niobium and tan-
talum carbides on graphite bodies (1958). The carbide
coatings of 50 to 500 μm in thickness were formed in the
reaction time of 15 min. to 2 hr.

Vla group (MoC and WC)　　Vapor platings of carbides
of Vla group metals had been performed before the begin-
ning of the studies on C.V.D. in lVa group metal carbides.
Pring and Fielding (39) obtained in 1909 the coating of
molybdenum or tungsten carbide in the vapor phase con-
taining metal chloride. The method employing chloride
vapors as the source of metals, however, have been rarely

used because metallic molybdenum or tungsten is easy to form. Molybdenum or tungsten filament was carburized by Westgren and Phragmen (40) in a CO atmosphere at 1,500 °C to find the presence of Mo_2C or W_2C and WC, respectively. Andrews et al. (41 & 42) investigated more carefully the carburization of tungsten filament in the temperature range of 2,000° to 2,300°C in the naphthalene vapor at the pressure of 2×10^{-3} torr. The main factor of the reaction process was determined to be the rate of diffusion of carbon through carbide. Becker heated tungsten wires of 2.4 to 12 mil in diameter using a mixture of hydrogen, and benzene vapor or methane as the carburizing agent (43) and obtained WC at the temperature up to 2,200°C, while α-W_2C and β-W_2C were formed in the higher temperature ranges of 2,200°-2,400°C and 2,400°-2,550°C, respectively. β-Mo_2C was identified by Kuo et al. in the carburization process of molybdenum in carbon monoxide gas at a relatively low temperature below 800 °C (44).

Lander and Germer (45) attempted in 1947 to obtain carbides by the thermal decomposition of molybdenum carbonyl, $Mo(CO)_6$ and tungsten carbonyl, $W(CO)_6$ at reduced pressures. The advantage of this process was to serve the purpose at lower deposition temperature than is required in the other methods as already described. Adherent β-Mo_2C (cubic) and β-W_2C (cubic) coatings were produced in the temperature range of 350° to 500°C. Cubic Mo_2C was obtained also on an iron specimen at temperatures as low as 170°C from a mixture of molybdenum carbonyl and hydrogen under the CO pressure of 0.05 torr. and the hydrogen pressure of 0.06 torr. It is interesting to be able to produce carbide by decomposition of

carbonyl, although this is limited to Vla group metal
carbides.

1.3 Theoretical Approach to Whisker Growth from the Vapor Phase.

<u>Dislocation mechanism</u>   In crystal growth of metals
or inorganic compounds from the vapor phase, one can
often encounter their one dimensional anisotropic growth
of "whiskers" —— so called by reason of their appear-
ance ——, which has become the subject of intense studies
in recent years. These whiskers are characterized re-
markably with the rapid growth under a relatively low
supersaturation, the filamentary and monocrystalline ap-
pearance, the ultra-high tensile strength, etc. The
growth mechanism of a whisker has been discussed in the
past 20 years by many crystallographers. In 1949, Frank
proposed a growth theory of a crystal which was based
on the screw dislocation (46 & 47), in order to explain
the crystal growth under low supersaturation which could
be often observed experimentally, but it was not coinci-
dent with the growth theory of a perfect crystal which
was proposed by Kossel and other investigators (48).
According to Frank's model, the step required for the
crystal growth is given by the screw dislocation around
a fixed point, so that the crystal can grow continuously
under low supersaturation without two dimensional nucle-
ation, where the activation free energy of nucleation,

$$\Delta F = \pi \rho_c \epsilon$$

is necessary (ρ_c: critical radius of curvature, and ϵ :
edge free energy of monolayer). Spiral growth due to
the dislocation could be verified in fact by the micro-

scopic observations of SiC or $C_{36}H_{74}$(for example, 49), Mg
(50), etc. This model was first applied also by Frank
to the growth mechanism of tin whiskers (51). The whisk-
er axis was considered to be parallel to the Burgers vec-
tor of the dislocation, namely a slip direction in the
crystal. After that, "Frank's mechanism" had been sup-
ported by many experimental or theoretical treatments
(52), until the V.L.S. mechanism was presented.

<u>V.L.S. mechanism</u>   In spite of its generaly applicabil-
ity of the theory by Frank, a few additional problems
remained why the side of the whisker did not grow at an
appreciable rate and how the impurity effects in whisker
growth were connected to the dislocation mechanism (53).
Therefore, it was considered by some workers that reser-
vations should have arisen regarding its universal appli-
cation. Greiner (54) found that the addition of small
traces of impurities was essential to promote the growth
of filamentary silicon crystals. Wagner and Ellis (55)
investigated further in detail the process of the dis-
proportionation reaction;

$$2SiI_2(g) = Si(s) + SiI_4(g),$$
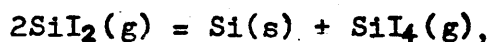
and proposed so called "Vapor-Liquid-Solid mechanism"
(V.L.S. mechanism) in 1964, and the characteristics of
silicon whisker growth by V.L.S. mechanism were summariz-
ed as follows:

   i) Silicon whiskers were free from dislocation.

  ii) Certain impurities were essential for whisker
     growth.

 iii) A "liquid-like" globule was observed occasion-
     ally at the tip of the whisker crystals during
     growth.

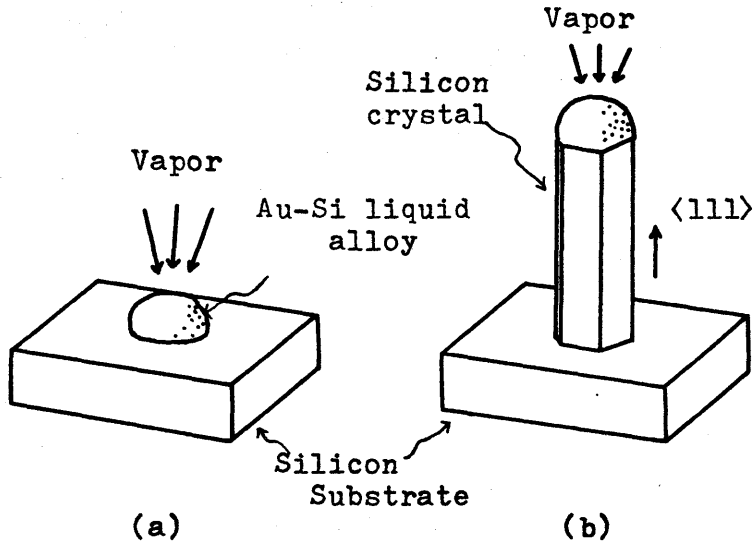The idealized drawing of V.L.S. mechanism is illustrated

Fig.1.3 Idealized drawing of V.L.S. mechanism
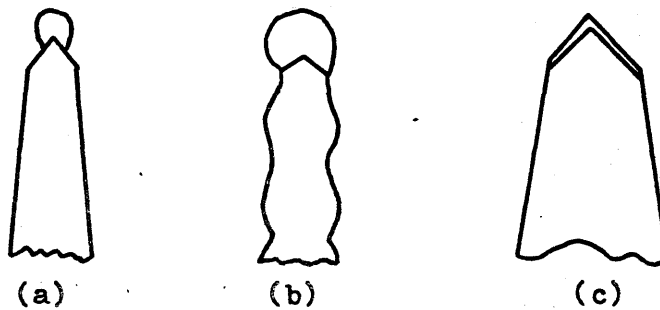for the whisker growth of Si. (55)

Fig.1.4 Schematic drawing suggesting the relation
between final whisker shape and shape of
molten alloy zone.(57)

(a) at slow flow rate

(b) at high flow rate

(c) at high temperatures and after consider-
able depletion of the available gold.

for the growth of a silicon crystal in Fig.1.3.   In the
first step of growth, the deposition may occur directly
on a solid substrate and then the liquid solution is
formed by incorporation of the impurities. The liquid
phase is supersaturated with silicon from the vapor (V-
L system) and the second step of the precipitation of
silicon single crystal at the liquid-solid interface
(L-S system) occurs. Wagner et al. showed that the im-
purities such as Au, Ni, Pd, Cu, Mg and Os produced ex-
tensive filamentary growth, while the following impu-
rities did not promote the growth: Zn, C, Mn, Sn, etc.
(56). The growth mechanism of comparatively thick needles
was considered by them to be based on the rapid extention
in length of a leader-like crystal, which was followed
by the slow thickening through the deposition on the
lateral face. The former may be concerned with the im-
purity effects and the latter with the side growth by
the movement of steps. The correlation between the whisk-
er morphology and the growth condition was studied by
Thorton et al. (57) and the final whisker shapes were
shown schematically in Fig.1.4. The detailed descrip-
tions about the controlled V.L.S. growth of silicon and
discussions on defects or kinkings were given in the lit-
erature by Wagner (58 & 59).

   The V.L.S. growth mechanism has been verified in
other whisker growth of the compounds such as $\alpha-Al_2O_3$
(60), GaAs, MgO (61), SiC, etc. In the recent study of
Berman and Ryan (62), single crystal needles of 2H-type
silicon carbide were grown by V.L.S. method in the pro-
cess of the hydrogen reduction of purified CH_3SiCl_3 .
They found that by making the mole fraction of CH_3SiCl_3
low, the liquid zone of silicon would be etched away by HCl

product and consequently no liquid globules could be observed apparently. Conversely, through the slight increase of the mole fraction of the reagent, the molten tip became saturated with silicon. Thus, various forms of needles could be obtained by adjustments of flow rate or temperature.

1.4　Applications to Chemical Industries

<u>Protective coatings</u>　As described in Section 1.2, a series of basic studies on syntheses of interstitial carbides by C.V.D. were originated above all by chemists in the 1930's. The studies were presumably stimulated by their academic interests in the chemical behaviors of heated lamp filaments in various atmospheres. The C.V.D. method of interstitial carbides had been noticed scarcely from the industrial point of view until World War Ⅱ. But after the war, the importance of coating techniques on materials has increased gradually as well as that of sintered interstitial carbides (TiC, WC, B_4C, etc.) which have made much progress in the practical applications to cermet materials and super-hard alloys (for example TiC-WC-Co system). In fact, they have been used commercially as cutting tools, braking materials, refractory and reinforced materials for vehicles or aircrafts, etc. The remarkable progress in recent material science seems to be based on the simultaneous combintion of materials with different properties. The demand for such "combined materials" has been increasing so as to allow the interstitial compound to serve to one of the elements which construct the new combined materials.

The researches on protective coatings of intersti-

tial carbides by C.V.D. have not always produced the
good results enough to be put to practical use. Adherent
and uniform (non-porous) coating on metals at low tem-
peratures is one of the present problems to be solved.
Titanium carbide coating on the steel surface, was in-
vestigated by Takahashi et al. (36) in the relatively
low temperature range of 850° to 1,000°C using a mixture
of $TiCl_4$ + H_2 + (C_3H_8). They found that the pre-elecro-
deposition of cobalt on low carbon steel was effective
to obtain adherent titanium carbide coating. The uni-
form coating of β-W_2C or β-Mo_2C on iron obtained by Lander
et al. (45) is also noteworthy as the coating technique
at low temperature which will applied to other compounds
in the future.

Composite materials   The whiskers or fibrous forms
of inorganic materials have been marked as the reinforce
components in composite materials since the production
of G.F.R.P. (glass-fibre reinforced plastics) was intro-
duced in the industries in the 1950's. The new composite
material is the subject of research and development in
today's material science. Especially, C.F.R.P. (carbon-
fibre reinforced prastics) is massproduced. Composite
materials are classified as F.R.P. (fibre reinforced plas-
tics), F.R.M. (fibre reinforced metal) and F.R.R. (fibre
reinforced rubber). These are composed of matrix mate-
rials (plastics, metals or rubbers) and reinforced fibres.
The fabrication process of whisker composites involves
the classification of the length and the alignment in
the matrix which were investigated by Lipp in the case
of silicon carbide whiskers (63). It was possible to
produce a highly oriented composite by means of the ex-
truding nozzle. The best combination of the matrix and

the fibres should be selected considering the problems
of wetting, bonding and chemical stability at the fibre-
matrix interface (64). The whisker or fibre reinforced
composites of interstitial compounds may be recommended
as the superior composite materials.

Other devices   Although the interstitial carbides ob-
tained by C.V.D. have not been applied to other devices,
one can expect further some possibilities of their prac-
tical uses, particularly in the field of electrical de-
vices. For example, the thermo-electrical or super-con-
ductive properties of interstitial carbides will become
more important in the near future. Indeed, the impor-
tance of C.V.D. techniques will be recognized as the
social demands for better materials increase.

1.5   The Aim and Scope of the Present Study
     As described previously, the interstitial compounds
have the chemical, mechanical and electrical properties
of interest (see Section 1.1). But the products obtain-
ed by C.V.D. have not always been connected immediately
with the chemical industries in spite of their potential-
ities in the future (see Section 1.4). This is not only
because the requirements have not been developed for
combined materials with the transition metals of small
Clarke numbers, but because the detailed informations
on C.V.D. have not been established in the coating or
whisker-forming technology (see Section 1.2). It is aim-
ed in the present study to investigate the chemical vapor
deposition of interstitial carbides, especially the car-
bides of titanium, tungsten and molybdenum, which are
relatively familiar in the refractory and super-hard ma-

terials. The originality of the study consists in the
one dimensional growth of carbides and some interesting
synthetic procedures are introduced. In performing this
investigation, the C.V.D. methods of silicon carbide and
other semiconducting compounds were quite instructive,
considering that the remarkable developments of recent
I.C. or L.S.I. technology have been indebted to a num-
ber of basic studies on C.V.D. of semiconductors such
as Si (65-67), SiC (68-72), and Si_3N_4 (73 &74).

In Chapter 2, the single crystal growth of titanium
carbide whiskers, needles or pillars is presented. In
a similar way, the vapor deposition of tungsten carbide
dendrites, including the needle or pillar forms, is de-
scribed in Chapter 5. Chapters 3 and 4 are concerned
with the fibrous growth of polycrystalline carbides of
titanium, tungsten and molybdenum. By the formation of
titanium carbide filaments, the vapor-solid reaction of
the titanization of carbon filament was employed. The
possibility of continuous fibrous growth of W_2C or Mo_2C
by discharge method is shown in Chapter 4.

REFERENCES

1) R.Kirk & D.Othmer, "Encyclopedia Chem. Tech." John
   Wiley & Sons, Inc. New York (1963-70).
2) R.E.Rundle, Acta Cryst. 1 180 (1949)
3) J.P.Nielsen, J. Metals 5 248 (1953)
4) R.Kirk & D.Othmer, "Encyclopedia Chem. Tech." John
   Wiley & Sons, Inc. New York Vol.4 p.80 (1964)
5) "Kagaku Binran" Maruzen Tokyo (1966)

6) W.W.Webb, J.T.Norton & C.Wagner, J. Electrochem. Soc. 103 112 (1956)

7) E.Nikolaiski, Z. Physik. Chem. 24 405 (1960)

8) R.W.Stewart & I.B.Clutler, J. Am. Ceram. Soc. 50 176 (1967)

9) K.Sugiyama & T.Takahashi, Kinzoku Hyomen Gijutsu 20 23 (1969)

10) J.M.Harris, H.C.Gatos & A.F.Witt, J. Electrochem. Soc. 116 380 (1969)

11) H.J.Schnabel, Phys. Chem. 241 177 (1969)

12) J.Bloem, J. Electrochem. Soc. 117 1397 (1970)

13) J.B.Higgins, A.Gatti & J.J.Gebhardt, J. Electrochem. Soc. 116 137 (1969)

14) K.E.Bean & P.S.Gleim, J. Electrochem. Soc. 114 1158 (1967)

15) G.E.Hellox & R.E.Smallman, J. Appl. Phys. 37 818 (1966)

16) D.W.Lee & J.S.Haggerty, J. Am. Ceram. Soc. 52 641 (1969)

17) F.W.Vahldick, J. Less-Common Metals 12 429 (1967)

18) A.Kelly & D.J.Rowcliffe, Phys. Status Solidi 14 K29 (1966)

19) R.S.Mehan & J.A.Herzog, "Whisker Technology" John Wiley & Sons, Inc. New York p157 (1970)

20) A.Gatti, C.Mancuso, E.Feingold & R.Mehan, J. Phys. Chem. Solid, Suppl. No. 1 317 (1967)

21) R.L.Mehan & E.Feingold, J. Materials 2 239 (1967)

22) T.Takahashi, K.Sugiyama & Y.Suzuki, J. Crystal Growth 10 139 (1971)

23) K.Sugiyama & T.Takahashi, Kogyo Kagaku Zasshi 73 1959 (1970)

24) М.И. Айвазов, И.А.Домашнев и Т.В.Резчикова,

Изв. Акад. Наук СССР Неорг. Матер. **5** 2195 (1969)

25) В.С.Нешпор, В.С.Давыдов, Б.Г.Ермаков и Б.Б.Могилевич,
Порошковая Металлургия **50** 65 (1967)

26) В.Г.Тревенкина и Е.Н.Денбновецкая,
Изв. Акад. Наук СССР Неорг. Матер. **4** 2196 (1968)

27) L.Ramquvist, Jernkont. Ann. **152** 456 (1968)

28) C.Kittel, "Introduction to Solid State Physics"
John Wiley & Sons, Inc. New York p338 (1967)

29) N.Pessall, C.K.Jones, H.A.Johansen & J.K.Hulm,
Appl. Phys. Letters **7** 38 (1965)

30) F.J.Darnell, P.E.Bierstedt, W.O.Forshey & R.K.Waring,
Phys. Rev. **140** 1581 (1965)

31) T.Takahashi, K.Sugiyama & K.Kitagawa, Kinzoku Hyomen
Gijutsu **18** 350 (1967)

32) A.E.van Arkel & J.H.de Boer, Z. anorg. allgem. Chem.
148 345 (1925)

33) K.Moers, Z. anorg. allgem. Chem. **198** 243 (1931)

34) W.Burgers & J.Besart, Z. anor. allgem. Chem. **216**
209 (1934)

35) C.F.Powell, J.H.Oxley & J.M.Blocher, "Vapor Deposi-
tion" John Wiley & Sons, Inc. New York p364-74
(1966)

36) T.Takahashi, K.Sugiyama & K.Tomita, J. Electrochem.
Soc. **114** 1230 (1967)

37) T.Takahashi, K.Sugiyama & K.Kitagawa, Kinzoku Hyo-
men Gijutsu **19** 514 (1968)

38) K.Becker and H.Ewest, Z. Tech. Phys. **11** 148, 216
(1930)

39) J.N.Pring & W.Fielding, J. Chem, Soc. **95** 1497 (1909)

40) A.Westgren & G.Phragmen, Z. anorg. allgem. Chem.
156 27 (1927)

41) M.R.Andrews, J. Phys. Chem. **27** 270 (1923)

42) M.R.Andrews & S.Dushman, J. Phys. Chem, 29 462 (1925)

43) K.Becker, Z. Metallk. 20 437 (1928)

44) K.Kuo & G.Hagg, Nature 170 245 (1952)

45) J.J.Lander & L.H.Germer, Am. Inst. Mining Met. Engrs. Tech. Publ. 2259 (1947)

46) W.K.Burton, N.Cabrera & F.C.Frank, Nature 163 398 (1949)

47) W.K.Burton, N.Cabrera & F.C.Frank, Phil. Trans. Roy. Soc. 243 299 (1951)

48) W.K.Burton & N.Cabrera, Disc. Faraday Soc. 5 33 (1949)

49) A.R.Verma, Nature 167 939 (1951)
L.M.Dawson & V.Vand, Nature 167 476 (1951)

50) A.J.Fortz, Phil. Mag. 43 481, 949 (1952)

51) F.C.Frank, Phil. Mag. 44 854 (1953)

52) F.R.Nabarro & P.J.Jackson, "Growth and Perfection of Crystals" John Wiley & Sons, Inc. New York p13 (1958)

53) N.Cabrera & R.V.Coleman, "The Art and Science of Growing Crystals" John Wiley & Sons, Inc. New York p23 (1963)

54) E.S.Greiner, J.A.Gutowski & W.C.Ellis, J. Appl. Phys. 32 2489 (1961)

55) R.S.Wagner & W.C.Ellis, Appl. Phys. Letters 4 89 (1964)

56) R.S.Wagner, W.C.Ellis, K.A.Jackson & S.M.Arnold, J. Appl. Phys. 35 2993 (1964)

57) P.R.Thorton, D.W.F.James, C.Lewis & A. Brandford, Phil. Mag. 14 165 (1966)

58) R.S.Wagner, "Whisker Technology" John Wiley & Sons, Inc. New York p47 (1970)

59) R.S.Wagner & C.J.Doherty, J. Electrochem. Soc. <u>115</u> 93 (1968)

60) D.J.Barher, Phil. Mag. <u>10</u> 75 (1964)

61) A.H.Hener & P.Burnett, J. Am. Ceram. Soc. <u>50</u> 627 (1967)

62) I.Berman & C.E.Ryan, J. Crystal Growth <u>9</u> 314 (1971)

63) A.Lipp, Feinwerktechnik <u>74</u> 150 (1970)

64) S.M.Wolf, "Whisker Technology" John Wiley & Sons, Inc. New York p273 (1970)

65) W.Steinmaiar, Phillips Res. Repts <u>18</u> 75 (1963)

66) T.O.Sedgwick, J. Electrochem. Soc. <u>111</u> 1381 (1964)

67) D.C.Gupta & R.Yee, J. Electrochem. Soc. <u>116</u> 1561 (1969)

68) R.B.Campbell & T.L.Chu, J. Electrochem. Soc. <u>113</u> 825 (1966)

69) I.L.Kalnin & J.Rosenstock, Electrochem. Tech. <u>4</u> 492 (1966)

70) J.J.Rohan & J.L.Sampson, J. Phys. Chem. Solids Suppl. No. 1 523 (1967)

71) R.S.Price, Am. Ceram. Soc. Bull. <u>48</u> 859 (1969)

72) J.M.Harris, H.C.Gatos & A.F.Witt, J. Electrochem. Soc. <u>118</u> 335 (1971)

73) J.V.Dalton & J.Drobek, J. Electrochem. Soc. <u>115</u> 865 (1968)

74) M.J.Griece, F.L.Worthing & B.Schwartz, J. Electro- chem. Soc. <u>115</u> 525 (1968)

CHAPTER   2

Single Crystal Growth of Titanium Carbide

by Chemical Vapor Deposition

2.1   Introduction

Titanium carbide, one of the typical interstitial
compounds having a high melting point of 3,250° C and
Vicker's hardness of 3,200 kg/mm^2, has been well known
as a super-hard and refractory material. Boule single
crystal of titanium carbide has been prepared by Arc-
Verneuil process and many studies (1-4) have been done
on its crystal structure (for example, "Mondrian precip-
itates", stacking faults, etc.) or physical properties
(see Section 1.1). Moers (5) obtained the monocrystal-
line deposits of titanium carbide on a tungsten filament
which was heated at 1,600° to 2,000° C in the atmosphere
of $TiCl_4 + H_2 + C_7H_8$, but the detailed study on crystal
morphology was not reported. On the other hand, few
papers have been published on the preparation of needle
or whisker forms of carbide from vapor phase, except a
brief report by Hertl (6) who obtained fibrous titanium

carbide from TiO_2 and colloidal carbon in chlorine atmosphere.

In this experiment, various forms of titanium carbide single crystal were grown on graphite substrate in the temperature range of 1,200° to 1,350° C from the vapor phase containing hydrocarbon and hydrogen saturated with titanium tetrachloride vapor. The purpose of this study was not only to investigate the correlation between the growth conditions (temperature, concentration, etc.) and the crystal morphology (needle, whisker, pillar or polyhedron), but also to clarify the growth direction and the growth mechanism. In discussing the crystal growth process, the theory on silicon whisker growth by Wagner et al. (7) was instructive as well as the experimental studies on whiskers of SiC (8-11), B_4C (12) and HfC (13). Finally, the tensile strength was measured by the buoyancy method and it could be compared with published values of other whisker materials.

2.2   Experimental

The schematic diagram of the experimental apparatus is illustrated in Fig.2.1.   Titanium carbide single crystal was prepared according to the reaction;

$$TiCl_4 + C_xH_y + H_2 \longrightarrow TiC + 4HCl + C_mH_n,$$
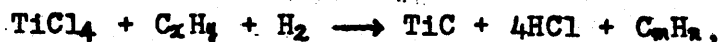
where C_xH_y was propane, taking account of the facility for pyrolysis of hydrocarbon (see Section 1.2). The reaction was performed in a horizontal quartz tube, the inside diameter of which was about 35 mm. A cylindrical graphite (50 mm in length, 30-32 and 10-23 mm in outside and inside diameters, respectively) was placed at the center of the tube, and was used as substrate for depo-
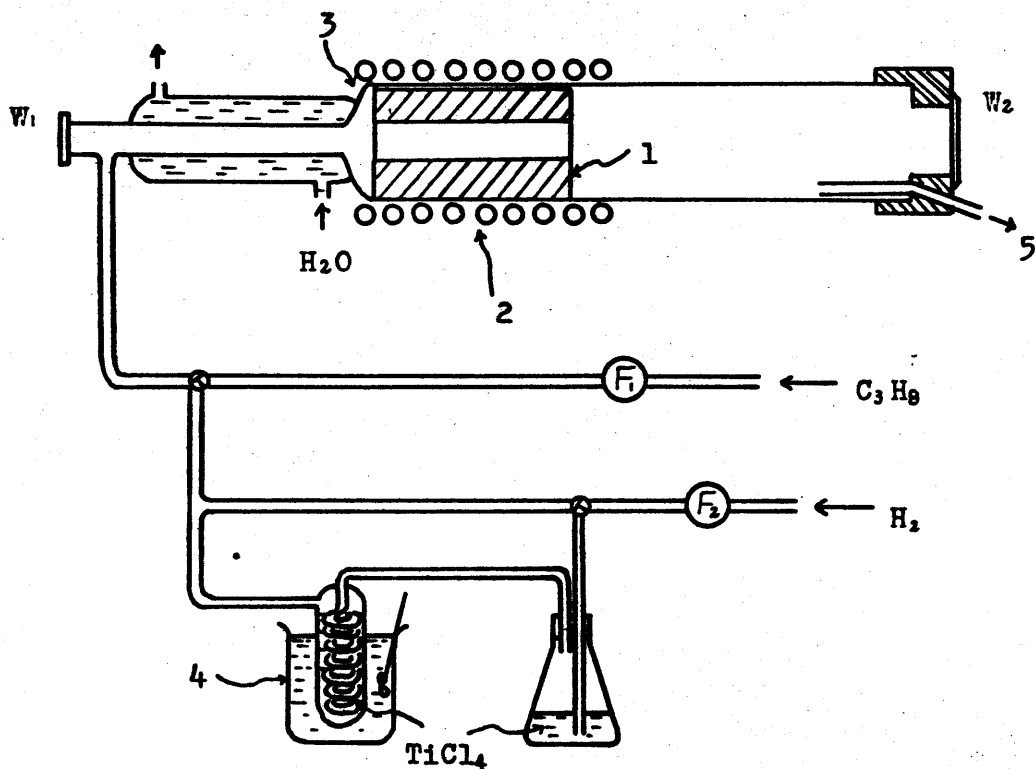
Fig.2.1 Schematic diagram of the experimental
apparatus.

(1) graphite substrate   (2) r.f. induction
coil   (3) quartz reactor   (4) $TiCl_4$ saturator
(5) outlet

F_1 , F_2 : flow meter

W_1 , W_2 : glass window

sition of titanium carbide which was heated by a radio frequency (r.f.) induction coil. Titanium tetrachloride (b.p. 136.5°C) was introduced into the hydrogen stream by means of a bubbling type saturator, maintained at 90 °C (vapor pressure of $TiCl_4$ at 90°C: 190 mmHg). The gas flow rates of dried hydrogen and propane were measured with the flow meter. After precleaning the reaction tube with hydrogen, the gas mixture of titanium tetrachloride, hydrogen and propane was thus led to the inlet. It was necessary to keep the gas mixture at 90° to 100°C by cooling water at the inlet which was 20-50 mm forward the surface of graphite substrate to prevent the propane from decomposing excessively due to the radiation of the heated graphite. The substrate temperature was measured through the glass window W_1 with the photo-pyrometer and the growth process was observed through the other window W_2. Impurities such as Au, Pd, H_2PtCl_6, HgCl, $MnCl_2$, $Mn(NO_3)_2$, Na_2SO_4, etc. were incorporated into the graphite and the impurity effect on the crystal growth was investigated.

The morphology of each single crystal was observed through the microscope. The deposits were identified by X-ray diffractometer and the growth directions were determined by Laue method. The needle and pillar crystals were embedded in the epoxy resin, the cross section of a crystal was abraded with diamond paste, and it was etched in hot concentrated nitric acid for five minutes.

The fracture strength along the crystal axis was measured by buoyancy method, whereby the crystal was fixed at both ends on copper tools, one of which was connected with a buoy via thin tungsten wire and was loaded continuously in tension by draining the water which sus-
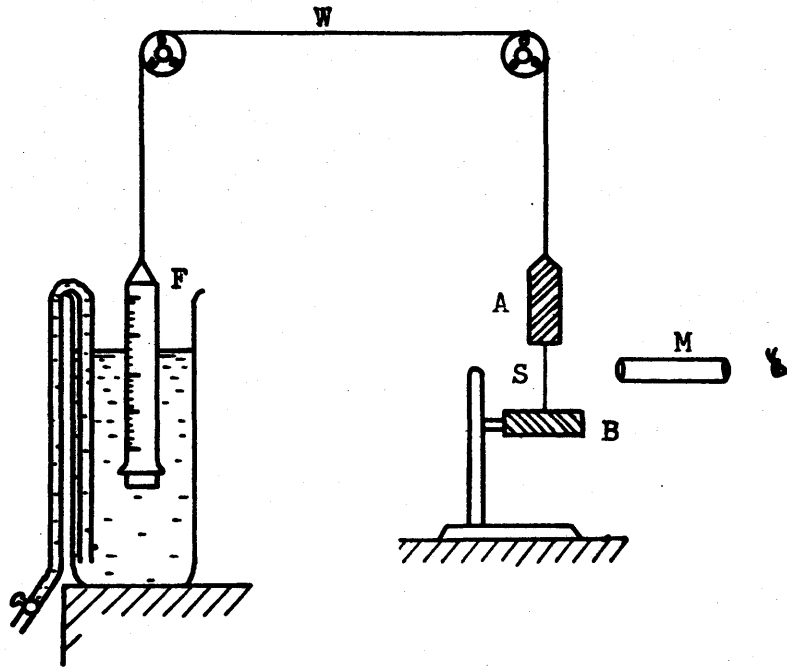
Fig.2.2 Schematic diagram of the apparatus for
        measurement of fracture strength.

(A) & (B)   copper supports

   (S)   specimen

   (W)   tungsten wire

   (F)   buoy

   (M)   microscope

tained the buoy (see Fig.2.2).

2.3   Results

<u>Growth conditions</u>   The conditions for single crystal
growth were investigated as a function of temperature,
gas flow rate and the shape of the graphite substrate in
the reaction tube. The temperature dependence was note-
worthy; when the temperature of the substrate was below
1,200°C, a thin film of titanium carbide (14) was coated
on the graphite surface, and when above 1,400°C, poly-
crystals were deposited rapidly. In this experiment,
the single crystal growth was studied in detail in the
temperature range of 1,200° to 1,400°C. Fig.2.3 shows
the influence of temperature and propane gas flow rate
on the crystal growth, when the hydrogen gas flow rate
was 4.0-8.0 ml/sec (linear velocity: 27.5-55.0 cm/sec
in the graphite tube). It should be noted from Fig.2.3
that a suitable temperature range for single crystal
growth is from 1,240° to 1,280°C. Using a propane gas
flow rate of 0.05 ml/sec (0.8 m/o) is essential. The
influence of hydrogen gas flow rate and temperature on
the crystal morphology is shown in Fig.2.4 at a fixed
propane gas flow rate of 0.05 ml/sec. Needle or whisker
crystals were found to deposit at a relatively high flow
rate of about 7.7 ml/sec (linear velocity: 53.1 cm/sec),
while pillar crystals were deposited at a lower flow rate
of 6.2 ml/sec (linear velocity: 43.8 cm/sec), and poly-
hedron crystals in a higher temperature range of 1,250°
to 1,300°C. These experimental data were obtained when
the inside diameter of substrate was 10 mm. As the in-
side diameter Di was increased, for example Di = 20-23
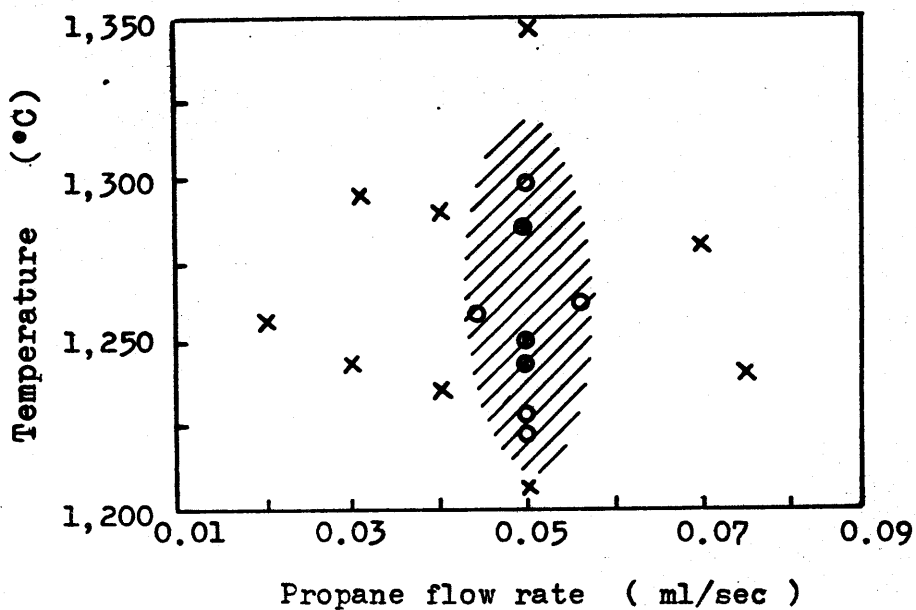
Fig.2.3 Influence of temperature and propane gas
        flow rate on crystal growth.
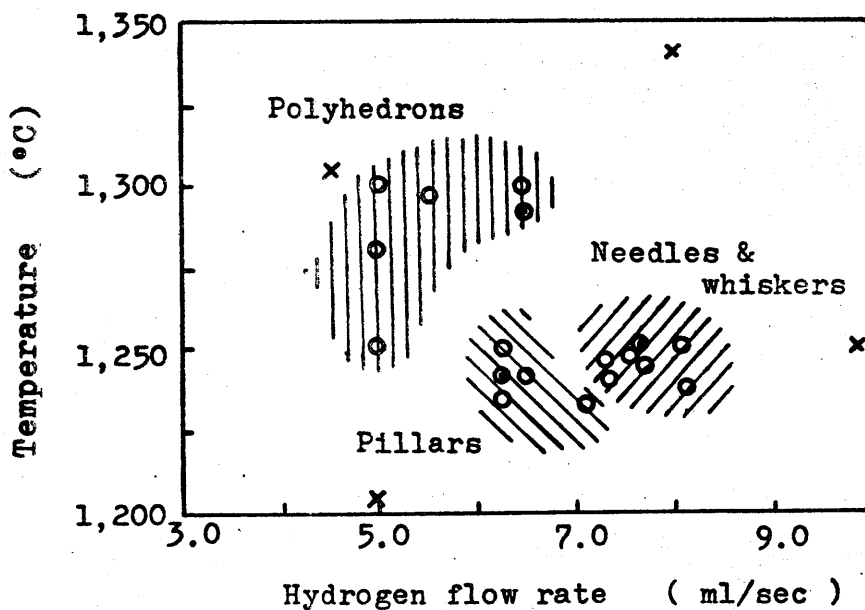
Fig.2.4 Influence of temperature and hydrogen gas flow
         rate on crystal morphology. (C_3H_8 flow rate:
         0.05 ml/sec)
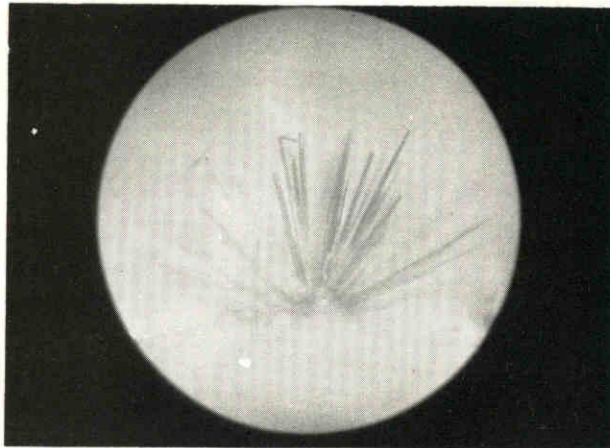
Fig.2.5 Micrograph of needle crystals. (front view)
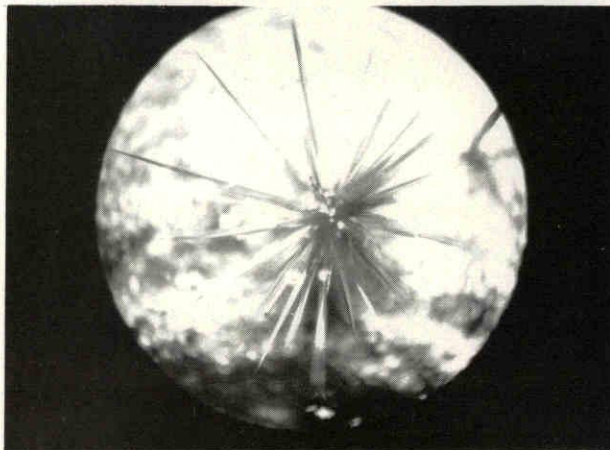Note that some crystal tips are kinked to-
wards appropriate atmosphere.

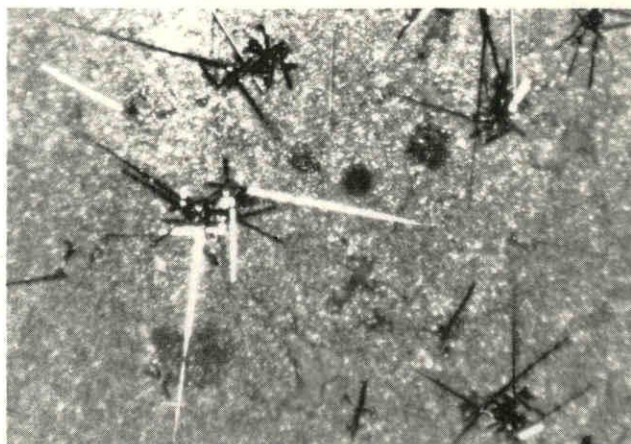Fig.2.6 Micrograph of needle crystals. (plane figure)

Fig.2.7 Micrograph of tapered needle crystals
grown in several groups on the graphite
substrate.

$\begin{cases} \text{Temperature:} & 1,250°C \\ C_3H_8 \text{ flow rate:} & 0.05 \text{ ml/sec} \\ H_2 \text{ flow rate:} & 8.0 \text{ ml/sec} \end{cases}$

mm, a number of needle crystals 6-7 mm long were grown,
but it was difficult to obtain reproducible data. How-
ever, relatively short but fine whiskers with the diam-
eter of 2-10 μm were obtained at the decreased cross sec-
tional area of the graphite tube, in which a graphite
cylinder (10-20 mm in diameter) was inserted. The mod-
erate deposition area in a run was limited to the graph-
ite surface at a proper distance from the inlet, which
was probably dependent on the temperature distribution
or the transport process of the agents in the furnace.
Crystal morphology   Figs.2.5 & 2.6 show the needle
crystals observed from two different directions.
They occur in radiating clusters, apparently from a sin-
gle nucleus. The initial growth rate is from 5 to 7
mm/hr, but the rate decreases abruptly in 60-80 minutes.
This seems to show that the growth region of needles is
limited to the thin gas film over the graphite surface,
because some long needles kink towards the appropriate
atmosphere at the tip. Needle crystals could be grown
in several groups on the substrate surface, as shown in
Fig.2.7, and some of them were tapered with metallic
luster. Whiskers from 2 to 12 μm in diameter were ob-
served together with fine needles at a higher linear flow
rate of hydrogen gas (Figs.2.8 & 2.9). A few pillar sin-
gle crystals, shown in Fig.2.10, grow in different direc-
tions from a single nucleus just like the needle crystals.
These are from 30 to 50 μm in diameter and from 1 to 5
mm in length, but the growth rate (2-5 mm/hr) is lower
than that of needles. One pillar crystal is magnified
in Fig.2.11, where the side plane of hexagonal prism and
the tip of the truncated pyramid are observed. Each side
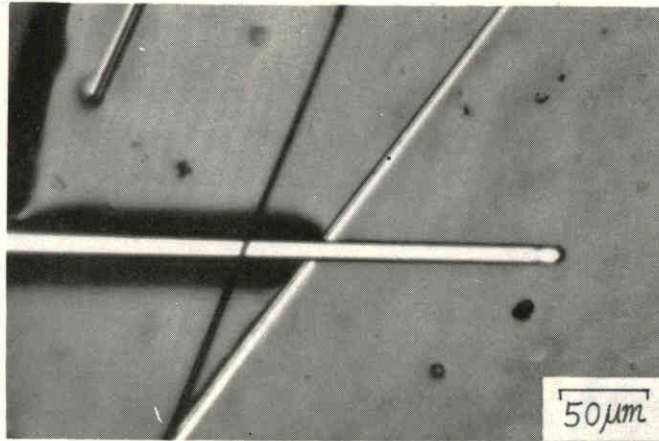has a smooth plane and a metallic gloss, except a special

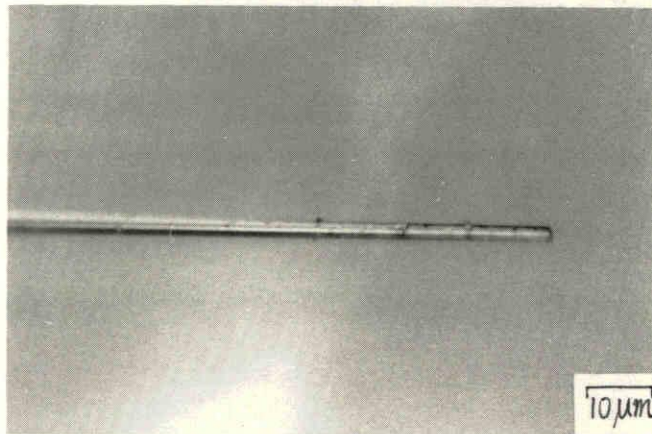Fig.2.8   Micrograph of whiskers.

(temperature: 1,240°C)

Fig.2.9   Micrograph of a magnified whisker
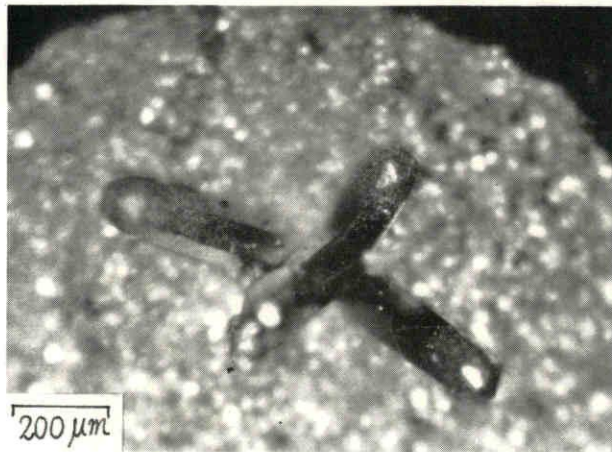
2μm in diameter.

Fig.2.10   Micrograph of a few pillar crystals.
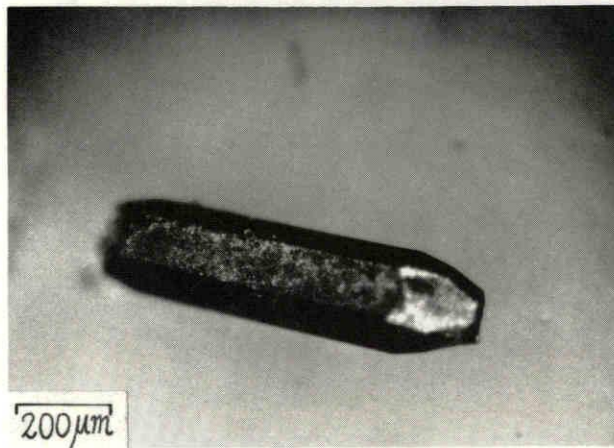
(temperature: 1,230°C)

Fig.2.11   Micrograph of a magnified pillar
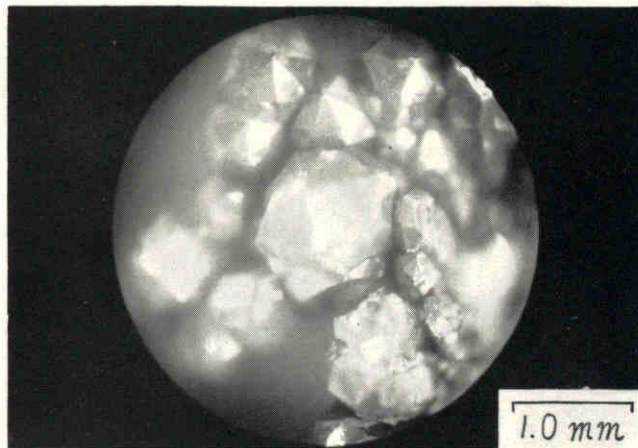
crystal like a hexagonal prism.

Fig.2.12 Micrograph of polyhedrons whose tips

are octagonal pyramids. (temperature: 1,280°C)

Fig.2.13 Micrograph of octahedral crystals

with impurities adhered at the lateral

faces.

case as described later. Polyhedron crystals, grown
for several hours in high temperature range, have a dif-
ferent sort of morphology, for example, hexahedron or
octahedron. Fig.2.12 shows the polyhedron crystals, whose
tips are octagonal pyramids, and they grow large enough
to become adjacent each other. Polyhedrons which adhere
impurities at the lateral faces, are shown in Fig.2.13.
They are similar to monocrystalline deposits apparently,
which were prepared in van Arkel type atmosphere by Moers
(5) and Chermant (15).

Crystallogrophic assignment and etching figure   After
the identification with the titanium carbide A.S.T.M.
card (16) by means of X-ray diffractometer, the growth
direction was determined with Laue method (front reflec-
tion type). X-ray beam from molybdenum target was radi-
ated for 90 minutes on a needle or a pillar crystal
mounted vertically on the goniometer head. Figs.2.14a
& b are transmission Laue photographs taken from a given
position (a), and from the rotated position by 60° (b)
around the axis. Two mirror symmetries can be confirmed
in the figures (a) and (b), where the equivalent Laue
patterns are at inverse directions each other. It is
suggested, therefore, that ⟨111⟩ is the growth direction,
since titanium carbide has a NaCl type crystal structure
(17). Consequently, each side of hexagonal prism of a
pillar crystal which was observed in Fig.2.11, is ap-
parently (110) plane. It is interesting that (110) plane
corresponds to the highly oriented plane in vapor plat-
ing on iron of titanium carbide at lower temperature
(14). Fig.2.15 shows the kinking of needle crystals
described previously, and the measured angle of the kink-
ed tip to the original direction ⟨111⟩, is about 108°,
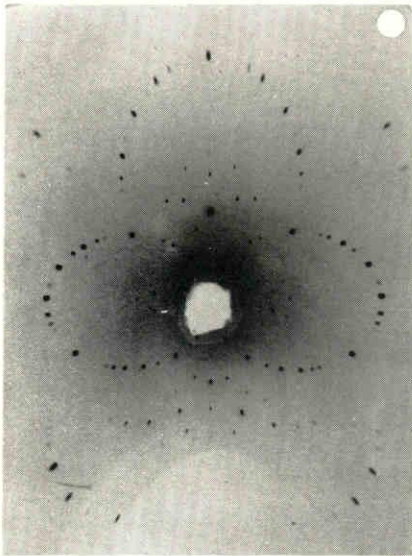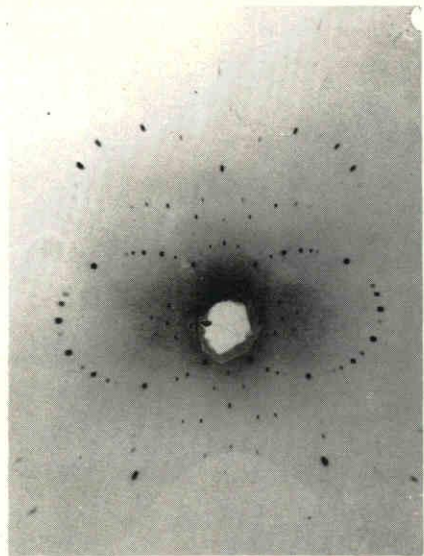
(a)   (b)

Fig.2.14   Laue photographs. (target: Mo, exposure: 40

   kV, 15 mA, 90 min., crystal-to-film distance: 16 mm)

   (a)   Laue spots with a mirror symmetry, radiated

      from a given direction.

   (b)   Laue spots with an inverse symmetry, radiated
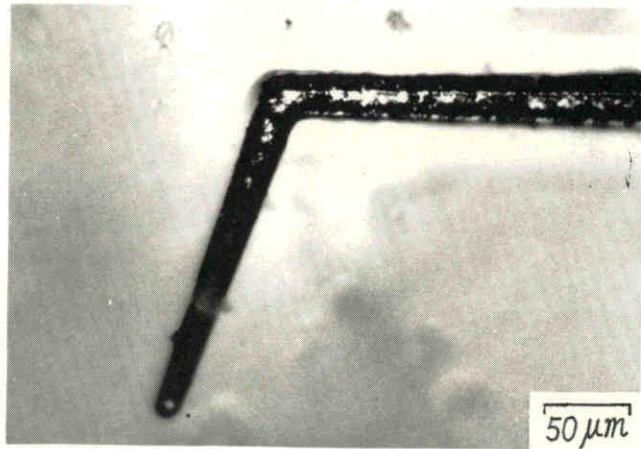
      from a rotated direction by 60° around the axis.

Fig.2.15   Micrograph of a needle crystal kinked
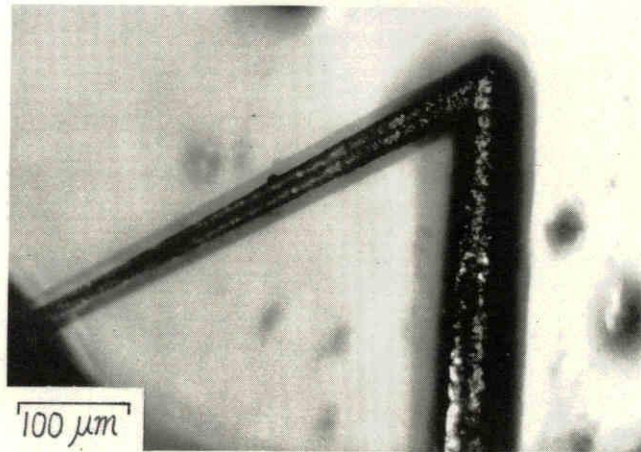
from $\langle 111 \rangle$ to $\langle 1\bar{1}1 \rangle$.

Fig.2.16   Micrograph of a needle crystal kinked

towards $\langle 100 \rangle$ at the tip.
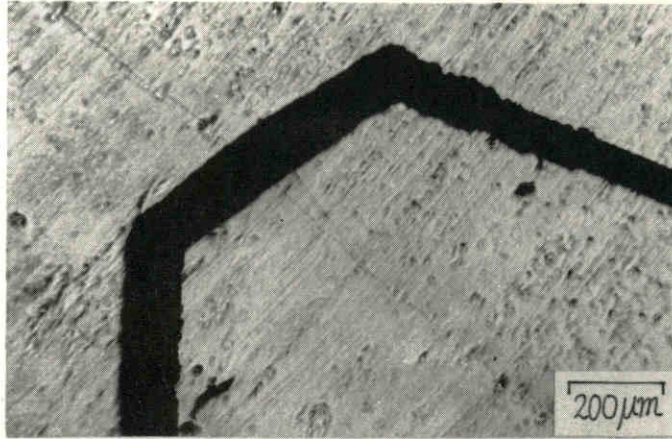
Fig.2.17 Micrograph of a dekinked needle

crystal (,which was observed occasionally

at the crystal tip of a relatively long

needle crystal).

so that the kinking direction is assigned the same form
$\langle 1\bar{1}1 \rangle$. From the analogous observation, the kinking di-
rection of a needle as shown in Fig.2.16, is probably
$\langle 100 \rangle$, for the kinked angle is about 60°. Dekinking was
also observed occasionally (see Fig.2.17).

Etching of the cross section in hot concentrated
nitric acid reveals the growth layers shown in Figs.2.18
& 2.19. Fig.2.18 shows the etching figure of a needle
crystal, where the nearly circular growth layers are ob-
served. On the other hand, there are regular hexagonal
growth layers in Fig.2.19, which show the etching figure
of a pillar crystal. Each side of the hexagon is found
to correspond to (110) plane indexed previously. At the
center of the cross section, there is a circular project-
ed part about 10 μm in both figures, which is difficult
to etch.

Impurity effects and shapes of crystal tips   When im-
purities were incorporated into the graphite substrate,
continuous large growth steps were easy to grow on the
side of a pillar crystal (Figs.2.20 & 2.21 magnified)
and each step has a secondary step at the edge. Fig.2.
22 shows a few irregular and larger growth steps for a
crystal which was grown in the higher temperature range.
Though it was difficult to get an exact quantitaive know-
ledge about the impurity effect on growth rate, it was
possible to establish the difference of the growth by
incorporating a few kinds of impurities. For example,
Mn and Au show a positive effect on the crystal growth,
as shown in Figs.2.23 & 2.24. A number of needles can
be seen to swarm up at the substrate which was impreg-
nated with $Mn(NO_3)_2$, while several long needles are grown
in the case of elemental Au. It was found similarly
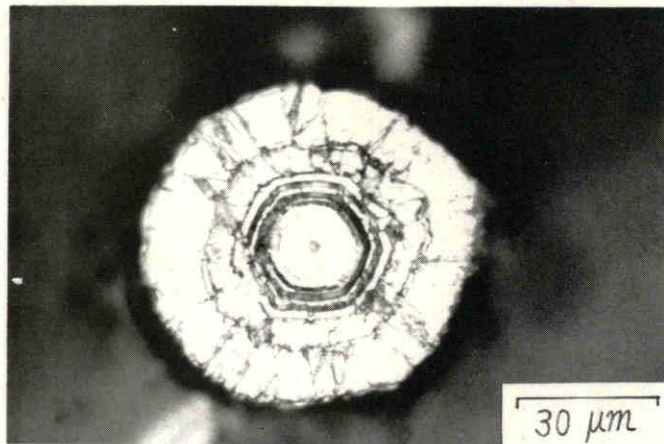
Fig.2.18   Etching figure of the cross section
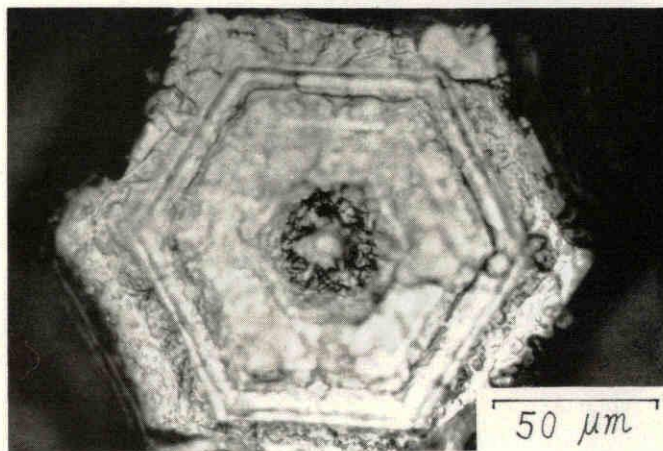
of a needle crystal.

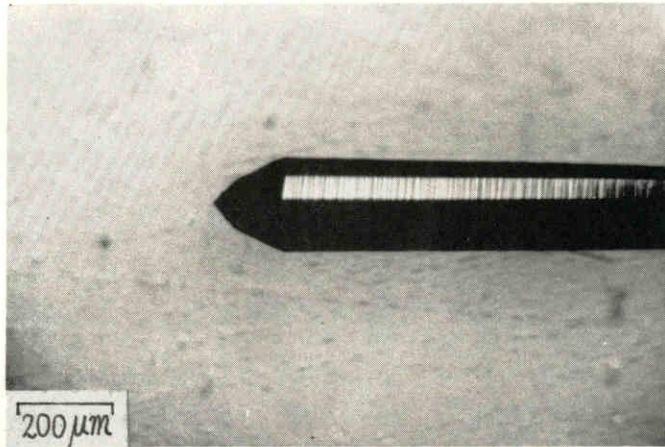Fig.2.19   Etching figure of the cross section

of a pillar crystal.

Fig.2.20 Micrograph of continuous large growth
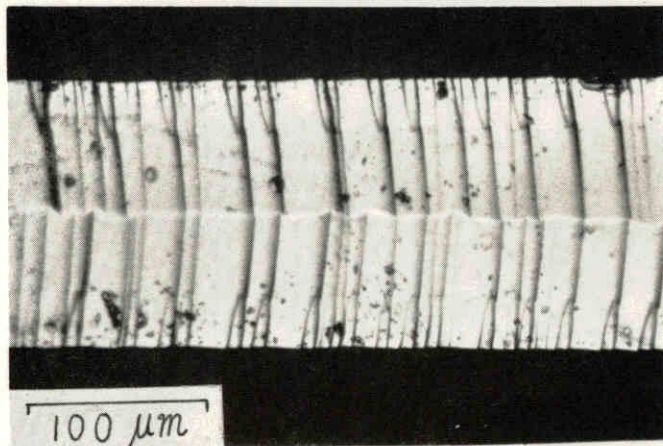
steps of a pillar crystal.

Fig.2.21 Micrograph of magnified large growth

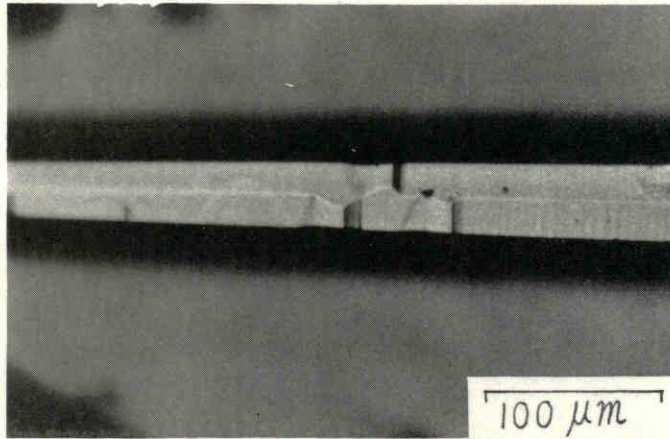steps followed by the secondary bunched

steps.

Fig.2.22 Micrograph of a few irregular and
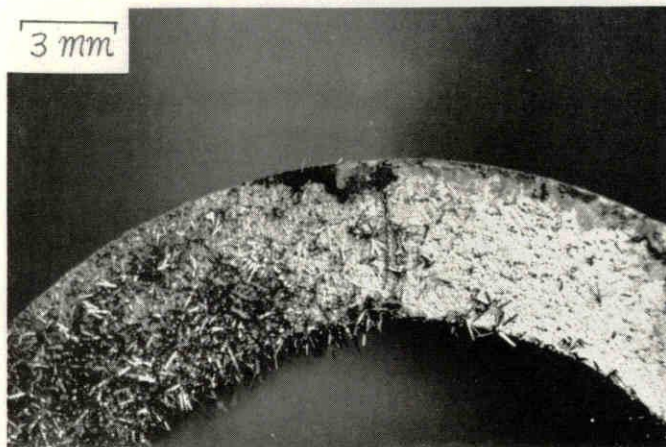large growth steps at the lateral faces
of a pillar crystal.

Fig.2.23 Impurity effect on the graphite sub-
strate incorporated with $Mn(NO_3)_2$ (left side)
and no impurity (right side).

that Pt, Pd, Ag, etc. represented positive effects, but Cu, Fe, Co, Zn, etc. showed negative effects.

The typical shape of a whisker tip is shown in Fig. 2.25. It seems that the tip has no globule cap, but has the growth planes with a right angle each other, which is analogous to the shape of a pillar crystal (see Fig. 2.26). The final shapes of tapered needle crystals are shown in Fig.2.27. These data on impurity effects stated above, will give an important suggestion in discussion of the growth mechanism.

Tensile strength   The fracture strength vs. the diameter of needle or pillar crystals is plotted on logarithmic scales in Fig.2.28. A linear relation can be seen from the figure, as expected from the measurements of other whiskers (see Fig.1.2). The extrapolated value to 5 μm in diameter is about 1,000 kg/mm^2. The tensile strength of titanium carbide whiskers, therefore, is estimated to exceed that of iron (250 kg/mm^2), sapphire (350 kg/mm^2) or alumina (560 kg/mm^2) in the same diameter (18). Fig.2.29 shows the micrograph of a fractured cross section, which was cracked radially with less possibility of the slip plane (111), (4).

2.4   Discussion

The vapor phase reaction and crystal morphology   As described earlier, the propane gas flow rate of 0.05 ml/sec (0.8 m/o) and cooling of gas mixture at 90°-100°C were essential for growth of a single crystal. It means that the decomposition reaction of hydrocarbon play an important part in the formation of titanium carbide single crystals. This suggestion seems to be supported by
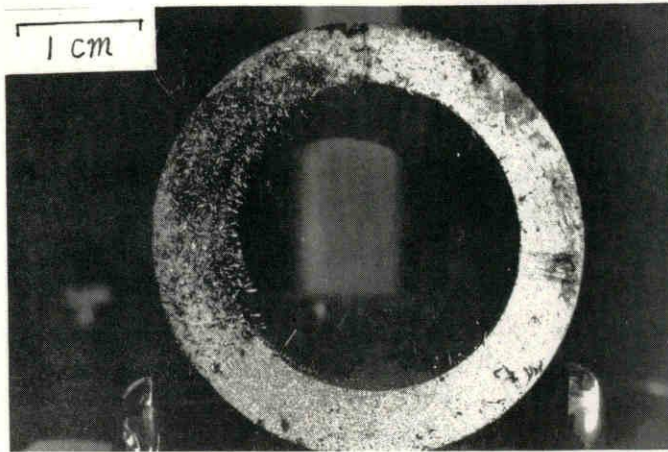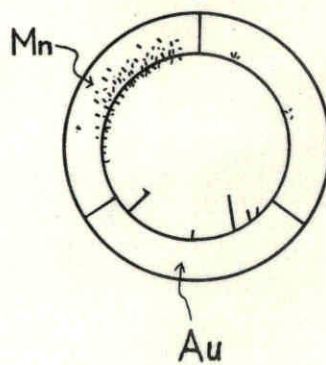
Fig.2.24   Impurity effect of Mn and Au.

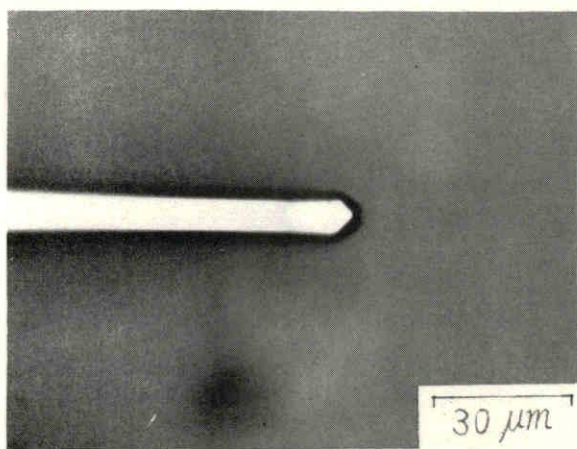The substrate portion where the impurity was incorporated is shown below.

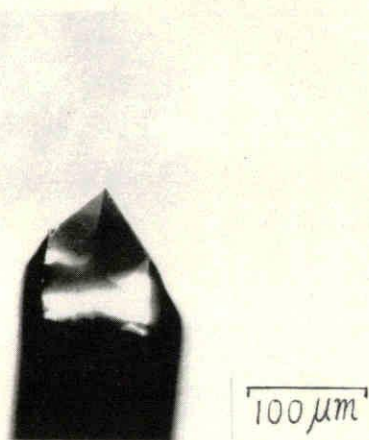Fig.2.25 Micrograph of the crystal tip of

a whisker.

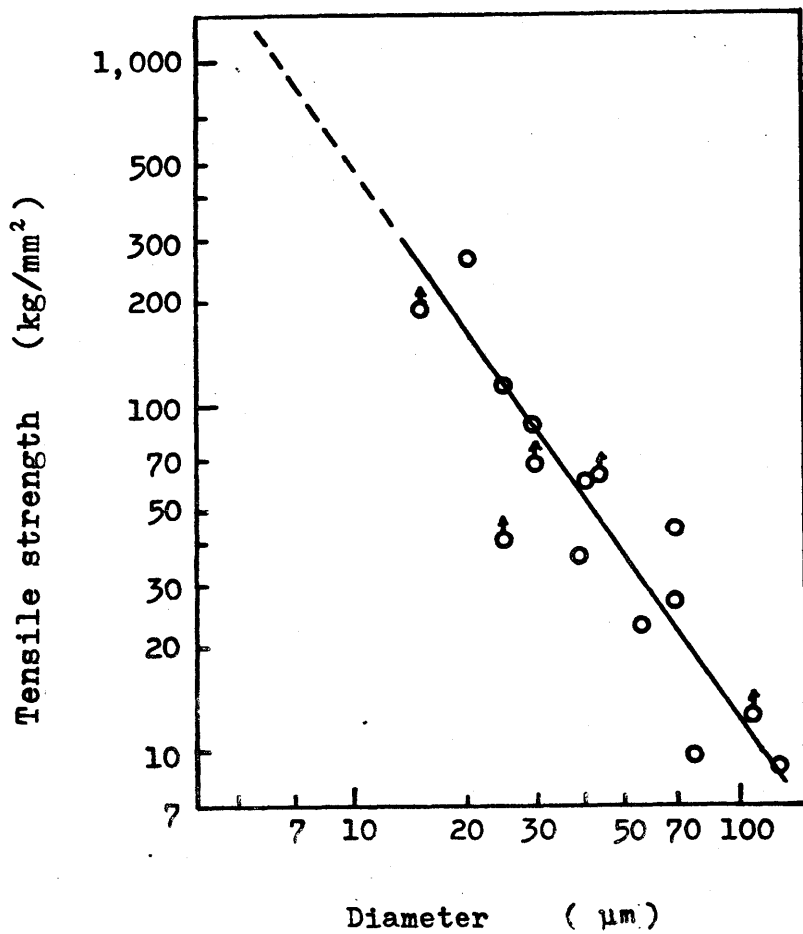Fig.2.26 Micrograph of the tip shape of a

pillar crystal.

Fig. 2.28 Fracture tensile strength vs. diameter
of needle or pillar crystals.

the study of Pearce (19) who discussed the reaction me-
chanism in the formation of TiC from the vapor. He con-
cluded with the help of thermodynamic data that the in-
itial formation of pyrocarbon was important rather than
the reduction to amorphous carbon. Since the reaction
does not involve the formation of titanium in the tem-
perature range employed, as suggested by Münster (20),
the net reaction may occur between titanium trichloride
and radical products (pyrocarbon) to form the addition
compounds such as CH_3TiCl_3. Therefore, appropriate tem-
perature distribution and gasous diffusion process in the
reaction tube should be given to provide pyrocarbon on
the surface of graphite substrate. In addition, it is
necessary to keep a constant supersaturation at the growth
tip in order to obtain a given crystal morphology as
pointed out by Gatti (12) in the whisker growth of B_4C.
When the inside diameter of the cylinder is large, for
example, it is difficult to introduce a proper quantity
of pyrocarbon while keeping the temperature or atmosphere
constant. As a result, the reproducibility decreases.
With small inside diameters, however, the linear flow
rate of hydrogen gas is higher, making it easier to grow
a fine whisker, as shown in Fig.2.3. Anyhow, it seems
a complicated problem to obtain longer whiskers than 7
mm unless completely controlled conditions are establish-
ed.

Growth mechanism   The growth mechanism of polyhedrons
can be explained by Kossel model on perfect crystal under
a high supersaturation (21). Also, it can be applied
to the process for lateral growth of a pillar single crys-
tal where the growth steps are observed in Fig.2.20. In
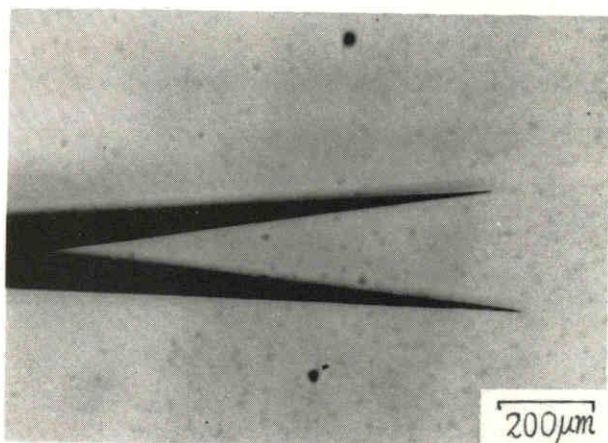fact, polyhedrons and pillars are found to be grown at

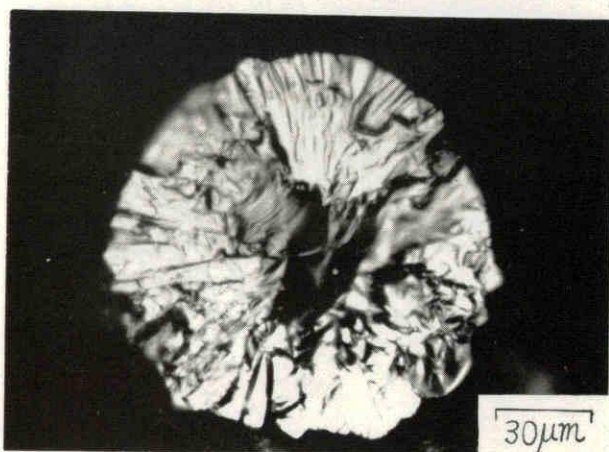Fig.2.27 Micrograph of crystal tips of tapered

needle crystals.

Fig.2.27 Micrograph of the fractured cross

section of a needle crystal.

higher concentration of TiCl$_4$, as shown in Fig.2.4. Observations of the etching figures (Figs.2.17 & 2.18) suggest the difference in the growth mechanism between the center and the circumference. It is convenient to describe two steps like silicon whisker growth (7); one is the whisker growth and the other is the lateral growth of needle or whisker. Through the micoscopic observations (see Figs.2.24-26), however, any small globule can not be found at the tip of the whisker or needle crystals. So it is doubtful to establish the TiC whisker growth mechanism by V.L.S. (see Figs.1.3 & 1.4). But, a particular case may be considered where the globule is etched away completely as reported by Berman et al. (11), so that more detailed investigations on the microstructure and the impurity effect should be made to learn the mechanism of whisker growth.

It seems that the growth layers in Figs.2.17 & 2.18 are due to the variation of chemical composition, and these can be connected with the lateral growth. From the appearance of the growth steps in Figs.2.20 & 2.21, the bunched steps were considered to grow in the presence of impurities. Such a "bunching effect" of mono-molecular steps which were caused by impurity, was discussed theoretically by Frank (22). The lateral growth rate increases when the bunched growth steps pass through any side, which results in the growth layers. It is concluded, therefore, that the pillar crystals are grown by the movement of steps on the side simultaneously with the tip growth, while in the case of the tapered needle crystals, the lateral growth is a little slower than the tip growth.

2.5　Conclusion

Single crystals of titanium carbide were grown on the graphite substrate from vapor phase in the temperature range of 1,200° to 1,350°C. The atmosphere employed consisted of hydrogen, titanium tetrachloride and propane. It was found that the gas flow rate, or the geometrical shape and impurities of the substrate greatly affected the crystal morphology. Above all, the contribution of propane concentration (0.8 m/o) was so remarkable that the decomposition of propane gas was considered to define strictly the growth range of single crystals. Impurities such as Mn, Au, Pd, Ag, etc. revealed the facility for crystal growth.

Polyhedron crystals were deposited in the high temperature range (1,250°-1,300°C), and have smooth and glossy planes on the crystal surface. Pillar crystals (30-50 μm in diameter) grew gradually as hexagonal prisms at the moderate temperature of 1,240°C, while needle crystals (6-7 cm in length and 10-40 μm in diameter) grew rapidly in radiating clusters from a growth nucleus at a higher concentration of hydrogen (8.0 ml/sec). The growth rate of needles was 5-7 mm/hr. Whisker crystals about 3 μm in diameter were observed among them, when the linear velocity of hydrogen was rather high.

The growth direction of needle or pillar crystals was found to be $\langle 111 \rangle$ by Laue method and the kinking direction was $\langle 1\bar{1}1 \rangle$, or sometimes $\langle 100 \rangle$. The lateral plane of hexagonal prism was assigned (110), as a result.

The etching figure of the cross section showed hexagonal growth layers, where the central portion was difficult to etch. The bunched growth steps and the impurity effects suggested the growth mechanism similar to Si

whisker growth by V.L.S. method, i.e. the tip growth of whiskers was followed by the movement of growth steps on the side. Thus the tapered needles or pillars were supposed to grow by two steps. But it is uncertain to accept the V.L.S. mechanism for TiC whisker growth, for no globule was observed on the crystal tip.

From the linear relation between the strength and the diameter, the tensile strength of 1,000 kg/mm^2 was estimated at 5 µm in diameter. Titanium carbide whiskers are worthy of note, as a material having superior high tensile strength as well as the other mechanical properties.

REFERENCES

1) S.Williams, J. Appl. Phys. 32 552 (1961)

2) G.E.Hollox & R.E.Smallman, J. Appl. Phys. 37 818 (1966)

3) J.Venables, Phys. Status Solodi 15 313 (1966)

4) F.W.Vahldick, J. Less-Common Metals 12 429 (1967)

5) K.Moers, Z. anorg. allgem. Chem. 198 243 (1931)

6) W.Hertl, J. Am. Ceram. Soc. 50 630 (1967)

7) R.S.Wagner, W.C.Ellis, K.A.Jackson & S.M.Arnold, J. Appl. Phys. 35 2993 (1964)

8) W.F.Knippenberg, H.B.Haanstra & J.R.M.Dekkers, Phillips Tech. Rev. 24 181 (1962-3)

9) H.P.Kirchner & P.Knoll, J. Am. Ceram. Soc. 46 299 (1963)

10) M.J.Noone & J.P.Roberts, Nature 212 71 (1966)

11) I.Berman & C.E.Ryan, J. Crystal Growth 9 314 (1971)

12) A.Gatti, C.Mancuso, E.Feingold & R.Mehan, J. Phys. Chem. Solids, Suppl. No. 1 317 (1967)

13) W.R.Wilcox, J.R.Tevioldale & R.A.Corley, Trans. Met. Soc. A.I.M.E. 242 588 (1968)

14) T.Takahashi, K.Sugiyama & K.Tomita, J. Electrochem. Soc. 114 1230 (1967)

15) J.L.Chermant, Rev. Int. Hautes Tempér. et Réfract. 6 299 (1969)

16) A.V.Smith et al., "Index (Inorganic) to the Powder Diffraction File" A.S.T.M. Philadelphia (1968) Card No. 6-0614

17) L.V.Azároff, "Elements of X-ray Crystallography" McGraw-Booh Comp. New York p390 (1968)

18) R.L.Mehan & W.H.Sutton, AIAA Journal 4 1889 (1966)

19) M.L.Pearce & R.W.Marek, J. Am.Ceram. Soc. 51 84 (1968)

20) A.Münster & W.Ruppert, Z. Electrochemie 57 558 (1953)

21) W.K.Burton & N.Cabrera, Disc. Faraday Soc. 5 33 (1949)

22) N.Cabrera & D.A.Vermilyea, "Growth and Perfection of Crystals" John Wiley & Sons, Inc. New York p411 (1958)

CHAPTER   3

Formation of Titanium Carbide Filament

by Titanization of Carbon Filament

3.1   Introduction

Titanium carbide filaments have received an increasing attention in recent years as the reinforce components of refractory composite materials as stated in Section 1.4. It may be possible to fabricate a super-hard F.R. M. (fibre reinforced metal), considering the favorable wetting behaviors of titanium carbide for cobalt, molybdenum, etc. (1). The preparation of fibrous or filamentary form of titanium carbide, however, has rarely been reported in the past 40 years. In the early study by Burgurs et al. (2), the coating of titanium carbide on a carbon filament (about 100 μm in diameter) was performed in the van Arkel type atmosphere, where titanium tetrachloride vapor and hydrogen gas were introduced into a lamp reactor. The temperature of the heated carbon was estimated to reach 1,800°-2,100° C. Recently, fibrous titanium carbide with the length of 7-15 μm was obtained by Hertl (3) in a temperature range of 1,250° to 1,500° C

from TiO$_2$ and C. In Chapter 2, the author presented the
preparation method of titanium carbide whiskers or needles
by C.V.D. Nevertheless, it was rather difficult to ob-
tain whiskers or filaments of several microns in diameter
and several centimeters in length by the methods describ-
ed in Chapter 2. For example, the growth in length was
strictly limited in the single crystal growth of TiC,
because it was a complicated problem to control suffi-
ciently the temperature and the gas concentration at the
growth tip.

In this experiment, the titanization of thin carbon
filament was employed rather than the carburization of
titanium filament (4), considering the free energy of
formation. The purpose was to prepare a lot of titanium
carbide filaments at the same time as simply as possible.
Although the products are polycrystalline, this method
is worthy of note from a viewpoint of producing a thin
but long filament of interstitial carbides as well as
the discharge method (5) which will be described later
in Chapter 4. Titanization was performed in an atmos-
phere of titanium tetrachloride and hydrogen gases for
a sufficient reaction time, and the moderate condition
for the formation was investigated. An interesting phe-
nomenon was found by X-ray diffraction where the titani-
zation mechanism was studied in detail in relation to
the diffusion process of carbon in titanium carbide (6-
8).

3.2   Experimental
    The illustration of the experimental apparatus is
shown in Fig.3.1. The graphite tube (inside diameter:

22 mm), in which the carbon filaments or texture were inserted, was heated by induction coil in the temperature range of 1,200° to 1,550°C. The titanium tetrachloride vapor was produced by passing the chlorine gas carried by argon through the sponge titanium, which was heated at 400°-600°C in a nichrome resistance furnace attached to the reactor. The generated chloride vapor was introduced into the reaction zone of the graphite tube after being mixed with a dry hydrogen at the inlet of the horizontal quartz reactor (inside diameter: 34 mm). Similarly, the titanization of graphite was performed by setting a cylindrical graphite (15 mm in diameter) in the tube. The temperature of the specimens were measured by the photopyrometer through the observation window at the left side in Fig.3.1. The flow rates of chlorine, argon and hydrogen gases were determined by the flow meters; F_1 -F_3 at room temperature. Carbon filaments were obtained in the same reactor, where several kinds of organic filaments such as acetate, rayon, vinylon, nitron (P.A. N.), etc. were carbonized for 15 minutes to 4 hours in an inert atmosphere. The commercial graphite wool was used also as the starting material. The weight of specimen before or after every run was measured by the automatic balance and the weight increase was calculated. A sufficient precleaning of the reaction zone and the $TiCl_4$ generator with argon gas was essential in order to obtain the reproducible data. The obtained titanium carbide filament or texture was observed by the microscope and identified by X-ray diffractometer. The cross section of the embedded filaments or plates in epoxy resin, were abraded by emery papers or diamond paste. The profile of the titanized graphite plate was investigated
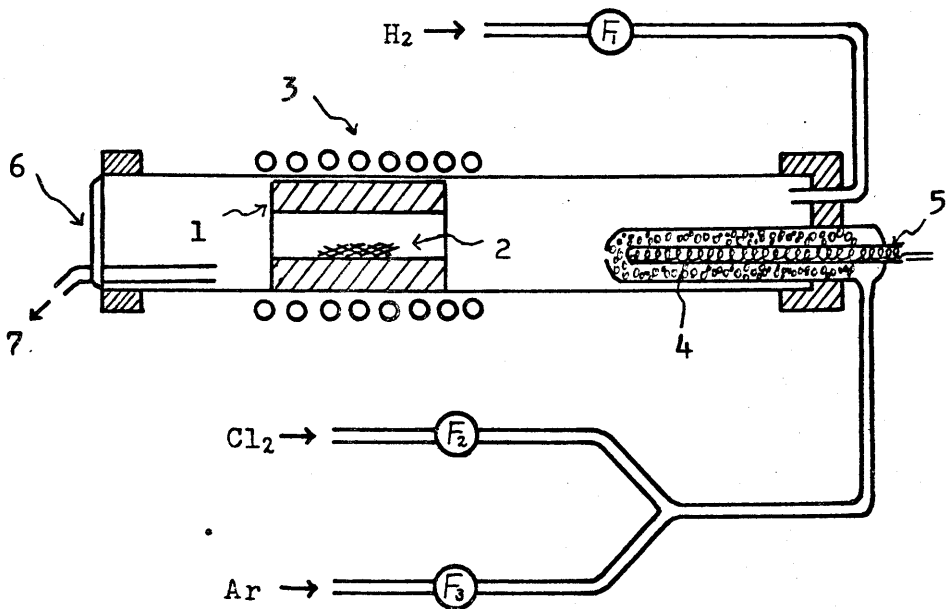
Fig.3.1 Schematic diagram of the experimental
         apparatus.

    (1) graphite tube (2) carbon filaments or
    texture (3) r.f. induction coil (4) sponge
    titanium (5) nichrome heater (6) observation
   window (7) outlet
    $F_1 - F_3$: flow meter

by X-ray microanalysis.

3.3   Results and Discussion
3.3.1   Moderate Condition for Titanization and Micro-
scopic Observation

The moderate condition for the formation of tita-
nium carbide filaments were studied as a function of tem-
perature, gaseous concentration and reaction time. The
moderate temperature range of titanization was between
1,200° and 1,550° C. The smooth and thin filaments were
obtained at a lower temperature, but the titanization
rate was remarkably low. On the other hand, carbon fil-
aments were titanized rapidly at a higher temperature,
accompanied by the deposition of polycrystalline grains
on the surface. Below 1,200° C, only the frailty of car-
bon filaments occurred without any visible titanization
product. It is found that the moderate temperature is
shifted to a higher temperature range than that of the
chemical vapor deposition of TiC (6), where the hydro-
carbon is used as a supplying agent for carbon. This
is supported by the thermodynamic study of Münster et
al. (9) on the vapor-solid reaction;

$$TiCl_4(g) + 2H_2 + C(s) \longrightarrow TiC + 4HCl,$$
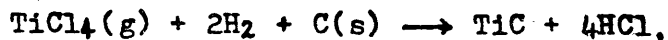
where $\Delta G^\circ = 44,000 - 33.5\,T$. The temperature range above
1,550° C was eliminated from the subject of the present
study in order to obtain the uniform filaments at the
temperature as low as possible.
The flow rates of hydrogen and argon turned out to have
minor influences on the formation of titanium carbide.
Relatively wide ranges of 2-4 ml/sec and 1.5-4.0 ml/sec
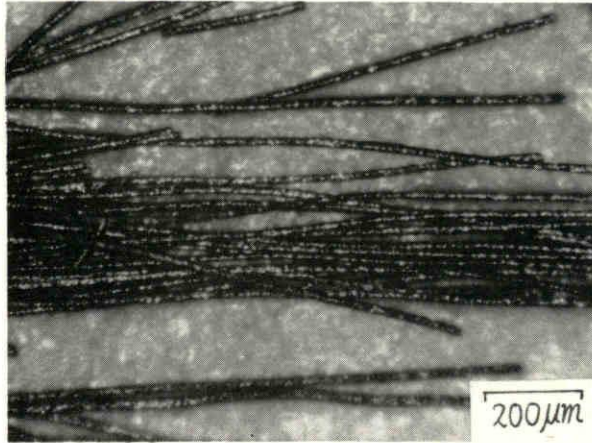were employed, respectively. The concentration of tita-

Fig.3.2 Micrograph of titanium carbide filaments.

(raw material: graphite wool in P.A.N. system)

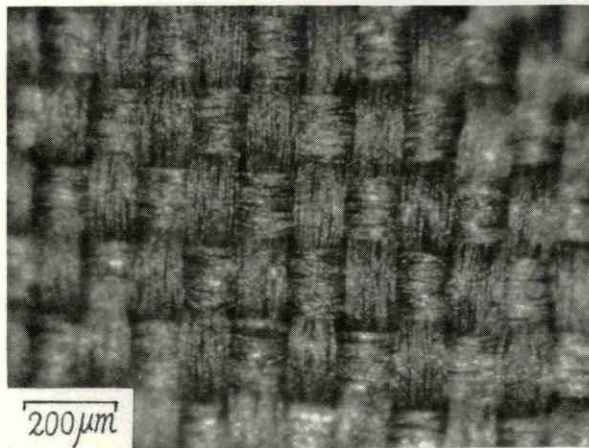Temperature: 1,420°C,   Reaction time: 30 min.

Fig.3.4 Micrograph of titanium carbide texture.

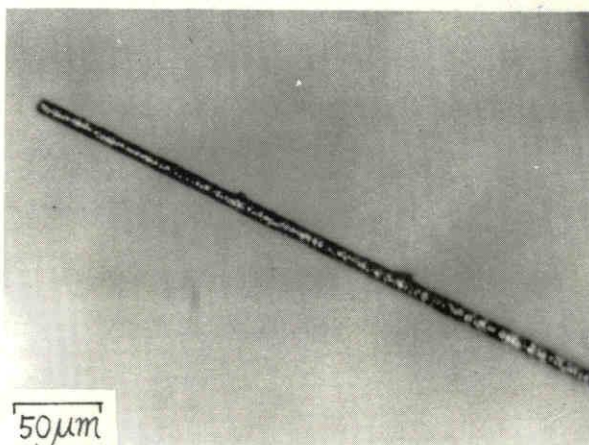(raw material: carbon texture in acetate system)

Temperature: 1,350°C,   Reaction time: 165 min.

nium tetrachloride vapor seemed so positively effective
on the titanization rate that a fairly high flow rate
range of 0.1 to 0.2 ml/sec (2-5 m/o) was used.

The carbon filaments adaptable for titanization are
those of acetate and acrylonitrile systems, which have
been recommended for industrial fabrication in relation
to carbon filaments in recent years (10). Fig.3.2 shows
the titanium carbide filaments obtained by titanization
of the commercial graphite wool (P.A.N. system) at 1,420
°C for 80 min. The flow rate of titanium tetrachloride
was 0.2 ml/sec (3.7 m/o). The diameters of filaments
were increased from the initial diameters of 13 μm to
about 16 μm. They become to have polycrystalline sur-
face with golden-yellow color as the titanization reac-
tion is proceeded. In Fig.3.3a, the titanized filaments
are shown, where after carbonizing the acetate filaments
in an argon atmosphere at 1,300°C for 15 min., the tita-
nization was performed under the following conditions;
temperature: 1,500°C, reaction time: 30 min., TiCl$_4$ flow
rate: 0.12 ml/sec (2.6 m/o), H$_2$ flow rate: 3.0 ml/sec
and Ar flow rate: 1.5 ml/sec. It is desirable for tita-
nization to use thinner carbon filament than 10 μm
in diameter as the raw material. An example of the ob-
tained single filament is shown in Fig.3.3b. Fig.3.4
shows a micrograph of the titanium carbide texture which
were obtained by titanization of acetate texture at 1,350
°C for 165 min. The weight of a texture decreased by
about 90 per cent during the carbonization, but the re-
sultant vacant spaces between the filaments were filled
progressively as the titanization was proceeded. The
flexibility of a texture decreased as its metallic luster
increased.

(a)

(b)

Fig.3.3   Micrograph of titanium carbide filaments

(a) and a single filament magnified (b).

Raw material: carbon filament in acetate system

Temperature: 1,420°C

Reaction time: 80 min.

3.3.2 Chemical Composition of Titanium Carbide Filament

<u>Weight increase</u>   Fig.3.5 shows the relation between the weight ratio Wr and the reaction time t on log-log scale, where Wr = (Weight of TiC_x texture) / (Weight of initial carbon texture) and t = 10-150 min. The carbon texture was obtained by the carbonization of an acetate texture at 1,300°C for 15 min. in an argon atmosphere. The gaseous flow rates in titanization were as follows; $TiCl_4$: 0.2 ml/sec (3.7 m/o), H_2: 2.0 ml/sec and Ar: 3.2 ml/sec. The weight ratios were plotted against the titanization temperatures of 1,490°, 1,420° and 1,350°C, and linear relations can be confirmed from Fig.3.5 obviously. It is suggested from the slope of about 0.5 in the figure that the rate determining step of the formation of titanium carbide is the diffusion process of carbon in it. If the titanium carbide filament has a homogeneous chemical composition, it is presumed that the stoichiometric $TiC_{1.0}$ (where Wr = 5.0) should be obtained for reaction time of 30 to 100 min. The slope remained to be constant, however, up to Wr ≒ 10, which suggested the formation of nonstoichiometric titanium carbide with an excess amount of titanium.

Fig.3.6 shows also the diagram of the weight ratio Wr vs. the reaction time t in log-log scale, where t = 40-900 min. The titanization conditions were as follows; temperature: 1,500°C and $TiCl_4$ flow rate: 0.12 ml /sec (2.6 m/o). It is found from Fig.3.6 that the weight ratio shows a linear increase up to Wr ≒ 9 like Fig.3.5, and then the slope decreases remarkably between Wr = 10-11. The saturated value of Wr = 11 is attained for the reaction time of 900 to 1,000 min. The chemical composition at Wr = 11 is nearly coincident with that on the
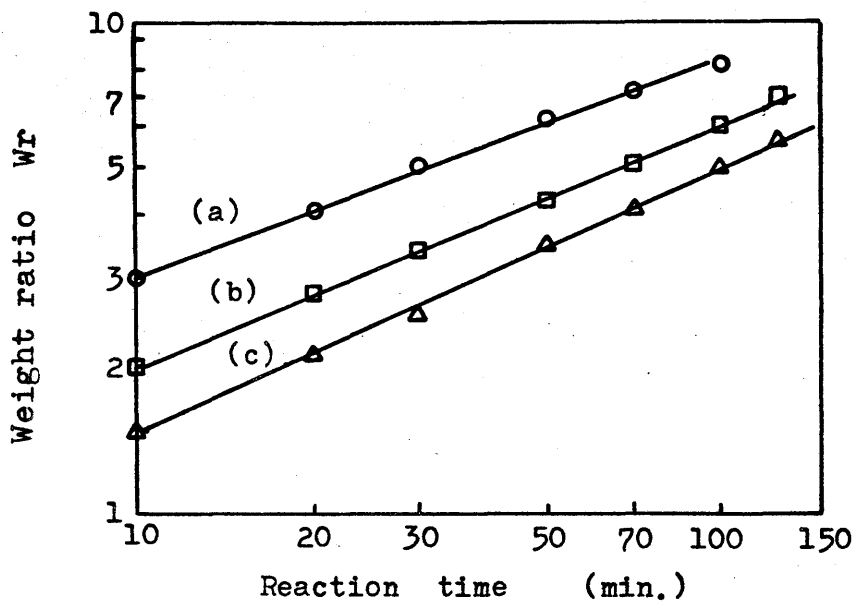
Fig.3.5 Weight ratio vs. reaction time. (10-150 min.)
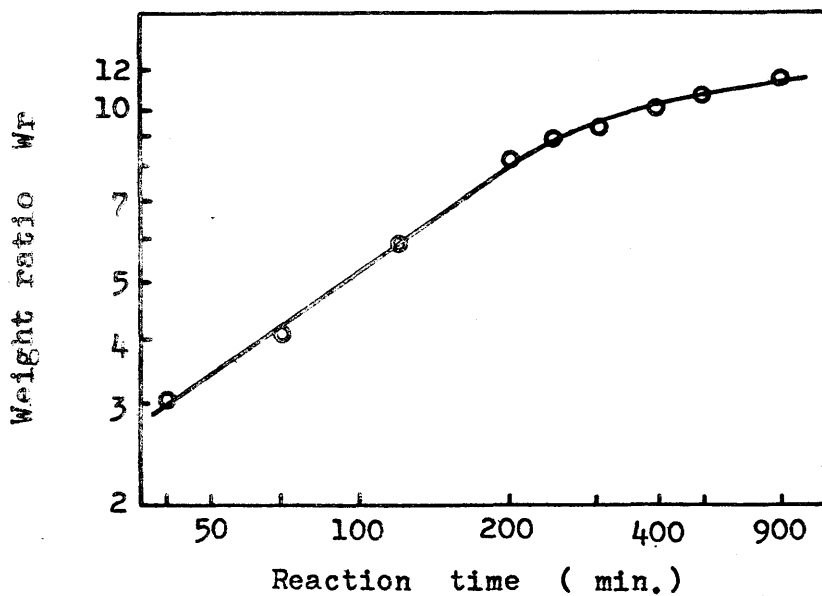
(a) 1,490° C (b) 1,420° C (c) 1,350° C

Fig.3.6 Weight ratio vs. reaction time. (40-900 min.)

Temperature: 1,500° C

solvus line in Ti-C phase diagram (see Fig.1.1) present
ed by Nielsen (11) or Bickerdike (12). Therefore, non-
stoichiometric composition, $TiC_{0.45}$ is formed, which shows
the maximum solubility of titanium (i.e. 10 carbon weight
per cent, $Wr = 10$). Probably, this was caused by the
excess concentration of titanium tetrachloride in the
vapor phase, for elemental titanium could not be detect-
ed at all by X-ray diffraction as is described later.
In the temperature range up to 1,700° C, the thermodynamic
data (9 & 13) suggest the less possibilities of formation
of metallic titanium;

$$TiCl_4(g) + 2H_2 \longrightarrow Ti(s) + 4HCl,$$

where $\Delta G° = 87,700 - 35.8\ T$.

<u>X-ray diffraction patterns</u>   Fig.3.7 shows X-ray dif-
fraction patterns of titanium carbide textures as a fun-
ction of the reaction time. The specimens were obtained
by titanization of the acetate texture at 1,420° C. It
is apparent from Fig.3.7 that at the initial stage of
titanization, the products can be identified with nearly
stoichiometric titanium carbide, though the peaks appear
at diffraction angles somewhat higher than those in A.S.
T.M. card (14). Further, another sub-peaks can be ob-
served at higher angles by 0.4-1.0° at the reaction time
of 30-60 min. Their intensities increase gradually in
advanced stages of the reaction (80-100 min.), while the
initial peaks drop down conversely. When the reaction
time exceeds 150 min., only the sub-peaks are confirmed.
This interesting behavior in X-ray diffraction shows that
the chemical compositions of the X-ray radiated surface
layers are differnt each other between the specimens of
(a) and (b) in Fig.3.7. The specimens of (b)-(e) in Fig.
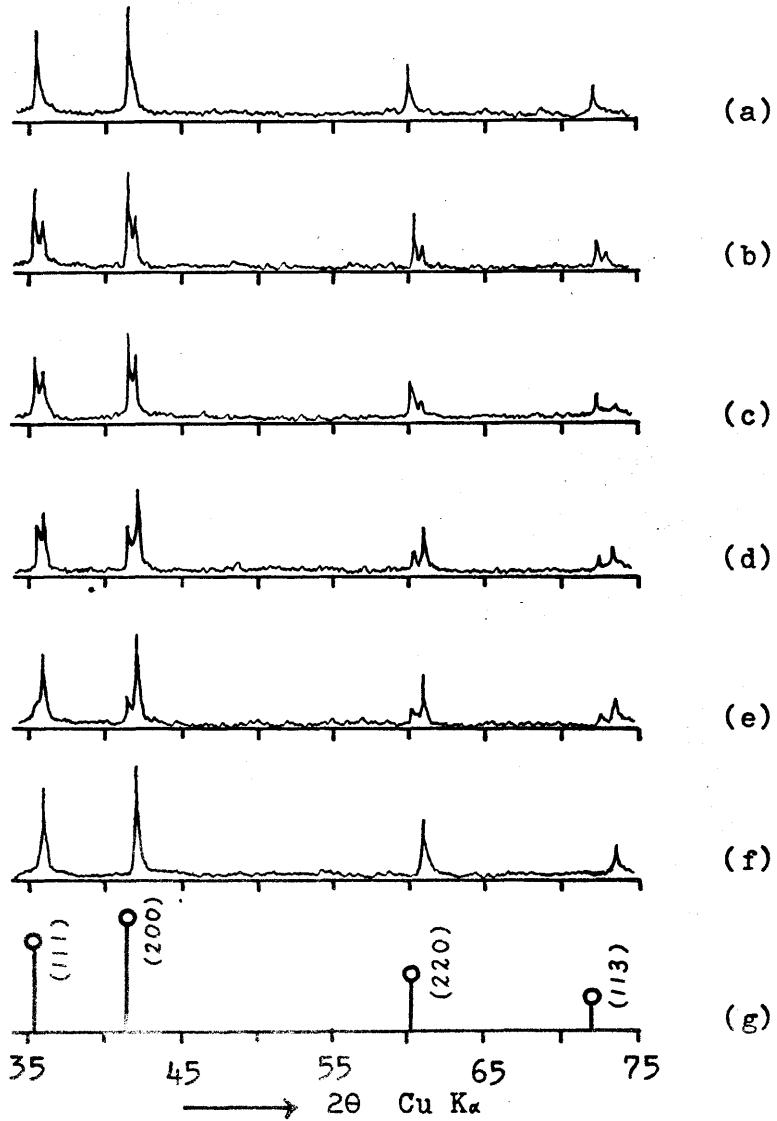3.7 are considered to represent the coexistence of the

Fig.3.7 Variation of the X-ray diffraction pattern
with reaction time. (specimen: TiC texture)
(a) 10 min. (b) 30 min. (c) 60 min. (d) 80 min.
(e) 100 min. (f) 150 min. (g) A.S.T.M. TiC

two different compositions. The lattice parameters of
the two carbides were calculated from the inter-planar
spacings of (200) as follows; $a_t = 4.31_2$Å at lower angle
(reaction time: 10 min.) and $a_t = 4.25_4$Å at higher angle
(reaction time: 150 min.). The former corresponds near-
ly to the parameter of the stoichiometric $TiC_{1.0}$, which
has not been determined precisely, however, in the refer-
ences (15 & 16). The latter is a considerably small val-
ue compared with the results of Ehrlich (15), who inves-
tigated the correlation between the lattice parameter
and nonstoichiometry of sintered titanium carbide. The
higher lattice parameter of 4.29 Å can be expected from
his result if $TiC_{0.45}$ is formed. This contradicts the pre-
sent experimental results apparently, the reason of which
is not distinct as the methods of preparation or measur-
ment are differnt. Anyhow, it would be concluded that
nonstoichiometric $TiC_{0.45}$ is coincident with the titanium
carbide with high density which reveals the sub-peaks in
Fig.3.7.

3.3.3   Titanization Mechanism of Carbon Filament:
<u>Titanization of graphite plate</u>   It is an important
problem to discuss the titanization mechanism of the fil-
ament, that is, to determine whether such an unfamiliar
phenomenon of the X-ray behavior is proper to the tita-
nization of "filaments" or is common to this sort of
"vapor-solid reaction". This sub-section 3.3.3 is con-
cerned with the chemical composition of titanized gra-
phite plates which are obtained in the same atmosphere
and temperature ranges as described previously in 3.3.2.
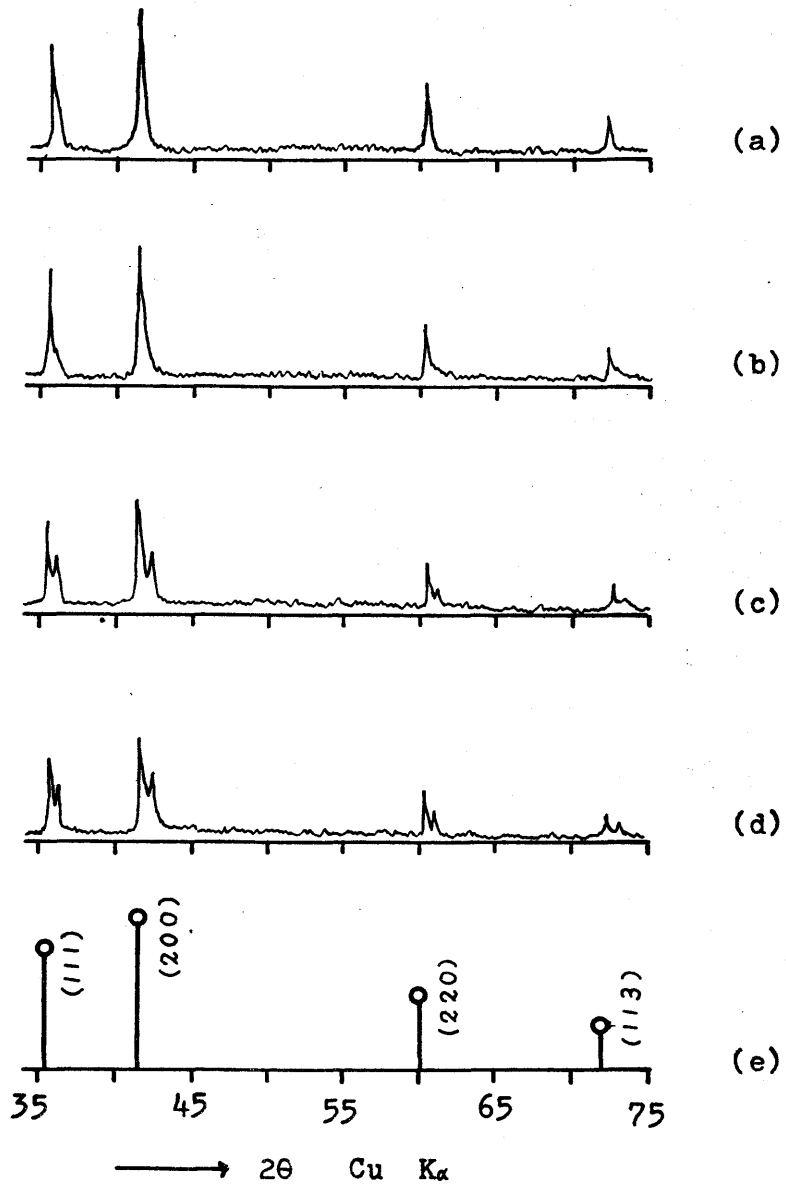The variations of X-ray patterns analogous to Fig.3.7

Fig.3.8 Variation of the X-ray diffraction pattern
with reaction time. (specimen: titanized plate)
(a) 10 min. (b) 30 min. (c) 70 min. (d) 120 min.
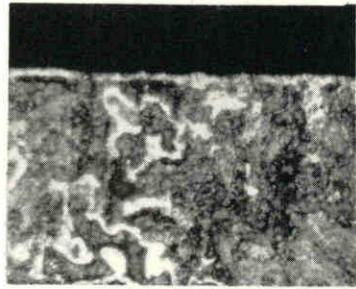(e) A.S.T.M. TiC

were confirmed in Fig.3.8, when the graphite plates were titanized at 1,450°C at the following flow rates of $TiCl_4$ and Ar, respectively; 4.0 ml/sec and 0.8 ml/sec. A comparatively slow titanization rate is due to a smaller diffusibility of carbon. Fig.3.9 shows the cross sectional micrograph of the same specimens. It is found that the thickness of the surface layer of titanium carbide increases from about 1.5 μm for the reaction time of 10 min. up to about 6.3 μm for that of 120 min. The tight layers with metallic luster, which seem to have the identical composition with the surface layer, can be observed on the grain boundaries of the bulk region in graphite plate. It is suggested, therefore, that the titanium tetrachloride vapor is easy to diffuse into the grain boundaries through the pores of the surface.

Fig.3.10 shows the variations of X-ray diffraction patterns by abrading the surface layer of the specimen shown in Fig.3.8d (reaction time: 120 min.). It is apparent that the sub-peaks at higher angles disappear gradually as the thickness of the abraded layer D is increased. When $D \gtrsim 6.3$ μm, the stoichiometric titanium carbide mixed with a small amount of graphite were identified. The intensities of the graphite peaks increased in the bulk region ($D \simeq 8$ μm). It is considered that the sub-peaks are coincident with those of tight surface layer of titanium carbide, while the stoichiometric titanium carbide lies on the boundary between the tight surface layer and the bulk region of the graphite plate.
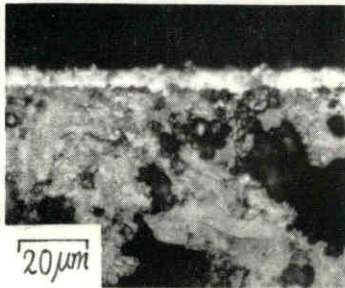
Fig.3.11 shows the result of X-ray microanalysis of the cross section of the two specimens of (a) and (d) in Fig.3.9. The intensity curves of titanium and carbon are drawn as a function of the distance from the surface.
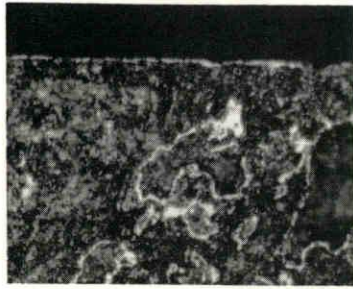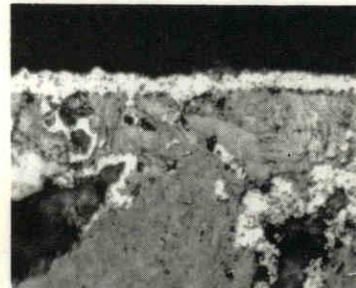
(a)

(b)

(c)

(d)

Fig.3.9   Micrograph of the cross section of tita-

nized graphite plate. (temperature: 1,450°C)

Reaction time;

    (a)   10 min.

    (b)   30 min.

    (c)   70 min.
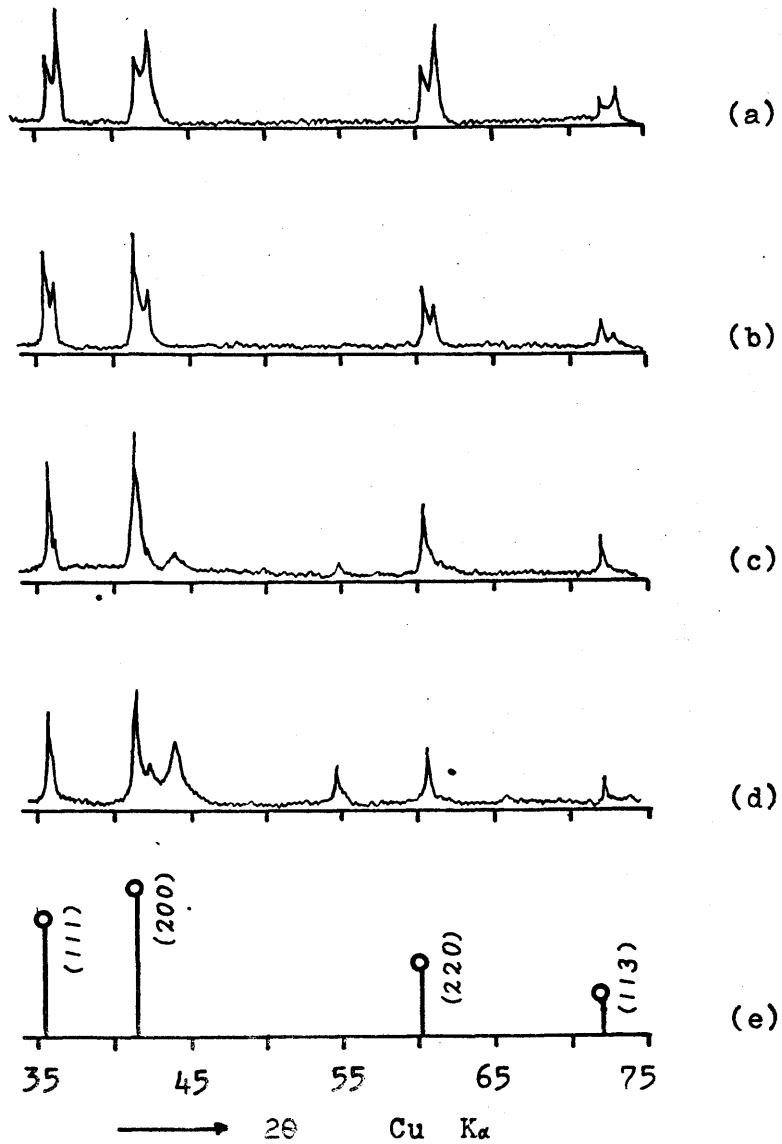
    (d)   120 min.

Fig.3.10 Variation of the X-ray diffraction pattern
of the abraded plate.

(a) D = 0 (b) D ≲ 6.3 μm (c) D ≳ 6.3 um

(d) D ≃ 8 μm (e) A.S.T.M. TiC
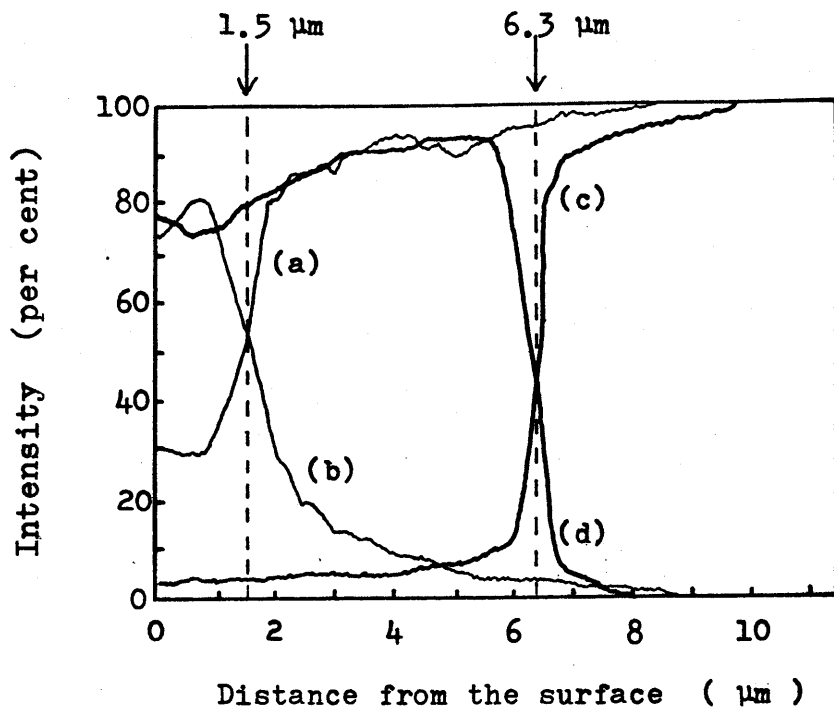
Fig.3.11 Diffusion profile obtained by X-ray
microanalysis of the titanized plate.

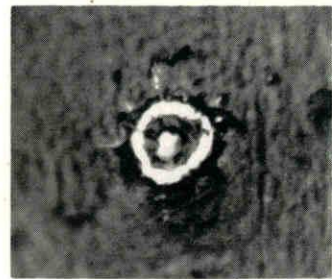| Element	Reaction time	
	10 min.	120 min.
Carbon	(a)	(c)
Titanium	(b)	(d)

Specimen: (a) and (b) in Fig.3.9

The heavy gradients of the titanium and carbon concentrations can be seen at the distance of 6.3 μm, which corresponds to the boundary between the surface layer and the bulk as can be observed in Fig.3.9. The disappearance of the sub-peaks in Fig.3.10c may be attributed to the remarkable decrease of titanium concentration at the boundary. The tight surface layer can be thought from the invariable slope to have a homogenous chemical composition which was previously assumed to be $TiC_{0.45}$. On the other hand, the variation of the both concentrations at the boundary are comparatively gentle for the specimen obtained at a reaction time of 10 min. There remains an appreciable amount of carbon in the surface layer, which can correspond to the absence of the sub-peaks in Fig.3.8a.

<u>Titanization mechanism</u>   It is found from the titanization of graphite plates described above, that the separation of the peaks of titanium carbide is caused by the marked variations of titanium and carbon concentrations. This can be applied to the growth mechanism of titanized filaments, if one notices the analogy of Figs. 3.7 & 3.8. The polished cross sections of titanium carbide filaments are shown in Fig.3.12 as a function of the reaction time. Apparently, the diameter of a filament increases progressively with the lapse of the reaction time in the following order; 7 μm (10 min.) → 10 μm (30 min.) → 11 μm (70 min.) → 13 μm (120 min.) → 24 μm (420 min.). The dense layer with metallic luster, which may have the composition of $TiC_{0.45}$, increases in thickness in the peripheral portion of the cross section (b)-(d), as expected from the titanization of graphite plates. The dense layer, however, can not be seen at a reaction
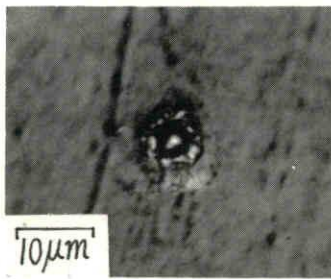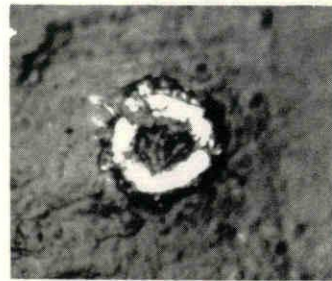
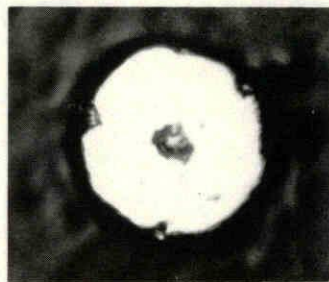Fig.3.12 Micrograph of the cross section of tita-

nium carbide filament.

Reaction time; (a) 10 min., (b) 30 min.,

(c) 70 min., (d) 120 min., (e) 420 min.

time of 10 min., in contrast to the case that almost all the parts consist of the dense titanium carbide at a reaction time of 420 min. Likeweise in Fig.3.9, these behaviors corresponds to the X-ray diffraction patterns in Fig.3.7, i.e. the black portions at the center are composed of amorphous carbon and stoichiometric $TiC_{1.0}$, the intensity of which decreases due to the formation of outer layer $TiC_{0.45}$.

Hence, it is advantageous to describe the two steps for the formation of titanium carbide layers. At the initial stage of the reaction, the gaseous diffusion of the titanium tetrachloride vapor into the carbon filament will permit the titanization which is proceeded for a short time by the surface reaction at grain boundaries;

$$TiCl_4(g) + 2H_2 + C(s) \longrightarrow TiC(s) + 4HCl.$$
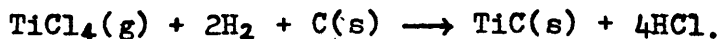
As a result, the stoichiometric $TiC_{1.0}$ and the remaining amorphous carbon are mixed in the central portion of the filament. Before the filament is titanized completely, the dense titanium carbide $TiC_{0.45}$ begins to form on the surface due to an excess titanium chloride vapor and then the gaseous diffusion into the grains is interrupted. In a sufficient reaction time, the solid diffusion of residual carbon atoms into the dense titanium carbide layer is prevailed. Consequently, the outer layer increased in thickness until the filament is saturated with $TiC_{0.45}$. Such schematic models in the diffusion process are illustrated in Fig.3.13.

There arise still fundamental questions, however, for the above discussions why the chemical composition does not vary continuously from $TiC_{1.0}$ to $TiC_{0.45}$ in the diffusion profile and whether the two distinct peaks in X-ray diffraction patterns predict the existence of two

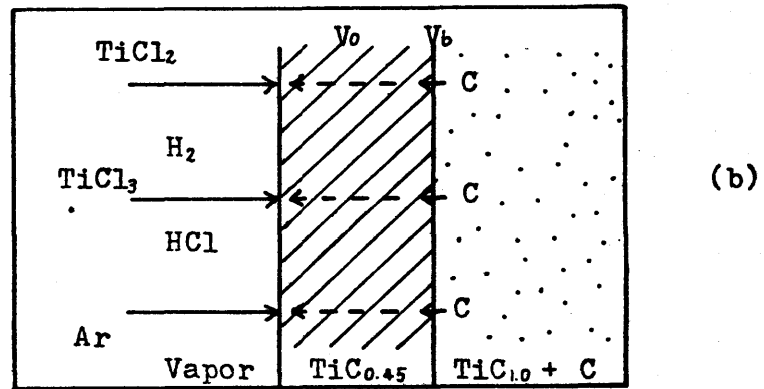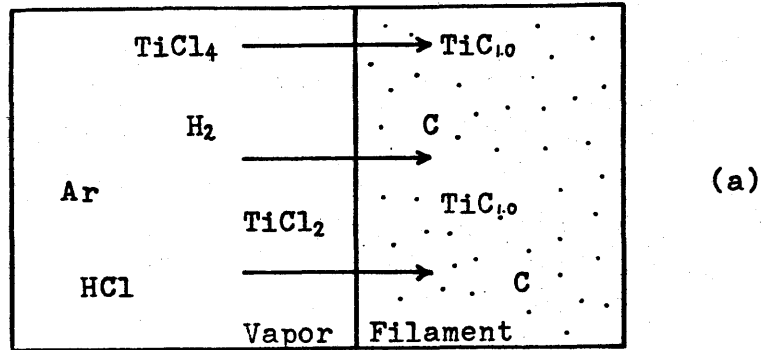Fig.3.13 Schematic model of the diffusion process.

(a) The initial stage for a short reaction time,
     when the gaseous diffusion of titanium chloride
     prevails to form $TiC_{1.0}$ by surface reaction.

(b) The latter stage for a sufficient reaction time,
     when the solid diffusion of carbon atom into
     the tight $TiC_{0.45}$ layer prevails.

     Diffusion velocity: $Vb \ll Vo$

stable compounds or not. These seems to be justified apparently, even though no report on the compound $TiC_{0.45}$ has been published, but only the phase diagram with a wide range of the solubility of carbon has been reported, as described in Section 1.1. Since the rate determining step of formation is not the chemical reaction, but the diffusion process, as shown in Section 3.3.2, it may be possible to explain the process without the assumption of a new compound $TiC_{0.45}$. As pointed out by Sarian or others (6-8), the transport species in the diffusion process are presumed to be carbon atoms, while the titanium sub-lattice is fixed in the crystal. Considering the diffusion profile in Fig.3.11, the net determining step is found to be the diffusion process of carbon at the boundary regions, where the diffusion velocity of carbon V_b is much smaller than that in the outer layer V_o. The thickness of boundary layer is so small not to be detected by X-ray analysis that the separation of the peaks can be occurred. Although it is not clear why the diffusion velocities are different between two regions, it would be explained by more detailed investigations.

3.4   Conclusion

The titanium carbide filaments with diameters of 5-20 μm were prepared by titanization of carbon filament in the atmosphere of titanium tetrachloride, hydrogen and argon gases. The carbon filaments were obtained by carbonization of organic filaments or textures such as acetate or acrylonitril. The titanization was performed for 10-700 min. in the temperature range of 1,200° to 1,550° C. The moderate gaseous concentrations were as follows; $TiCl_4$: 0.1-0.2 ml/sec (2-5 m/o), H_2: 2-4 ml/sec and Ar: 1.5-4.0 ml/sec. The inflexible but tight fila-

ment with metallic luster was obtained at a reaction time
of more than 60 min. Linear relations with the slope of
0.5 could be confirmed on log-log scale between the weight
increase and the reaction time. The saturated weight
ratio for titanization, $Wr = 11$ was found equal to the
chemical composition $TiC_{0.45}$ on the solvus line in Ti-C
phase diagram. The X-ray diffraction patterns showed
some sub-peaks at the higher angles than the peaks of the
stoichiometric titanium carbide. The sub-peaks increased
in their intensities with the lapse of a reaction time
and the lattice parameter was found to be $a_t = 4.25_4 \text{Å}$.
The identical behaviors were observed also in the tita-
nization of the graphite plate. It was found from X-ray
microanalysis of the cross section of the titanized plate
that the inner layer of the plate consisted of nearly
stoichiometric titanium carbide and graphite, while the
outer layer contained excess titanium and its chemical
composition was $TiC_{0.45}$ probably. The observation of the
titanium carbide double layers of the filaments suggest-
ed that the inner layer was produced by the surface re-
action on the carbon grain boundaries and it was follow-
ed by the formation of the outer layer. The net rate
determining step of the carbide formation was considered
to be the diffusion process of elemental carbon at the
boundary region between the surface layer and the bulk
region. The formation of double layers with different
composition is not described in the report by Амбарцуман
(17), who studied the analogous vapor-solid reaction of
titanium carbide. However, such an interesting phenom-
enon as has been found in the present study seems to
occur conspicuously at a high concentration of titanium
tetrachloride in the vapor.

REFERENCES

1) N.M.Parikh & M.Humenik, J. Am. Ceram. Soc. 40 315 (1957)

2) W.G.Burgers & J.C.M.Basart, Z. anorg. allgem. Chem. 216 209 (1934)

3) W.Hertl, J. Am. Ceram. Soc. 50 630 (1967)

4) F.H.Pollard & P.Woodward, Trans. Faraday Soc. 46 190 (1950)

5) K.Sugiyama & T.Takahashi, Kogyo Kagaku Zasshi 73 2105 (1970)

6) T.Takahashi, K.Sugiyama & K.Tomita, J. Electrochem. Soc. 114 1230 (1967)

7) S.Sarian, J. Appl. Phys. 39 3305 (1968)

8) S.Sarian, J. Appl. Pyys. 39 5036 (1968)

9) A.Münster & W.Ruppert, Z. Elektrochemie 57 558 (1953)

10) A.Shindo, Yogyo Kyokai-Shi 69 C195 (1961)

11) J.P.Nielsen, J. Mitals 5 248 (1953)

12) R.L.Bickerdike, G.Hughs, in E.R.Stoner & J.Wurff, A.I.M.E. Trans. 251 127 (1959)

13) M.L.Pearce & R.W.Marek, J. Am. Ceram. Soc. 51 84 (1968)

14) A.V.Smith et al. "Index (Inorganic) to the Powder Diffraction File" A.S.T.M. Philadelphia (1968). Card No. 6-0164

15) P.Ehrlich, Z. anorg. allgem. Chem. 259 1 (1949)

16) R.Kirk & D.Othmer, "Encyclopedia Chem. Tech." John Wiley & Sons, Inc. New York Vol.29 p415 (1969)

17) Р.С.Амбарцумян и Б.Н.Бабин, Изв. Акад. Наук СССР Неорг. Матер. 5 301(1969)

CHAPTER 4

Fibrous Growth of Tungsten and Molybdenum

Carbides by Discharge Method

4.1 Introduction

Fibrous carbides of tungsten and molybdenum have
the possibilities of applications not only to the rein-
forced composites, but also to the thermo-electrical and
thermionic emissive materials in higher temprature range.
The chemical vapor deposition of carbides of VIa group
metals has been studied for a long time as stated in Sec-
tion 1.2. In the most cases, however, the direct car-
burization of metallic sheet has been employed in an at-
mosphere composed of hydrogen and hydrocarbon. There
are a few reports on the fibrous growth of carbide, even
though the techniques of the protective coating with car-
bides has been made progress to some extent (for example,
1.& 2).

On the other hand, the fibrous growth of intersti-
tial compounds, such as TiB_2 (3), TiN (4), ZrB_2 (5), ZrC
(6) and TaC (7), has been reported recently in the au-

thor's laboratory. It was found in those studies that
the thin fibres with the length of several centimeters
could be obtained by A.C. arc-discharge method (thermo-
electron emissive type). The growth was performed under
the discharge current of 0.2 to 5.0 mA, where the dis-
charge electrodes were pulled apart manually, keeping
the inter-electrode distance constant.

In the present chapter, the fibrous growth of car-
bides of tungsten and molybdenum was investigated by dis-
charge method under the similar conditions to those de-
scribed above. The atmosphere was composed of hydrogen,
argon, hydrocarbon and metal chloride and a new mechan-
ical pulling apparatus was used to obtain a constant
growth rate. The purpose was to prepare the long but
thin fibres as rapidly as possible. The influences of
various factors on fibrous growth were studied in detail
and the optimum growth condition was determined. Struc-
tures and properties of the products are presented in the
latter half of the chapter.

4.2   Experimental
Fig.4.1 shows the illustration of the experimental
apparatus. The discharge growth was performed in a ver-
tical quartz reactor with the inside diameter of 23 mm.
The reactor was heated at 200° to 600° C by the external
nichrome heater. The upper half was composed of a double
tube. Chlorine and argon gases were introduced into the
outer tube, in which the coil pieces of tungsten wire
(0.2 mm in diameter) or molybdenum wire (0.5 mm in diam-
eter) were filled up. Tungsten hexachloride or molybde-
num pentachloride was generated stationarily from the
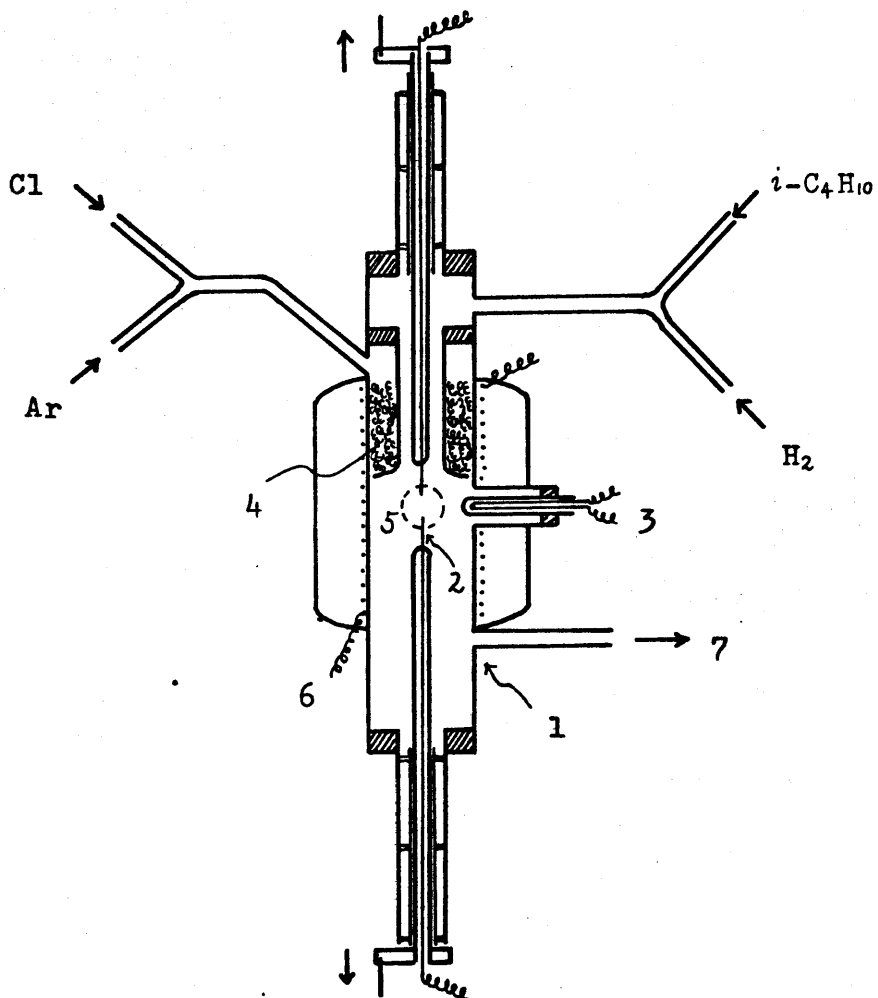
Fig.4.1 Schematic diagram of the experimental
apparatus.

(1) quartz reactor (2) molybdenum discharge
electrode (3) thermo-couple (4) coil pieces
of W or Mo (5) observation window (6) ni-
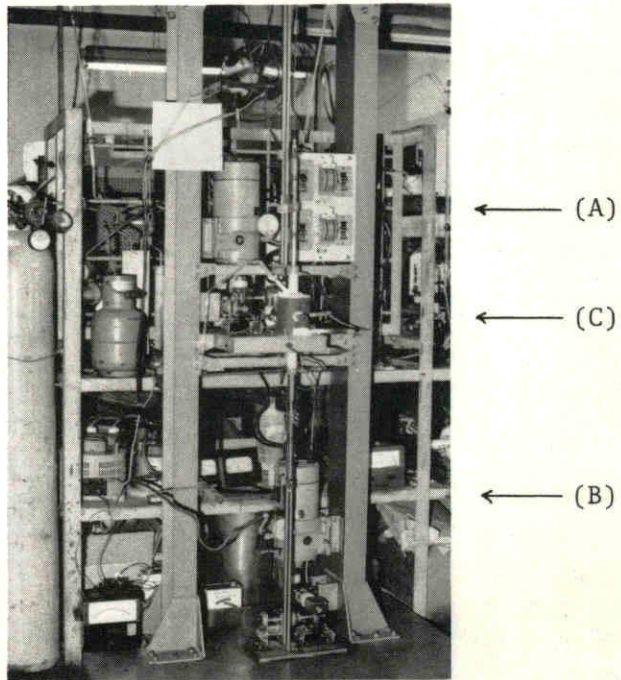chrome heater (7) outlet

Fig.4.2   Experimental apparatus for discharge

growth with the two electrodes pulled by

speed motors; (A) & (B).

(C) : Reactor illustrated in Fig.4.1.

bottom of the outer tube above 300°C. A mixture of hydrogen and iso-butane was passed into the inner tube (16 mm in diameter) and mixed with metal chloride and argon in the reaction zone. Argon gas was deoxygenated beforehand, passing it over the heated titanium sponge to prevent the formation of oxychloride ($WOCl_4$ or $MoOCl_3$) in the reaction tube (8). Hydrogen gas was also deoxygenated by heated copper. $i\text{-}C_4H_{10}$ was employed as the supplying source for carbon considering the availability for the reaction (see Section 1.2). A.C. voltage with a discharge frequency of 60 Hz was applied to the electrodes which were connected to a high voltage transformer. Molybdenum wire of 0.1 mm in diameter was used as the electrode material at the growth tip and it was connected to the A.C. source via the nickel wire sealed in the syringe quartz tube. Two electrodes were moved up and down by means of the speed motor (see Fig.4.2). As a result, it was possible to move the electrodes at a constant pulling rate in the range of 2 to 30 mm/min. The atmospheric temperature was measured by the thermo-couple which was inserted into the reaction zone. The sparkling tips of fibres were observed through the glass window. The flow rates of Cl_2, Ar, $i\text{-}C_4H_{10}$ and H_2 were measured by the flow meters at room temperature. The grown fibres were separated from the electrodes and washed with a hot HNO_3 : HCl (3 : 1) solution. After being dried, they were observed through the microscope and identified by X-ray diffractometer. The fracture strength was determined using the nichrome spring.

4.3   Results and Discussion

4.3.1   Moderate Conditions for Fibrous Growth

It is supposed that various factors such as dis-
charge current, reactor temperature and gas flow rates
affect the discharge growth of fibres.   In the present
sub-section, the effects of these factors on the thick-
ness or the discharge stability were investigated in de-
tail in order to obtain favorable fibres which filfill
the purpose of this study.   Preliminary experiments show-
ed that the fibres could be prepared roughly under the
following conditions;   discharge current: 0.5-4.0 mA,
reactor temperature: 300°-600°C, growth rate: 4-12 mm/
min, i-C_4H_{10} flow rate: 0.05-0.25 ml/sec, Cl_2 flow rate:
0.02-0.18 ml/sec and the flow rate ratio of H_2/Ar: 0.4-
1.6.   These were used as the initial condition for more
detailed experiments as described below.

Effect of discharge current   Fig.4.3 shows the effect
of discharge current (1.0-4.5 mA) on the diameter of the
tungsten carbide fibre.   It is found from the figure that
the diameter is proportional to the discharge current.
Fine fibres of about 20 μm in diameter were obtained at
the current as low as 2.5 mA when they were grown at a
growth rate higher than 9 mm/min.   Below 2.5 mA, however,
it was difficult to keep a constant discharge current,
so the uniform and long fibres could not be obtained.
The moderate current of 2.5-3.0 mA is found to be a con-
siderably high value compared with that (0.2-1.5 mA) for
the fibrous growth of TiB_2 (3) or ZrC (6).   This may be
caused by the following reasons: i) Tungsten carbide has
a smaller thermo-electronic emissivity than that of car-
bide or boride of 1Va group metals (9),   ii) The heat
efficiency at the growth tip is low, since a large amount
of thermal conductive hydrogen gas is required in the
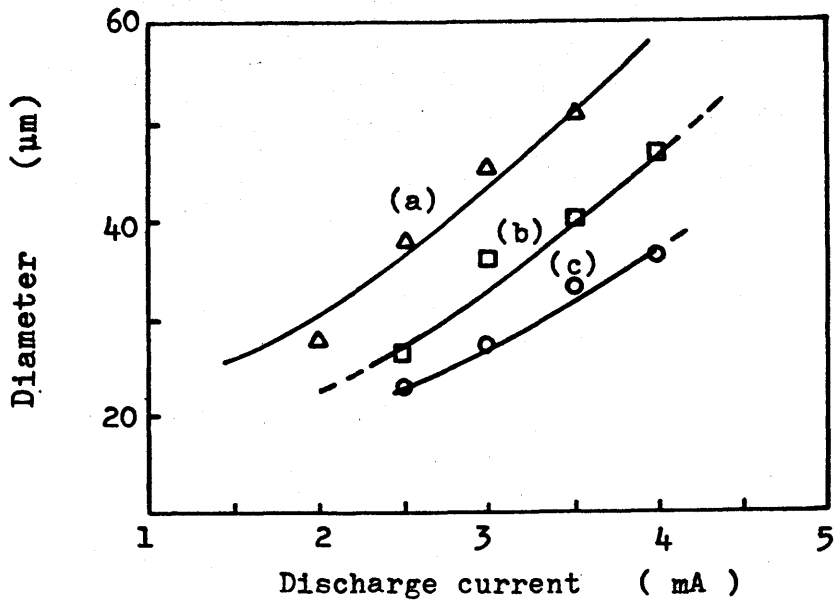
Fig.4.3   Discharge current vs. diameter.   (tungsten
          carbide)   (a) 5 mm/min   (b) 7 mm/min
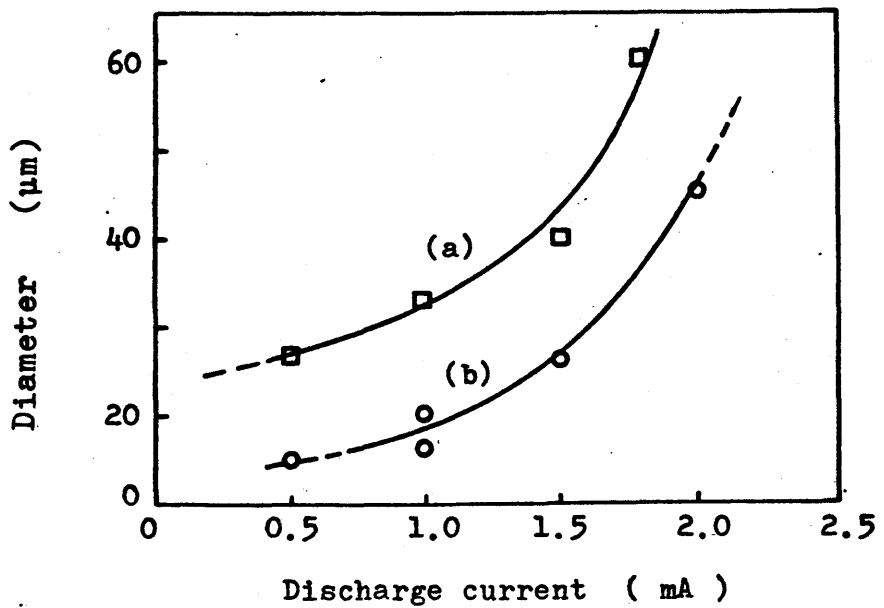   (c) 9 mm/min

Fig.4.4   Discharge current vs. diameter.   (molybdenum
          carbide)   (a) 6 mm/min   (b) 8 mm/min

present experiment as described later. On the other hand, the thick and dendritic deposits were obtained above the discharge current of 4.0 mA, when the crystal was grown from the molten state at higher than 2,600° C. Thus the temperature at the growth tip was dependent so much on the discharge current that the remarkable effect on the diameter or the growth rate resulted.

Fig.4.4 shows the relation between the discharge current and the diameter of molybdenum carbide fibre at the growth rates of 6 to 8 mm/min. The favorable range of discharge current is relatively wide and shifted to the lower values than those of tungsten carbide. The thin fibres with the diameter of 15 µm could be grown at the current of 0.5 mA and at the growth rate of 8 mm/min, although the discharge condition was unstable. Therefore, the moderate discharge current of 0.8 to 1.5 mA was required to obtain the uniform fibres with the length of more than 4 cm.

Effect of reactor temperature   The effect of the reactor temperature on the diameter of the fibre is shown in Fig.4.5, where the influence of the temperature at the growth tip on the reactor temperature can be neglected. Apparently, the minimum diameters of 25 µm and 15 µm can be seen at the reactor temperature of 480° C and 360° C for the growth of tungsten and molybdenum carbides, respec÷ tively. The moderate temperature is considered to occur due to the competing effect among the following factors; i) to produce gaseous metal chloride continuously without the deposition of solid lower chloride, ii) to produce the pyrocarbon sufficiently by the thermal decomposition of hydrocarbon, iii) to keep the local temperature region high at the growth tip. In the case of
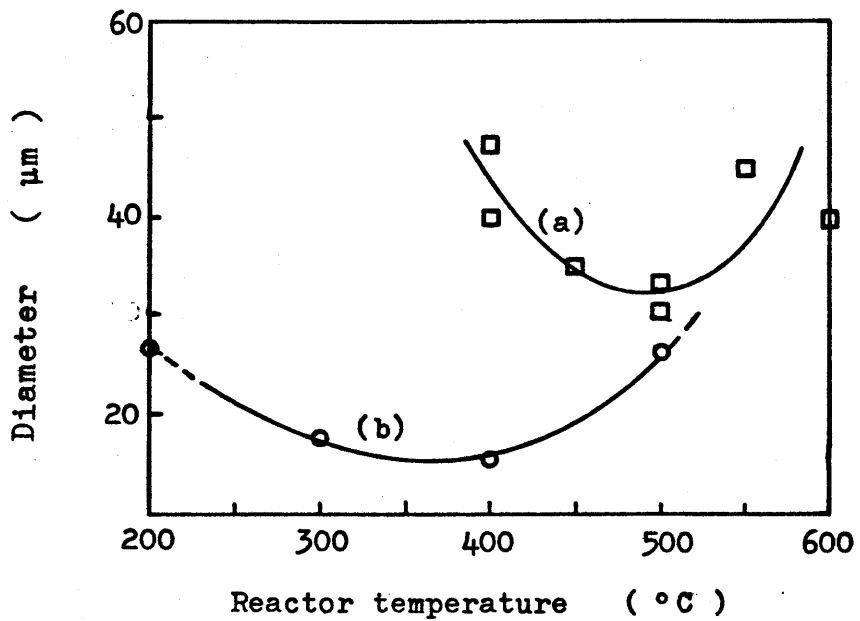
Fig.4.5 Reactor temperature vs. diameter

  (a) Tungsten carbide (discharge current: 2.5 mA)

  (b) Molybdenum carbide (discharge current: 1.0 mA)

tungsten carbide, the diameter increased below 400° C with the adhered lower chloride on the lateral face and the discharge current became unstable for the lack of hexa-chloride vapor, while the deposition of amorphous carbon resulted in the increased diameter above 550° C. The thin molybdenum carbide fibre with the diameter of 18 to 20 μm could be prepared in the wide temperature range of 300° to 450° C. Below 200° C, however, both the chlorina-tion of metal and the decomposition of i-C_4H_{10} were not proceeded enough, and above 500° C the fibrous growth was prevented by the formation of excess hydrogen chloride.

Effect of growth rate   Figs.4.6 & 4.7 show the cor-relation between the growth rate and the diameter of tung-sten and molybdenum carbides, respectively. It is found that the diameter decreased with the increase of growth rate in both cases. This is coincident with the fact that a negative correlation between the diameter and the growth rate was confirmed when the electrodes were pulled manually in the preparation of TiB_2 (3), etc. Such cor-relations suggest that a nearly constant deposition rate of the fibre prevails at a given discharge current. The uniform tungsten carbide fibre of 25 μm in diameter was obtained at the growth rate of 7 to 9 mm/min, as shown in Fig.4.6. But, the discharge became easy to be inter-rupted at more than 10 mm/min due to the increase of inter-electrode distance, where the axial growth could not fol-low the movement of the electrode. In Fig.4.7, the max-imum growth rate is found to decrease at the discharge current less than 1.0 mA. In the growth rate range of 4 to 6 mm/min, thick fibres were obtained easily with the deposits composed of amorphous carbon and lower chlo-rides on the surface.
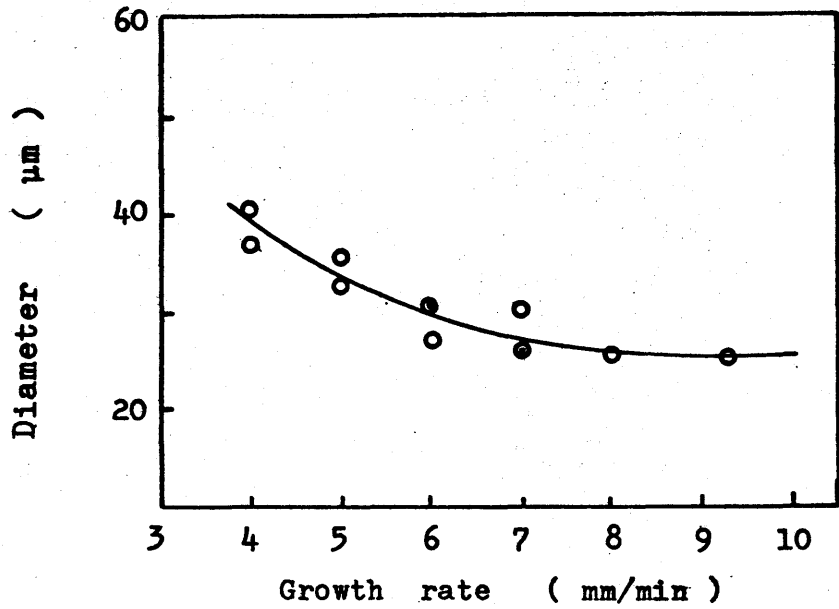
Fig.4.6 Growth rate vs. diameter. (tungsten carbide)
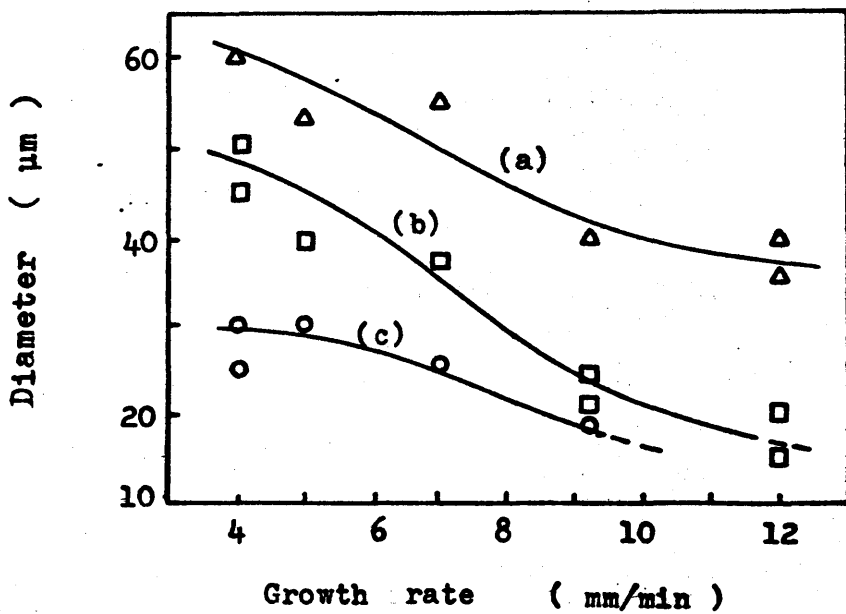
Temperature: 450° C   Discharge current: 2 mA

Fig.4.7 Growth rate vs. diameter. (molybdenum carbide)

400° C, (a) 2.0 mA (b) 1.0 mA (c) 0.5 mA

<u>Effect of gaseous composition</u>   The influence of gas-
eous concentration on the fibrous growth was investigat-
ed, where the flow rates of i-C_4H_{10} and Cl_2 affect the
chemical reaction of the carbide formation, while those
of H_2 and Ar affect mainly the stability of arc-discharge.

Fig.4.8 shows the diagram of the i-C_4H_{10} flow rate
vs. the diameter. The flow rate of i-C_4H_{10} had a minor
influence on the diameter of tungsten carbide, but a rel-
atively narrow flow rate range of 0.1 to 0.2 ml/sec was
required to stabilize the discharge growth. The black
and uneven fibre was obtained at the flow rate greater
than 0.2 ml/sec (5.3 m/o) probably because of the com-
petitive deposition reaction between carbide and amor-
phous carbon. Continuous fibrous growth was strictly
limited at the flow rate less than 0.1 ml/sec. The di-
lution of pyrocarbon in a gas mixture (10) can be attri-
buted to the production of a large amount of hydrogen
chloride vapor by the following reaction:

$$8WCl_6 + i\text{-}C_4H_{10} + 19H \longrightarrow 4W_2C + 48HCl,$$
$$8MoCl_5 + i\text{-}C_4H_{10} + 15H \longrightarrow 4Mo_2C + 40HCl.$$

For the formation of molybdenum carbide, the availability
of i-C_4H_{10} is calculated to be about a tenth as small as
that of molybdenum pentachloride.

Fig.4.9 shows the effect of the chlorine gas flow
rate. It is found from the figure that the chloride con-
centration is almost independent of the discharge stabil-
ity. The moderate flow rate for molybdenum chloride (0.15
ml/sec) is appreciably higher than that for tungsten chlo-
ride (0.06 ml/sec). This will be explained in the follow-
ing way. As suggested from the study of Saeki et al.
(11 & 12), $MoCl_{2.9\sim3.3}$ in solid state is deposited on the
reactor wall by the disproportionation reaction;
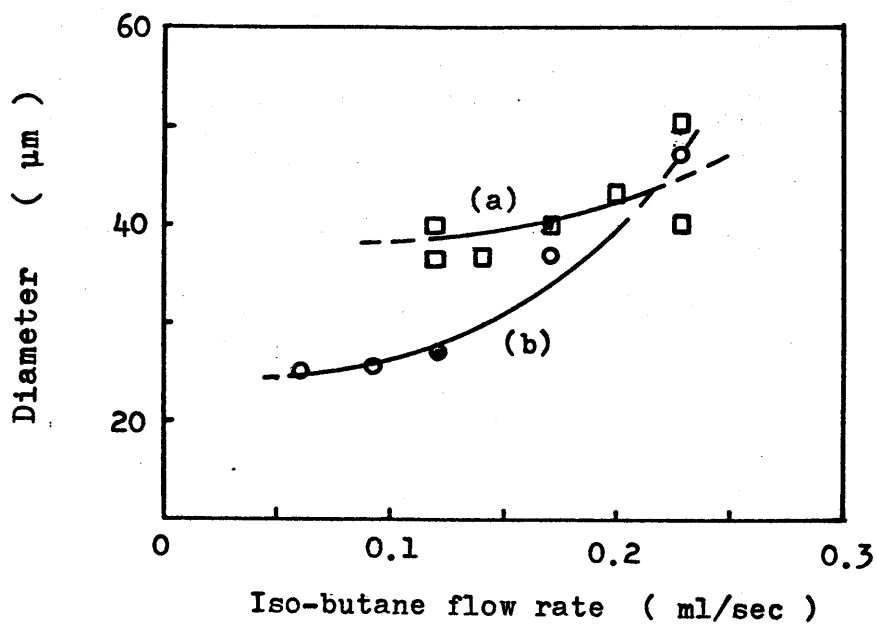
Fig.4.8 Iso-butane flow rate vs. diameter
          (growth rate: 7 mm/min)

(a) Tungsten carbide (450° C, 3.0 mA, Cl_2: 0.08
    ml/sec, Ar: 1.7 ml/sec, H_2: 1.8 ml/sec)
(b) Molybdenum carbide (400° C, 1.5 mA, Cl_2: 0.11
    ml/sec, Ar: 1.7 ml/sec, H_2: 1.2 ml/sec)
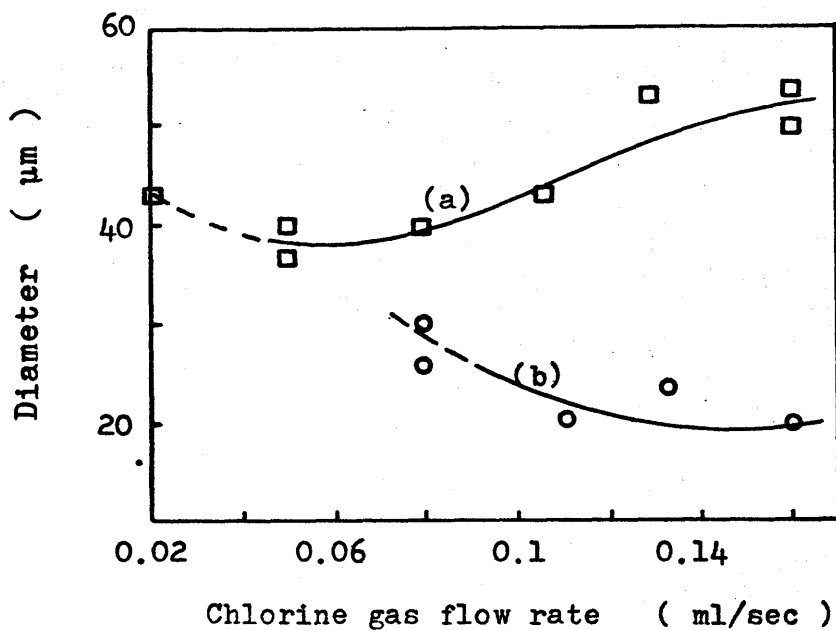
Fig.4.9 Chlorine gas flow rate vs. diameter.
. (growth rate: 7 mm/min)
(a) Tungsten carbide ($450°$ C, 3.0 mA, i-C_4H_{10}:
0.17 ml/sec, Ar: 1.7 ml/sec, H_2: 1.8 ml/sec)
(b) Molybdenum carbide ($400°$ C, 1.0 mA, i-C_4H_{10}:
0.12 ml/sec, Ar: 1.9 ml/sec, H_2: 1.2 ml/sec)
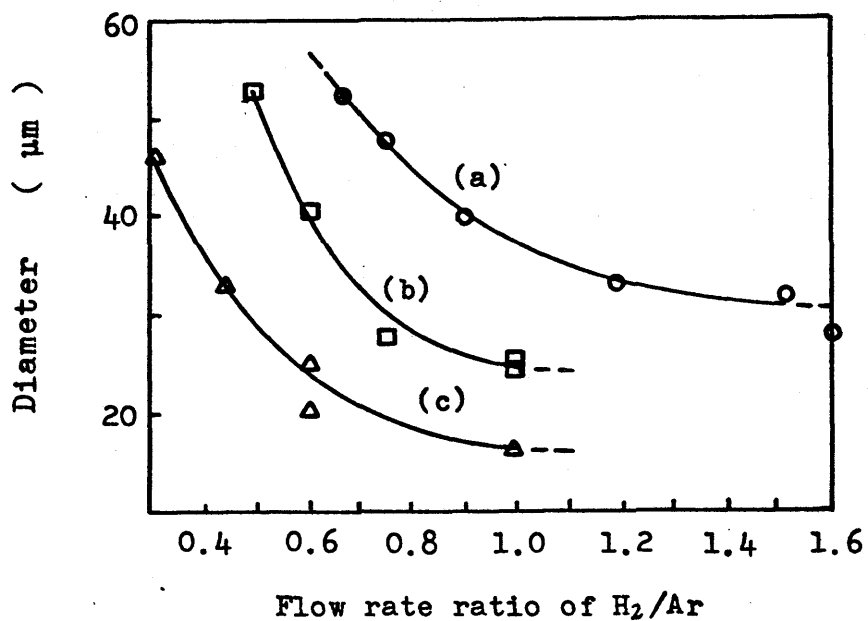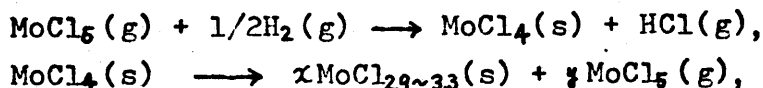
Fig.4.10 Flow rate ratio of H_2/Ar vs. diameter.
(growth rate: 7 mm/min.)

(a) Tungsten carbide (3.0 mA, 450° C, Cl_2 : 0.08
   ml/sec, i-C_4H_{10}: 0.14 ml/sec)

(b) Molybdenum carbide (1.5 mA)
(c) Molybdenum carbide (1.0 mA) } (400° C,
   Cl_2 : 0.11 ml/sec, i-C_4H_{10}: 0.12 ml/sec)

$$MoCl_5(g) + 1/2H_2(g) \longrightarrow MoCl_4(s) + HCl(g),$$

$$MoCl_4(s) \longrightarrow \chi MoCl_{2.9\sim3.3}(s) + \frac{1}{3}MoCl_5(g),$$

while the main product for the hydrogen reduction of WCl_6 (g) seems to consist of gaseous WCl_5 (13), so that the availability of WCl_6 is higher than that of $MoCl_5$.

The flow rate ratio of H_2/Ar is an important factor in order to keep the stable arc-discharge. The dependence of the flow rate ratio on the diameter is shown in Fig.4.10. The minimum diameter of molybdenum or tungsten carbide was attained at the flow rate ratio of 1.0 or 1.5, respectively. Above these ratios, the arc-discharge was sometimes changed into the glow discharge region where no fibre could be grown. The atmospheric temperature might decrease due to the excess amount of hydrogen with a high thermal conductivity which resulted in the glow discharge.

4.3.2 Microscopic Observation and X-ray Analysis
Appearance of fibres The mechanical pulling apparatus in Fig.4.2 made it possible to obtain the uniform and thin fibres as long as 5 to 6 cm under the stable discharge conditions. Fig.4.11 shows the straight tungsten carbide fibres with constant diameters of 30 to 50 μm. The growth conditions were as follows; reactor temperature: 500°C, discharge current: 3.0 mA, growth rate: 7 mm/min and the gaseous composition as shown in the figure caption. A globular deposit due to the high initial discharge current can be observed at the root of a fibre. The final shape at a growth tip is spindle-shaped, which suggests that the lateral growth of a fibre follows the axial growth. This was verified by the observation of
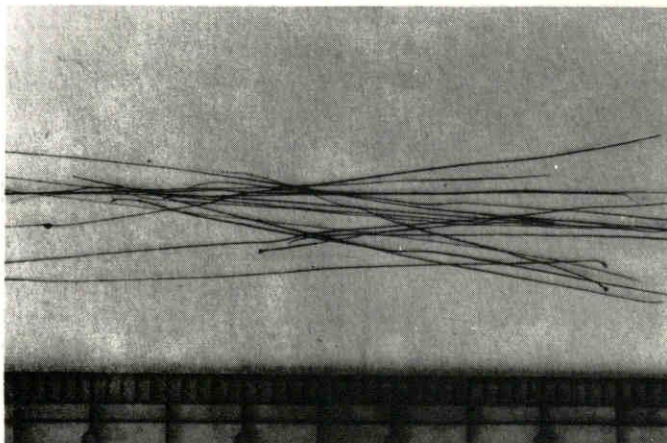
Fig.4.11 Tungsten carbide fibres obtained by
discharge method.

Discharge current: 3.0 mA

Growth rate: 7 mm/min

Reactor temperature: 500°C

Gas flow rates; Cl_2: 0.1 ml/sec

i-C_4H_{10}: 0.15-0.23 ml/sec

Ar: 1.7 ml/sec

H_2: 1.8 ml/sec
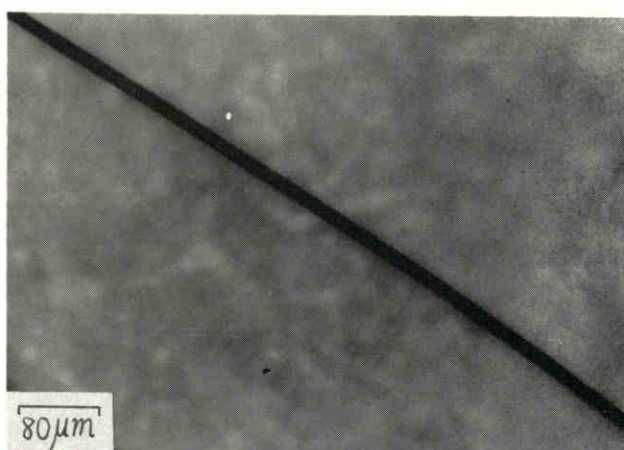
(a)
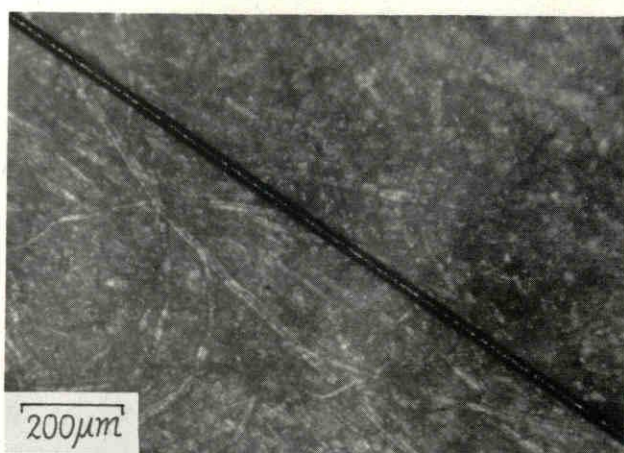
(b)

Fig.4.12   Micrograph of a thin fibre of tung-

sten carbide (a) or molybdenum carbide (b).

	(a)	(b)
Cl_2 flow rate	0.09 ml/sec	0.11 ml/sec
i-C_4H_{10} flow rate	0.14	0.08
H_2 flow rate	1.8	1.2

the fractured edge (see Section 4.3.3). When a fibre
was grown too long in length, the growth tip began to
sway sideways under the influence of a turbulent atmos-
phere, until the fibre tumbled down from the molybdenum
electrode into the receiver at the bottom or sometimes
bent towards the reactor wall with the discharge contin-
ued. Fig.4.12a shows the micrograph of a tungsten car-
bide fibre (diameter: 25 μm), which was prepared at the
reactor temperature of 450° C, the discharge current of
2.0 mA and the growth rate of 8.0 mm/min. Relatively
rough crystal grains could be observed under natural light.
A molybdenum carbide fibre (diameter: 20 μm) with the
smooth surface can be observed in Fig.4.12b. Growth con-
ditions were as follows; reactor temperature: 400° C, dis-
charge current: 1.5 mA and growth rate: 7 mm/min. Thus
the favorable fibre with metallic luster could be pre-
pared especially at i-C_4H_{10} flow rate of 0.08 ml/sec.
<u>Chemical composition</u>   Washed and dried carbides were
analyzed by X-ray diffraction. The specimen was prepared
on a glass plate which was spread with the powdered fi-
bres. Figs.4.13a & b show the X-ray diffraction patterns
for tungsten and molybdnum carbides, respectively. It
is apparent that both represent identical patterns of
cubic system.. The diffraction patterns of (b) could be
identified with cubic β-Mo_2C of A.S.T.M. card (14), the
strongest lines of which were shown in Fig.4.13c. Other
diffraction peaks of such as hexgonal MoC, α-Mo_2C, etc.
could not be confirmed. Each peak for the specimen can
be seen at lower diffraction angle by 1.0-2.0° than that
for A.S.T.M. β-Mo_2C. The lattice parameter was found
a = 4.25$_2$Å from the measurement of (200) interplanar spac-
ing. It is larger than that for A.S.T.M. β-Mo_2C, a_0 =
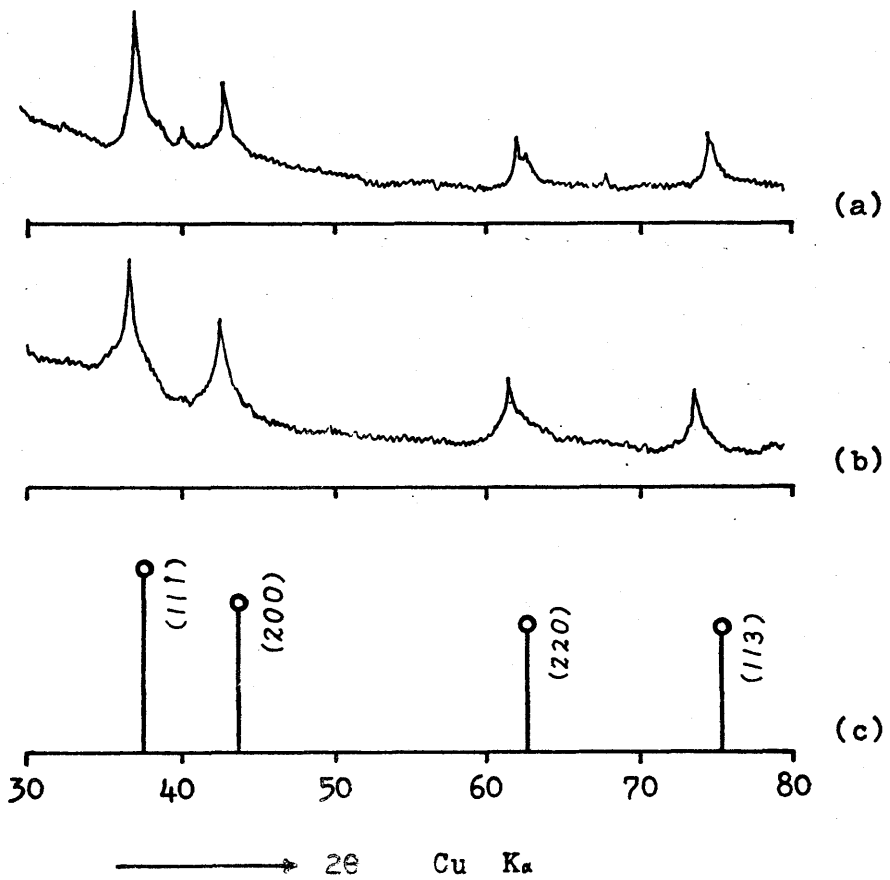
Fig.4.13 X-ray diffraction patterns of the prod-
     ucts.
   (a) β-W₂C   (b) β-Mo₂C   (c) A.S.T.M. Mo₂C

4.14 Å. The lattice parameter of cubic β-W_2C in Fig.4.
13a was also determined to be a = 4.23$_0$Å. But the dif-
fraction of β-W_2C is not registered in A.S.T.M. cards.

Cubic Mo_2C and W_2C were discovered in 1947 by Lander
and Germer (15) when they investigated the thermal decom-
position of carbonyls, $Mo(CO)_6$ and $W(CO)_6$ in the low tem-
perature range of 350° to 500° C (see Section 1.2). More
detailed study on the chemical composition or the growth
condition, however, has not been reported. Also, cubic
phases are not presented in the phase diagram of W-C sys-
tem (see Fig.1.1) and Mo-C system (16). According to
Lander et al. the lattice parameter of cubic W_2C is $a_0 =$
4.16 Å which is somewhat smaller than that measured in
the present study. The carbide fibres are presumed to
contain more carbon atoms than cubic W_2C identified by
Lander et al. from the analogy to the relation between
the lattice parameter and the composition as stated in
Chapter 3. Such inconsistent parameters can often be con-
firmed in this sort of interstitial carbide, which is
caused by the wide range of solubility of carbon atom
(see Section 1.1). It is interesting that cubic carbides
were formed from the vapor phase in this experiment, al-
though the familiar products of C.V.D. of VIa group metal
carbides were crystallized in hexagonal system. If the
β-phase of W_2C, which was reported by Becker (17), is
equivalent to cubic system, it is suggested that cubic
W_2C is formed at increased temperatures above 2,400° C.
Therefore, it is instructive to consider for the discharge
growth that the cubic W_2C or Mo_2C which is deposited at
the sparkling growth tip above 2,000° C, is frozen by
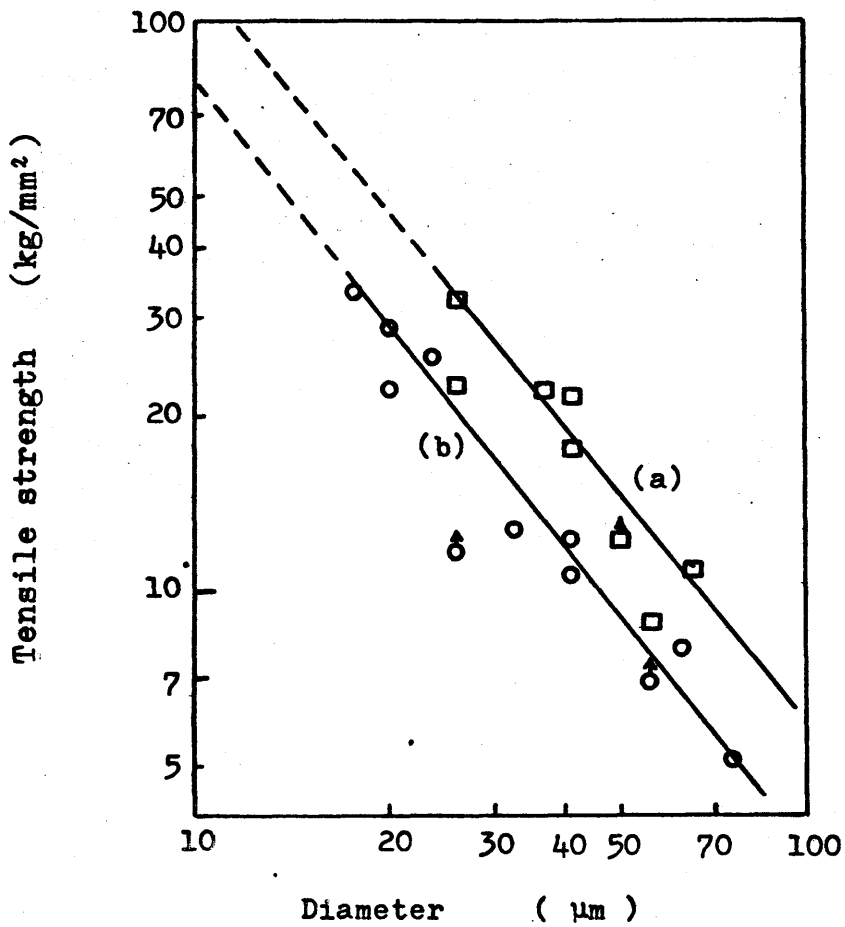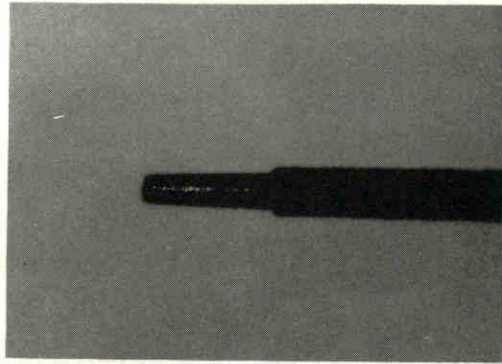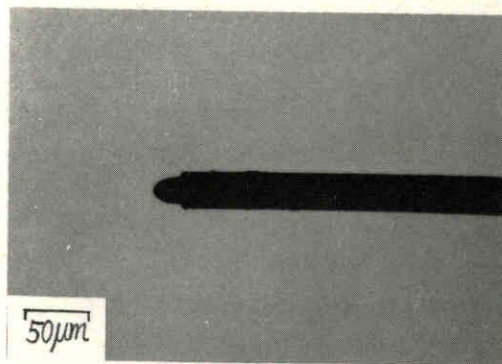quenching in the lower temperature atmosphere.

Fig.4.14 Fracture tensile strength vs. diameter.

    (a)   Tungsten carbide fibres

    (b)   Molybdenum carbide fibres

(a)

50μm

(b)

Fig.4.15 Micrograph of the fractured edge

of a tungsten carbide fibre.

4.3.3　Fracture Strength of Fibres

Fig.4.14 shows the diameter of the fracture strength vs. the diameter of fibre on logarithmic scales. Linear relationship can be seen in both cases. The tensile strength of tungsten carbide is a little higher than that of molybdenum carbide. Maximum strength of 35 kg/mm^2 was measured at 18 μm in diameter for the molybdenum carbide fibre. The extrapolated value to 10 μm showed about 100 kg/mm^2. This is a rather small value compared with that of titanium carbide whisker (500 kg/mm^2) as shown in Fig.2.28, but is comparable with the fibre strength of ZrB_2 (300 kg/mm^2), TiB_2 (150 kg/mm^2), ZrC (20-60 kg/mm^2) and TiN (10-30 kg/mm^2), which are obtained by discharge method (3-6).

Micrograph of the fractured edge of a tungsten carbide fibre is shown in Fig.4.15. It is considered from Fig.4.15a that the central portion consists of dense carbide with metallic luster, while the peripheral portion contains an excess amount of carbon. The fractured shape in Fig.4.15b suggests that the tensile strength of the center is higher than that of peripheral portion. Hence, the fibre growth may be proceeded by two steps like ZrC fibre (6): The first is the axial growth at the sparkling spot and the next is the lateral growth, as supported by the final shape of the growth tip.

4.4　Conclusion

Fibrous growth of tungsten and molybdenum carbides by A.C. discharge method was investigated in a gas mixture of H_2, Ar, $i-C_4H_{10}$ and metal chloride (WCl_6 or $MoCl_5$). Fibres with 3 to 6 cm in length and 15 to 40 μm in dia-

meter were obtained by moving the discharge elecrodes
with mechanical pulling apparatus. The optimum condi-
tions for the growth of tungsten and molybdenum carbide
fibres were respectively as follows; discharge current:
2.3 mA and 0.8 mA, atmospheric temperature: 480° C and
360° C, growth rate: 7 mm/min and 9 mm/min. The concen-
tration ratio of H_2/Ar between 0.8 to 1.4 was found to
give the minimum diameter. The moderate gaseous flow
rates for the fibre growth of tungsten and molybdenum
carbides were respectively as follows; i-C_4H_{10}: 0.15 ml/
sec and 0.08 ml/sec, Cl_2 : 0.06 ml/sec and 0.16 ml/sec.

By X-ray diffraction, the products were identified
with β-W_2C (cubic) and β-Mo_2C (cubic), which had been
found by Lander et al. The lattice parameters of W_2C
and Mo_2C were respectively as follows: 4.23_0Å and 4.25_2
Å. Cubic carbides were considered to be obtained by
quenching of the β-phase deposits in the lower tempera-
ture atmosphere. Further detailed investigation, however,
should be done in relation to cubic carbide. A linear
relation was confirmed between the fracture strength and
the diameter on log-log scale. The tensile strength of
100 kg/mm^2 at 10 μm in diameter was presumed by extra-
polation. The observation of the fractured edge suggest-
ed the growth mechanism of a fibre by two steps, i.e.
the axial growth and the lateral growth. It would be
possible to obtain the stronger and thinner fibres, if
the lateral growth can be further limited.

REFERENCES

1) J.R.Darnell & D.A.Tarver, C.A. 68 71567e, U.S. Patent (1967)

2) D.A.Tarver, C.A. 69 38202e, U.S. Patent (1968)

3) T.Takahashi, K.Sugiyama & Y.Suzuki, J. Crystal Growth 10 139 (1971)

4) T.Takahashi, K.Sugiyama, H.Itoh & Y.Suzuki, Kogyo Kagaku Zasshi 73 498 (1970)

5) K.Sugiyama & T.Takshashi, Kogyo Kagaku Zasshi 73 1959 (1970)

6) K.Sugiyama & T.Takahashi, Kogyo Kagaku Zasshi 73 2105 (1970)

7) T.Takahashi & K.Sugiyama, J. Elecrochem. Soc. (to be published)

8) "Jikken Kagaku Kohza" Maruzen Tokyo Vol.9 p297 (1958)

9) "Hohden Hando Bukku" Denki Gakkai Tokyo p27 (1958)

10) T.Takahashi, K.Sugiyama & K.Kitagawa, Kinzoku Hyo-men Gijutsu 18 350 (1967)

11) Y.Saeki, R.Matsuzaki & T.Matsushima, Denki Kagaku 35 46 (1967)

12) Y.Saeki & R.Matsuzaki, Denki Kagaku 38 615 (1970)

13) E.J.Mehalchilk & M.B.Maclnmis, Electrochem. Tech. 6 66 (1968)

14) A.V.Smith et al., "Index (Inorganic) to the Powder Diffraction File" A.S.T.M. Philadelphia (1968) Card No. 5-467

15) J.J.Lander & L.H.Germer, Am. Inst. Mining Met. Engrs. Tech. Publ. 2259 (1947)

16) R.Kirk & D.Othmer, "Encyclopedia Chem. Tech." John Wiley & Sons, Inc. New York Vol.4 p80 (1964)

17) K.Becker, Z.Metalk. 20 437 (1928)

CHAPTER   5

Chemical Vapor Deposition

of Tungsten Carbide Dendrites

5.1   Introduction

Protective coating or fibres of tungsten carbide
are important refractory materials used for some mechan-
ical and electrical devices. Most deposits of tungsten
carbide have been obtained from the vapor phase by the
carburization of a tungsten wire or sheet in an atmos-
phere containing hydrocarbons or carbon monoxide (1-3).
A comparatively higher temperature of more than 1,500° C
was sometimes necessary for the carbide formation. On
the other hand, the growth of WC single crystal by slowly
cooling of WC-Co solution (4) or a modified Czochralski
method (5) has been investigated together with the study
on its slip system (6). Recently, Mader et al. (7-9)
in Austria found WC and W whiskers of 1 to 4 mm long in
the sintered tungsten carbide. But the monocrystalline
or fibrous growth of tungsten carbide from the vapor
phase has not been reported.

The preparation of tungsten metal has been perform-

ed easily by the thermal decomposition or hydrogen re-
duction of tungsten chloride. Lamprey, for example, pro-
duced tungsten metal powder by reducing the metal chlo-
ride at $430° - 900° C$ (10). The chemical vapor deposition
of the carbide from a gas mixture containing tungsten
hexachloride, however, has been considered to be diffi-
cult because the free metal is easy to deposit out at
a low temperature as reported by Powell et al. (11). It
was found in this study that tungsten carbide was depos-
ited under restricted conditions in an atmosphere of
tungsten chloride, propane, hydrogen and argon gases.
Particularly, it was aimed to obtain one dimensional de-
posits as long as possible. The growth of WC-dendrites,
needles, etc. could be accomplished, when the experimen-
tal method was similar to that used for the deposition
of titanium carbide single crystals as described in Chap-
ter 2. The growth conditions of tungsten carbide were
investigated in detail as a function of geometry in the
furnace, gas flow rates and temperature. Various micro-
scopic crystal morphologies and the growth mechanism
are also included in the latter half.

5.2   Experimental

     Fig.5.1 shows the schematic diagram of the experi-
mental apparatus. A graphite tube susceptor (46 mm in
length, 33 mm and 22 mm in outside and inside diameters,
respectively) was placed in the quartz reactor. A cyl-
indrical graphite substrate was inserted into the tube.
Various types of cylinders were used preliminarily to
investigate the affection of the geometrical arrangement
in the furnace. The graphite cylinder for final experi-
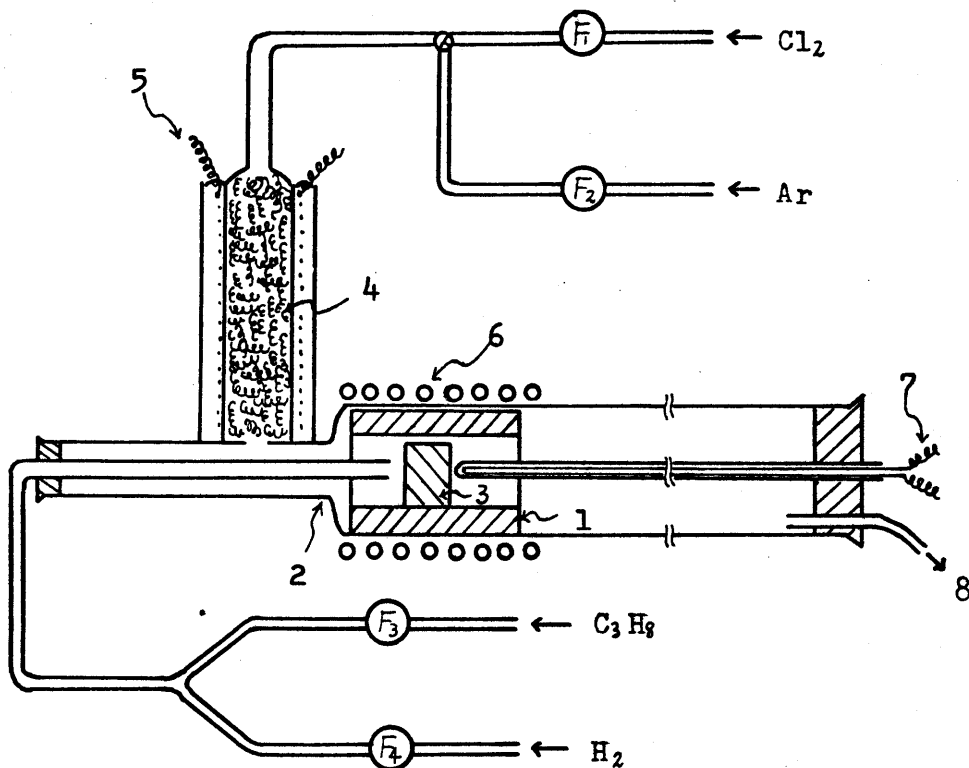
Fig.5.2 Schematic diagram of the experimental
         apparatus.

(1) graphite tube susceptor (2) quartz reactor
(3) graphite substrate (4) tungsten metal
coils (5) nichrome heater (6) r.f. induc-
tion coil (7) Pt-PtRh thermo-couple (8) out-
let
F_1 - F_4: flow meter

ments was 15 mm in length and 14-20.5 mm in diameter.
Tungsten hexachloride (b.p. 347°C) was prepared by com-
plete chlorination of the tungsten metal coils. Chlorine
gas, carried by argon, was passed over the coils and
heated at about 600°C in the nichrome resistance fur-
nace. Dehydrated propane and hydrogen gases were intro-
duced through the inner quartz tube (6 mm in diameter)
and mixed with the stream of tungsten chloride and argon
near the surface of the substrate. The inner tube could
be shifted on either side to adjust the mixing zone ap-
propriately. The graphite tube was heated at 800° to
1,500°C by an induction coil. The overall reaction seems
to be as follows:

$$WCl_6 + C_3H_8 + H_2 \longrightarrow WC \text{ (or } 1/2 W_2C) + 6HCl + xC_mH_n.$$
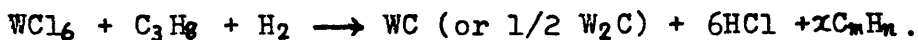
The substrate temperature was measured by a Pt-PtRh
thermo-couple. The flow rate of each gas at room tem-
perature and atmospheric pressure was measured by the
flow meter (F_1 -F_4). A constant reaction time of 50 min-
utes was employed in each run to allow comparison of the
weight increase which was measured by the automatic bal-
ance. The products were identified by the X-ray dif-
fractometer and observed through the microscope.

5.3   Results and Discussion

5.3.1   Growth Condition of Tungsten Carbide

There are several papers which describe the depo-
sition of tungsten carbide from a mixture of tungsten
chloride, hydrogen and hydrocarbon. The conditions for
the formation of tungsten carbide were investigated in
detail. Several factors, for example, the geometrical
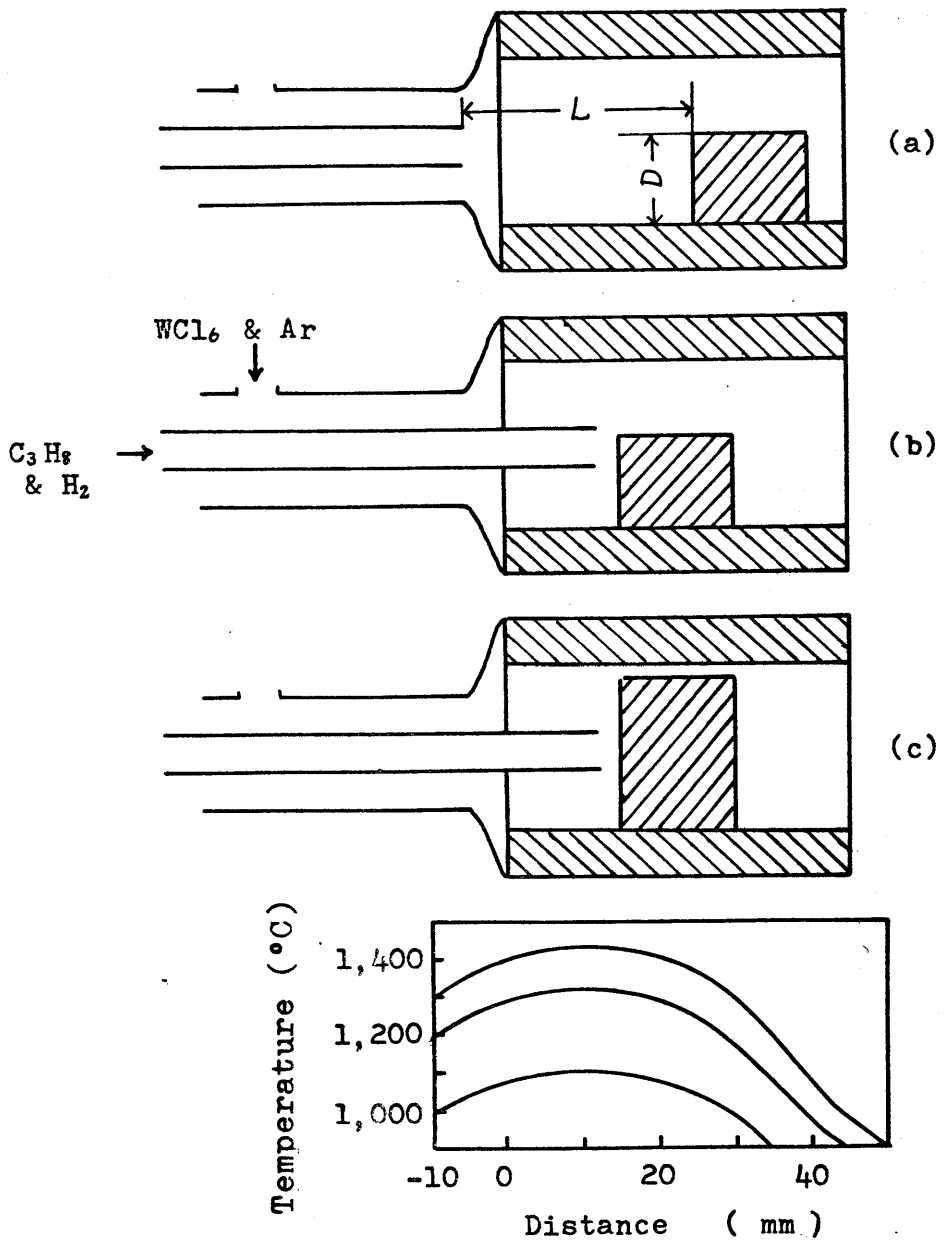factor, substrate temperature, gas flow rates, etc. were

Fig. 5.2 Geometrical models and temperature distribution in the furnace.

considered to affect on the deposition of the carbide. This sub-section is concerned with the study of these effects while keeping all other growth conditions constant in order to obtain reproducible data.

<u>Effect of geometrical factor</u>   The process of crystallization was much influenced by the geometry of the reaction furnace. Some typical diagrams of the arrangement in the furnace and the temperature profile are shown in Figs.5.2a-c. The graphite substrate which had a diameter D = 14 mm was placed at a comparatively long distance apart from the edge of the inner puartz tube (L = 30 mm), as shown in Fig.5.2a. A uniform coating of tungsten carbide mixed with a small quantity of tungsten metal was deposited in this case. It is thought that the hydrogen stream before it reaches the substrate surface, has enough time to reduce the tungsten hexachloride vapor to the free metal. The formation of tungsten metal could be avoided, when the conditions (b) and (c) of Fig.5.2 were used (L = 3 mm). It is necessary to separate the flow path of hydrogen from that of tungsten chloride in the transport process ahead of the substrate. In the case of condition (c) of Fig.5.2, where D equals to 20.5 mm, the dendritic or network-like crystals of tungsten carbide were formed on the front surface of the substrate. This means that a turbulent flow zone of the gas mixture is necessary in the vicinity of the substrate for one dimensional growth of a crystal. All the experimental results described next were obtained using condition (c).

<u>Effect of WCl_6 and H_2 concentrations</u>   The X-ray diffraction patterns of the specimens obtained at 1,230°C and 1,300°C are shown in Figs.5.3a-d.   The patterns
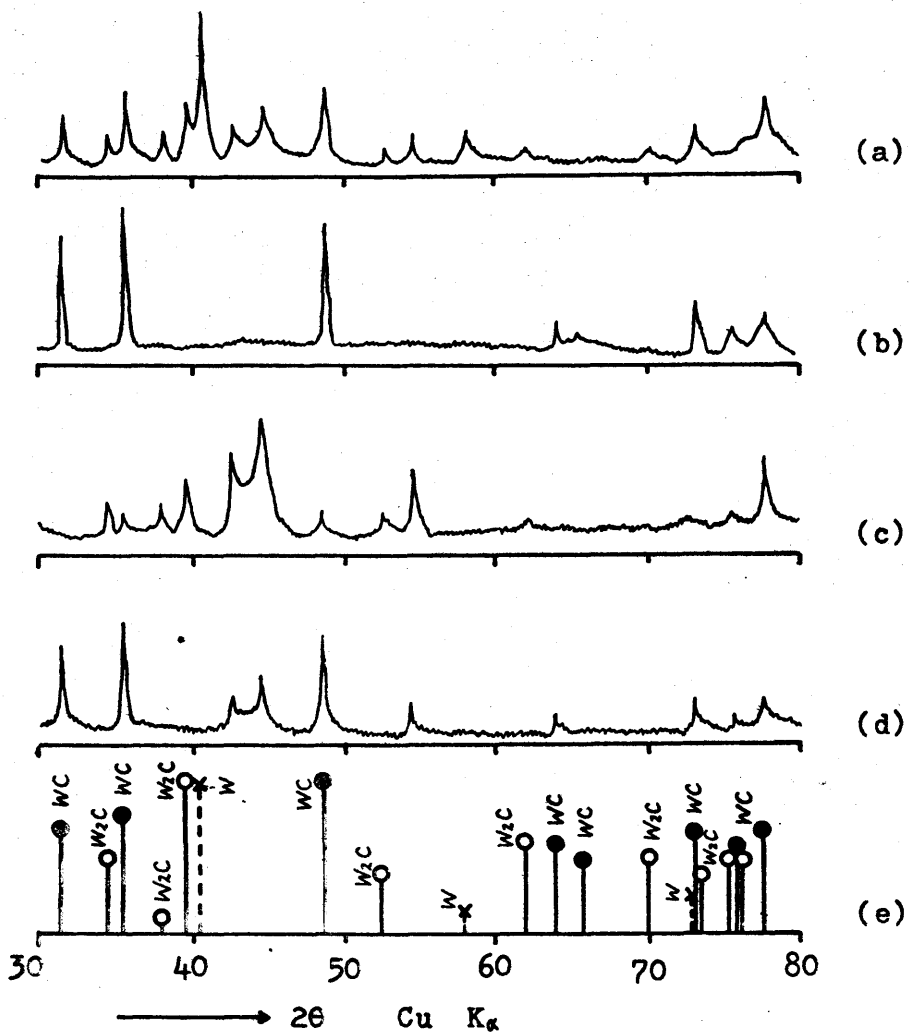
Fig.5.3 X-ray diffraction patterns

	Substrate temperature	Gas flow rates (ml/sec)			
		WCl_4	H_2	C_3H_8	Ar
(a)	1,230 °C	0.09	0.2	0.01	1.5
(b)	1,230	0.02	0.2	0.01	1.5
(c)	1,300	0.02	0.8	0.03	1.5
(d)	1,300	0.02	0.2	0.03	1.5
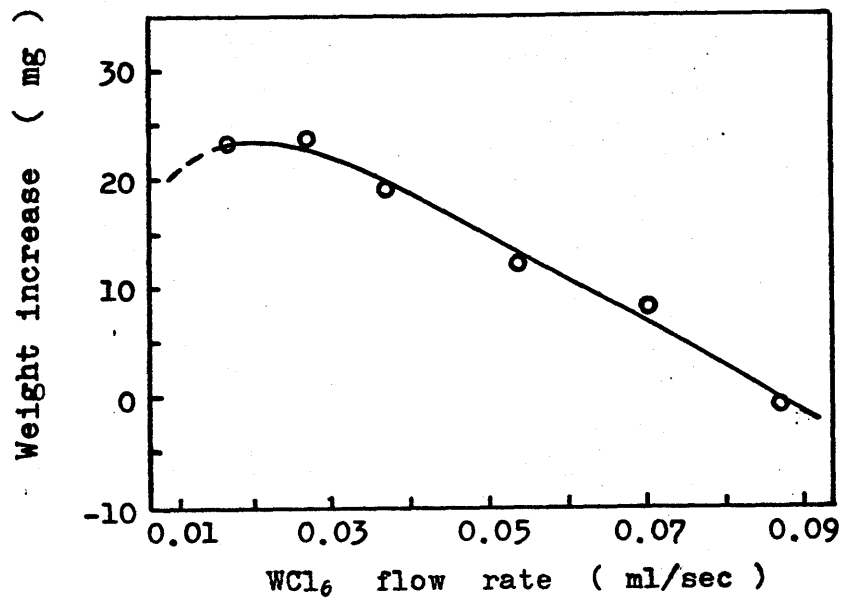
Fig. 5.4 Weight increase of the specimen vs.

WCl$_6$ flow rate.

shown in Fig.5.3e correspond to the strongest lines of
W, $\alpha-W_2C$ and WC as listed in the A.S.T.M. cards (7). In
Fig.5.3a, metallic tungsten, WC, $\alpha-W_2C$ and graphite were
identified for flow rates of WCl_6 of 0.09 ml/sec. The
WC was formed in large quantities only at lower concen-
trations of tungsten chloride (Fig.5.3b). Figs.5.3a &
b suggest that metallic tungsten or $\alpha-W_2C$ are easy to
deposit at higher concentration ratios of WCl_6/C_3H_8 .
This is shown in Fig.5.4 which plots the weight increase
of the specimen vs. the flow rate of tungsten hexachlo-
ride. The decrease in weight can be attributed to the
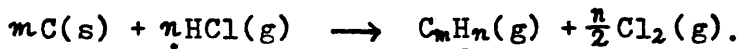thermal etching of the graphite cylinder by hydrogen
chloride, which is produced in the process of reducing
the excess of tungsten chloride:

$$mC(s) + nHCl(g) \longrightarrow C_mH_n(g) + \frac{n}{2}Cl_2(g).$$

Figs.5.3c & d show the dependence of the hydrogen
flow rate on the identity of the deposited species, when
the flow rate of tungsten chloride is held constant at
0.02 ml/sec. It can be seen that small amounts of $\alpha-$
W_2C and WC can be identified at hydrogen flow rate of
0.8 ml/sec. The reduction of tungsten hexachloride to
lower chlorides such as WCl_3 was considered to make the
formation ot $\alpha-W_2C$ possible. In the case of a lower con-
centration of hydrogen (0.2 ml/sec), the peaks of WC
which have a slight preferred orientation to <100> di-
rection, were observed similarly as for the condition
shown in Fig.5.3b.

Moderate condition for WC formation   On the basis of
the study on geometrical effect, the separation of the
H_2 and WCl_6 flow paths was found to be essential for the
formation of tungsten carbide. It was also confirmed by
X-ray diffraction that a hydrogen flow rate less than

0.4 ml/sec and a tungsten hexachloride flow rate less
than 0.05 ml/sec are required to produce pure hexagonal
WC on a graphite substrate. It is of major importance,
therefore, to prevent the following reaction, which has
been known to be fast even at the temperature as low as
700° C (10 & 13):

$$WCl_6(g) + 3H_2(g) \longrightarrow W(s) + 6HCl(g),$$

while the formation reaction of WC is considered to occur
at the intermediate stage of hydrogen reduction of WCl_6
or C_3H_8.

5.3.2   Crystal Morphology of Vapor-Deposited WC

<u>Temperature dependence</u>   Various crystal morphologies
of WC were observed by varying the concentrations of
tungsten chloride and hydrogen described above. The var-
iation of the morphology with the temperature is summa-
rized in Table 5.1. A small amount of $\alpha-W_2C$ was depos-
ited on the graphite substrate at a temperature below
950° C, but an adherent and uniform film of WC could be
obtained above 1,000° C. The weight of vapor-deposited
products increased as the temperature was raised. Pure
WC was identified by X-ray analysis in the temperature
range of 1,000° to 1,400° C. The deposition of WC was
prevented above 1,400° C, forming instead amorphous car-
bon and a slight amount of $\alpha-W_2C$. The decomposition of
propane to free carbon may have caused a deficiency of
pyrocarbon in the higher temperature region which grew
a small amount of $\alpha-W_2C$. The importance of the role of
pyrocarbon in the formation of titanium carbide was also
emphasized by Pearce et al. (see Section 1.2).

    When the growth experiments were performed in the

Table 5.1   Temperature dependence of the products.

Substrate temperature	Deposits	Crystal forms	Weight increase
950 (°C)	$\alpha-W_2C$	films	26 (mg)
1,080	WC	films	52
1,190	WC	films & networks	87
1,250	WC	films & dendrites	70
1,360	WC	films & pillars	36
1,450	WC & $\alpha-W_2C$	films	12

WCl_6 flow rate: 0.02 ml/sec
C_3H_8 flow rate: 0.03 ml/sec
H_2 flow rate: 0.2 ml/sec
Ar   flow rate: 1.5 ml/sec
Reaction time: 50 minutes

(a)

40 μm
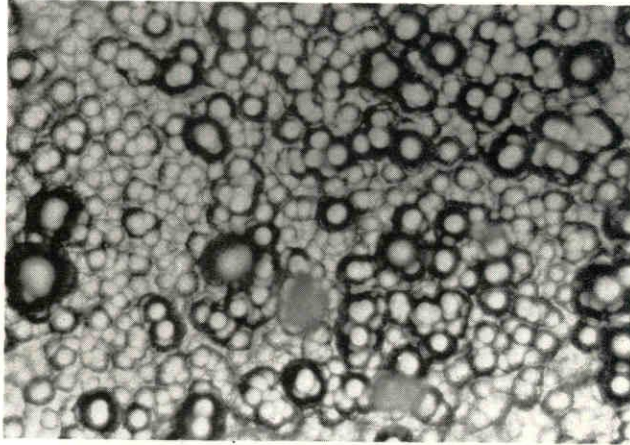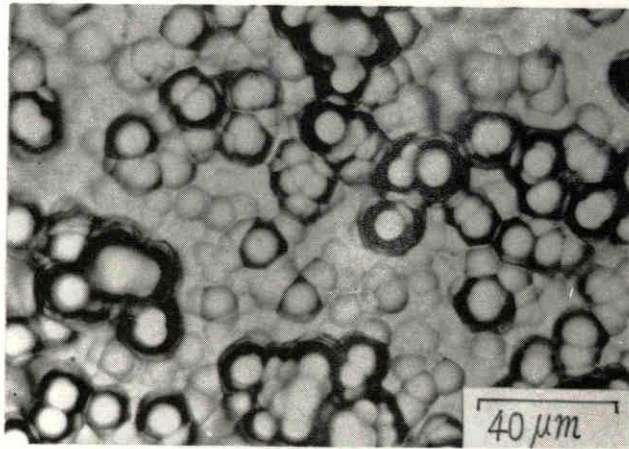
(b)

Fig.5.5 Heterogeneous coating of WC on graphite.

(temperature: 1,360°C)

(a) Peripheral portion of the substrate.

(b) Central portion of the substrate.

temperature range of 1,200° to 1,400°C, the heated graph-
ite substrate was coated heterogeneously with a film of
polycrystalline WC as shown in Fig.5.5. Small crystal
grains of 5 μm in diameter were observed in the periph-
eral portion of the substrate (see Fig.5.5a). On the
other hand, the grain sizes of the crystallites with di-
ameters of about 10 μm were packed together closely in
the central portion of the substrate (see Fig.5.5b),
where the degree of supersaturation of the gas mixture
seemed to be high. These crystallites may be slightly
oriented towards the ⟨100⟩ direction as implied by X-
ray diffraction (see Fig.5.3b).

The correlation between the weight increase of spe-
cimens and the propane flow rate is shown in Fig.5.6,
where the temperature of the substrate is 1,200°C and
the reaction time is 50 minutes. Linear relationships
can be seen in the figure, which suggests that the rate
determining step is the transport process of propane gas.
The deposition range of WC-networks or dendrites, how-
ever, was restricted to a flow rate of 0.03 to 0.05 ml/
sec. At higher concentration than 0.06 ml/sec, the ex-
cess free carbon adhered to the side of the cylindrical
graphite. The weight decrease at the flow rate of 0.01
ml/sec shows the thermal etching of the graphite surface,
as described earliar. Fine networks parallel to the
substrate surface (see Fig.5.7a) were deposited at pro-
pane and tungsten hexachloride flow rates of 0.03 ml/sec
and 0.02 ml/sec, respectively. It is found from the
figure that each branch is like a string of beads about
2 to 5 μm in diameter. When the temperature was raised
a little (see Fig.5.7b), linear fibrous crystals were
formed easily, especially in the peripheral or lateral

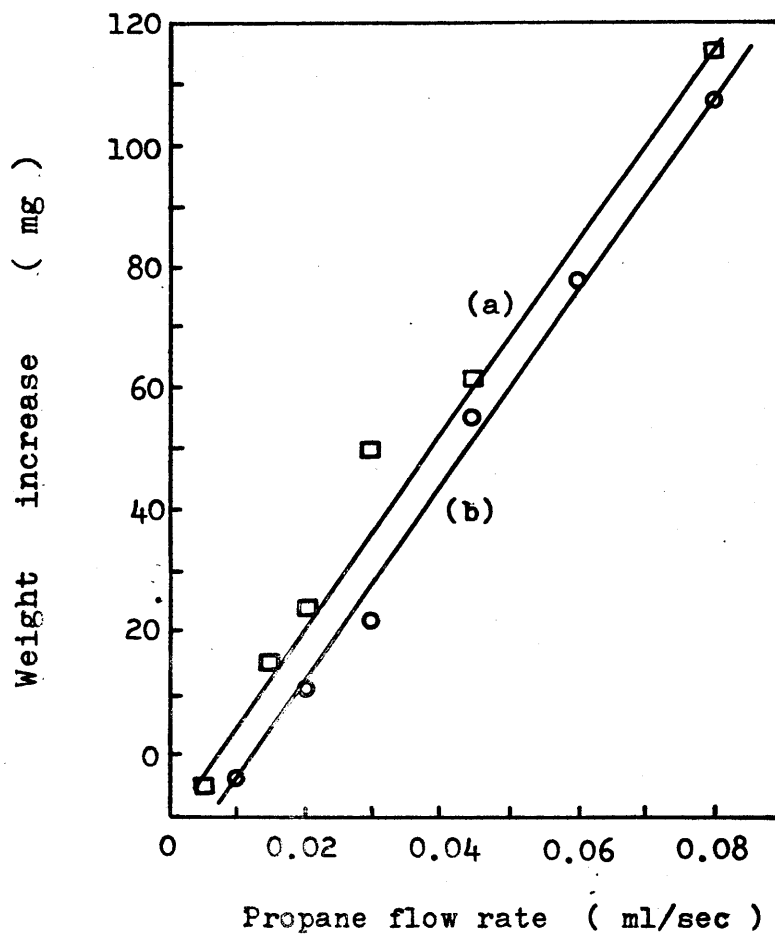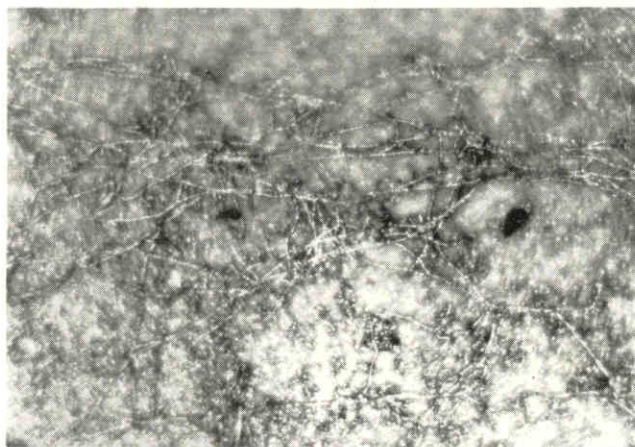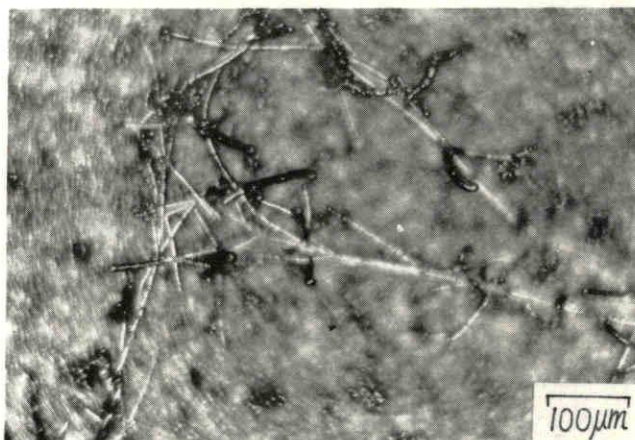Fig.5.6 Weight increase of the specimen vs.
propane flow rate.

WCl$_6$ flow rate: (a) 0.02 ml/sec (b) 0.09

ml/sec, H$_2$ flow rate: 0.2 ml/sec, Ar flow

rate: 1.5 ml/sec

Temperature: 1,200° C, Reaction time: 50 min.

(a)

(b)

Fig.5.7   Micrograph of WC-networks.

|	(a)	(b)
Temperature	1,200°C	1,250°C
C_3H_8 flow rate	0.03 ml/sec	
WCl_6 flow rate	0.02 ml/sec	

portion of the graphite cylinder.

Fig.5.8a shows the micrograph of WC-dendrites. They were formed as large clusters in various parts of the substrate at the temperature of 1,300° C. Some of the dendrites were needle-like crystals with metallic luster, which were 50 to 100 μm in length and 1 to 2 μm in diameter (see Fig.5.8b). The lower hydrogen flow rate of 0.1 ml/sec was suited for the growth of the dendritic WC, but none could be grown in the case of zero hydrogen flow rate. Typical forms of dendrites are represented in Fig.5.9. It is found from the figure that several straight needles which are assumed to have some crystallographic axis, aggregate together to form branched crystals. A globular crystal is observed at each branch point, from which branching appears to be initiated. It is instructive to consider that a sufficiently high supersaturation and a turbulent atmosphere in the gas mixture contribute to the formation of a vapor-deposited nucleus on the side of a branch. In addition, the process of nucleation may be facilitated by the impurities in a gas mixture or the graphite substrate.

At a substrate temperature of 1,300° C, thicker dendritic crystals were observed at the central portion of the substrate, as seen in Figs.5.10a & b. Globular crystals with smooth surfaces are formed on the tips of the dendritic branches. Fig.5.11 shows a pillar crystal, which was obtained at an elevated temperature of 1,360° C. Similar crystals with lengths of 50 to 200 μm were formed at a reaction time of 50 minutes at the center of the substrate. Preparation of a larger single crystal of tungsten carbide can be expected for a longer reaction time.

(a)

100 μm
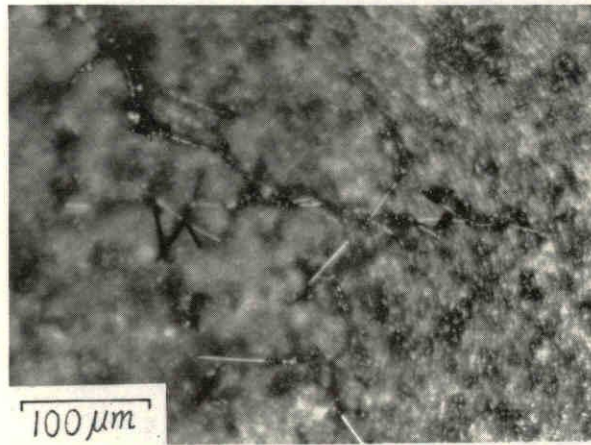
(b)

Fig.5.8 Micrograph of bush-like (a) or needle-

like (b) crystals of WC. (temperature: 1,300°C)
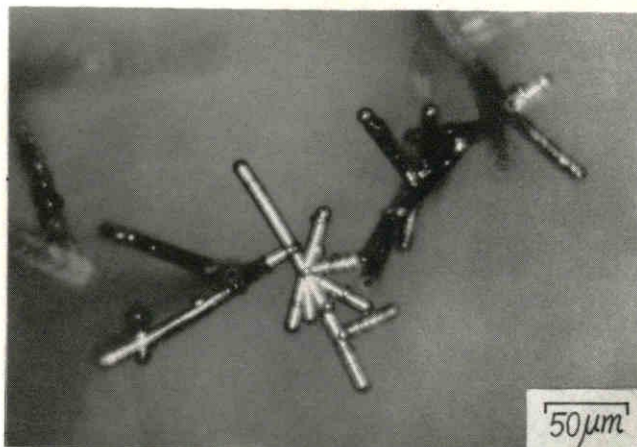
Fig.5.9   Micrograph of typical WC-dendrites

with straight branches.

Temperature: 1,300°C

C_3H_8 flow rate: 0.03 ml/sec

WCl_6 flow rate: 0.02 ml/sec

H_2 flow rate: 0.1 ml/sec
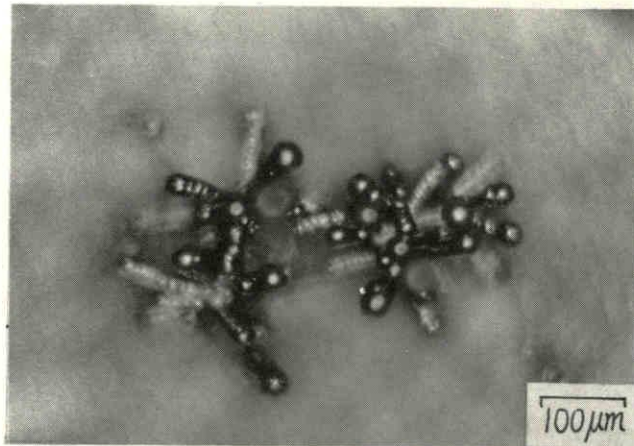
Ar flow rate: 1.5 ml/sec

It is found that the temperature dependence of the deposited crystal morphologies can be summarized as follows; networks: $1,200°-1,300°$ C, dendrites: $1,250°-1,350°$ C and pillars: $1,350°-1,400°$ C. The dendritic crystals have a tendency to grow vertically to the substrate surface at increased temperatures. In the much higher temperature range, however, the axial growth was limited and crystals with relatively large diameters could be obtained.

Effect of total flow rate   The influence of the total flow rate on crystal growth was also investigated. Crystal grains were found to become larger at a total flow rate of 3.5 ml/sec. But fine dendritic or fibrous crystals were formed at lower total flow rates of 1.78 ml/sec, where the moderate composition of the gas mixture was WCl_6: 1.5 m/o, C_3H_8: 1.7 m/o, H_2: 15 m/o and Ar: 82 m/o. The flow rate of argon was considered to have a minor influence on the crystal morphology, so that the flow rate of 1.5 ml/sec was maintained in every run.

Growth mechanism   It is understood in general that dendritic crystals are grown under a little higher supersaturation than that necessary for whisker growth (14). This seemed to be applicable to the present experimental result, i.e. a large number of dendrites which had many irregular branches could be found in the lower temperature range of the substrate or at a higher total concentration of the gas mixture. In such cases, the influence of external gaseous stream on the crystal morphology was predominant. Network-like crystals were a typical example of this type. As the temperature was raised, however, the whisker or needle-like crystals could be grown, because the crystal growth was no longer affected by the

(a)

(b)

Fig.5.10 Micrograph of thick WC-dendrites

with globular caps. (temperature: 1,300°C)

Fig.5.11 Micrograph of a WC-pillar.

(temperature: 1,360°C)

C_3H_8 flow rate: 0.03 ml/sec

WCl_6 flow rate: 0.02 ml/sec

H_2 flow rate: 0.2 ml/sec

Ar flow rate: 1.5 ml/sec

small supersaturation, but was controlled under the internal conditions of the crystal (i.e. whisker growth mechanism). In the highly turbulent atmosphere, nucleation would be occurred easily under a local high supersaturation with the result of the regular dendritic growth as shown in Fig.5.9. The V.L.S. mechanism of whisker growth (15) may be true in the case of the growth of each dendritic branch illustrated in Fig.5.10, where the globular crystals are observed on the tips. But, more detailed investigations on the impurity effects would be necessary to know a growth mechanism of the branch. Above 1,350° C, the thick but monocrystalline pillar crystal with no branch could be grown as was suggested by C.V.D. of titanium carbide single crystals described in Chapter 2.

5.4   Conclusion

Tungsten carbide was prepared by chemical vapor deposition from a mixture of WCl_6, C_3H_8, H_2 and Ar on a graphite substrate in the temperature range of 1,200° to 1,500° C. The influences of various factors (geometry in the reactor, gaseous concentration, temperature, etc.) on the crystal growth were investigated. Especially, the geomery in the furnace proved to be an important factor for the process of crystallization. It was necessary for one dimensional growth of a crystal to mix the stream of (WCl_6 + Ar) with that of (C_3H_8 + H_2) in a turbulent flow zone on the substrate surface. The adherent coating of α-W_2C could be obtained at relatively high flow rates of H_2 and WCl_6, while pure dendritic crystals of WC were obtained at the restricted flow rates of H_2

(<0.4 ml/sec) and WCl (<0.05 ml/sec), when the forma-
tion of metallic tungsten by hydrogen reduction of ex-
cess WCl_6 could be prevented. The appropriate gaseous
concentrations for the growth of WC were as follows;
WCl_6: 1.0-1.5 m/o, C_3H_8: 1.7-2.8 m/o, H_2: 10-20 m/o and
Ar: 75-85 m/o, where the total flow rate was 1.78 ml/sec.

Various types of crystals composed of uniform films,
networks, dendrites and pillars with diameters of 2 to
40 µm were deposited on the WC-plated graphite. The
dendritic or pillar crystals were obtained at temperature
between 1,250° and 1,400°C, while the network-like crys-
tals were formed at lower temperatures of 1,200° to 1,300
°C on the substrate. It was also found that the den-
dritic crystals tend to grow vertically to the substrate
surface with the increase of temperature, although the
axial growth is limited. The dendritic growth of WC was
supposed to be facilitated by a number of nucleations
on the side of a needle crystals, from which each branch
could be grown by a whisker growth mechanism such as V.
L.S. Irregular network-like crystals, however, were con-
sidered to be deposited under a higher supersaturation
with the predominant affection of the gaseous flow on
the morphology.

REFERENCES

1) A.Westgren & G.Phragmen, Z. anorg. allgem. Chem.
   156 27 (1926)
2) R.Schenck, Fr.Kurzen & H.Wesselkock, Z. anorg.
   allgem. Chem. 203 159 (1931)

3) G.F.Huttig, V.Fattinger & K.Kohla, Powder Met. Bull. $\underline{5}$ 30 (1950)

4) T.Takahashi & F.J.Freise, Phil. Mag. $\underline{12}$ 1 (1965)

5) A.P.Gerk & J.J.Gilman, J. Appl. Phys. $\underline{39}$ 4497 (1968)

6) J.Corteville & L.Pous, Compt. Rend. $\underline{260}$ 4477 (1965)

7) W.Mader, C.A. $\underline{66}$ 13441g, Redex Rundschan 600 (1965)

8) C.A. $\underline{68}$ 52462a, Austrian Patent (1968)

9) W.Mader, H.Horn & R. Ziegelhecker, C.A. $\underline{69}$ 39426t (1966)

10) H.Lamprey & R.L.Ripley, J. Electrochem. Soc. $\underline{109}$ 713 (1962)

11) C.F.Powell, J.H.Oxley & J.M.Blocher, "Vapor Deposition" John Wiley & Sons, Inc. New York p373 (1966)

12) J.V.Smith et al. "Index (Inorganic) to the Powder Diffraction File", A.S.T.M. Philadelphia (1968) Card No. 4-806, 2-1134 & 5-728

13) Y.Saeki & R.Matsuzaki, Denki Kagaku $\underline{38}$ 615 (1970)

14) "Kessho Kogaku Hando Bukku" Kyoritsu Shuppan Tokyo p214 (1971)

15) R.S.Wagner & W.C.Ellis, Appl. Phys. Letters. $\underline{4}$ 89 (1964)

CHAPTER   6

Summary

The transition metals in lVa, Va and Vla groups
combine with nonmetallic elements such as carbon, nitro-
gen and boron to form so called "interstitial compounds".
These compounds are well known for the high melting
point, super-hardness and high electrical conductivity
which are based on the strong metallic M-M and covalent
M-X bonds. The study on chemical vapor deposition of
interstitial carbide was originated mainly by chemists
in Germany in the 1930's, after which a little attention
was payed on its synthesis in contrast to the remarkable
progress of C.V.D. techniques of semiconductors. Re-
cently, however, stimulated by the increasing demand for
the new combined materials, the C.V.D. of interstitial
compound has become the subject of today's research and
development.

The purpose of the present work is to investigate
the chemical vapor deposition of interstitial carbides
in lVa group metal (TiC) and Vla group metals (WC, α-
W_2C, $\beta-W_2C$ and $\beta-Mo_2C$). Especially, it was aimed to

prepare the one dimensional deposits, for example, whisker, pillar, fibre, dendrite, etc., for the information of such crystal morphologies has been less known even nowadays. The synthetic condition, the crystal structure and the growth mechanism of the carbide crystals were investigated which were prepared by various methods as described below. (Chapter 1)

Various forms of TiC sigle crystals such as needle, whisker, pillar and polyhedron were deposited on a graphite substrate from the vapor phase consisting of H_2, $TiCl_4$ and C_3H_8 in the temperature range of 1,200° to 1,350° C. The correlation between the crystal morphology and the growth condition (temperature, gas flow rate, impurities, etc.) were investigated. The decomposition of the hydrocarbon was found to play an important role on the growth process. By X-ray diffraction, it was concluded that the growth direction of these crystals was mainly ⟨111⟩. The growth mechanism was further studied by the observation of the etching figure, the shape of crystal tip or the large growth step. A linear relation on log-log scale was confirmed between the fractured strength and the diameter. (Chapter 2)

Titanium carbide filament was prepared by titanization of the carbon filament in an atmosphere of $TiCl_4$, H_2 and Ar. The titanization was performed for 10-700 minutes in the temperature range of 1,200°-1,550° C. The X-ray diffraction patterns showed some sub-peaks at the higher angles other than the peaks of the stoichiometric TiC. It was found from X-ray microanalysis of the cross section of the titanized graphite plate that the inner layer of the plate consisted of nearly stoichiometric titanium carbide and free carbon, while the outer

layer contained excess titanium. This titanium carbide
double layer suggested that the inner layer ($TiC_{1.0}$) was
produced by the surface reaction and it was followed by
the formation of the outer layer ($TiC_{0.45}$) which was due
to the diffusion process of elemental carbon. (Chapter 3)

Fibrous growth of β-W_2C and β-Mo_2C by discharge
method was investigated in a gas mixture of H_2, Ar, i-
C_4H_{10} and metal chloride (WCl_6 or $MoCl_5$). Fibres with
3 to 6 cm in length and 15 to 40 μm in diameter were ob-
tained by moving the discharge electrodes with mechan-
ical pulling apparatus. The optimum conditions for fi-
brous growth were as follows; discharge current: 0.8-
2.3 mA, atmospheric temperature: $360°$-$480°$C and growth
rate: 7-9 mm/min. The concentration of i-C_4H_{10} and metal
chloride had minor effects on diameter. But the concen-
tration ratio of H_2/Ar between 0.8 and 1.4 was found to
give the minimum diameter. By X-ray diffraction, both
crystal structures were confirmed to belong to cubic sys-
tem. The growth mechanism of a gibre by two steps was
suggested from the observation of the fractured edge.
(Chapter 4)

Tungsten carbide was obtained by C.V.D. from a mix-
ture of WCl_6, C_3H_8, H_2 and Ar on a graphite substrate
in the temperature range of 1,200° to 1,500°C. The in-
fluence of various factors on the crystal growth was in-
vestigated. The geometry in the furnace proved to be an
important factor for the process of crystallization.
The adherent coating of α-W_2C could be obtained at rel-
atively high flow rates of H_2 and WCl , while pure WC
was obtained at the restricted flow rates of H_2 and WCl_6.
Various crystals composed of uniform film, network, den-
drite and pillar were deposited on the graphite substrate.

The dendritic or pillar crystals were obtained at the
temperature between 1,250° and 1,400°C, while the network-
like crystal was formed at lower temperatures of 1,200°
to 1,300°C. (Chapter 5)

Further, some comments on the above conclusion are
summarized as follows:
i)   It is suggested from the synthetic study of TiC
and WC (Chapter 2 & 5), that the monocrystalline deposits
such as whiskers, needles or dendrites may be obtained
possibly for the syntheses of other interstitial carbides
by the analogous preparation method using the gaseous
transtort agents, i.e. hydrocarbon, metal chloride, etc.
These crystals can be grown at an appropriate gaseous
composition and under relatively low supersaturation.
The growth in length, however, is apt to be limited to
a reaction time of 30 to 100 minutes, and it is follow-
ed by the lateral growth, so it seems to be a rather
difficult problem to prepare the filamentary crystals
longer than a few cetimeters unless the completely con-
trolling method of unstable factors is established. Fur-
ther, detailed informations on such factors will be re-
quired in order to solve this problem. The obtained
monocrystalline whiskers will have a comparable ten-
sile strength with other ceramic whiskers.
ii)   On the other hand, the thin but long fibres can
be produced for a lelatively short reaction time by the
vapor-solid reaction as titanization of carbon filament
(Chapter 3) or the A.C. discharge method (Chapter 4),
although the products are polycrystalline and consequent-
ly the tensile strength as high as single crystal whisk-
ers can not be expected. These methods are interesting

from the industrial or engineering point of view, since there is a possibility of the massproduction for fibres longer than several centimeters.

iii)   The chemical vapor deposition in the present study (Chapter 2-5) is performed in an atmosphere containing metal chloride or hydrocarbon (C_3H_8, C_4H_{10}, etc.), at temperatures above 1,000°C. It is necessary, therefore, to take a special care of the gaseous transport method and the geometrical factor in the reactor in order to supply a moderate amount of pyrocarbon or lower metal chloride on the deposition surface. The thermodynamic data on the hydrogen reduction or thermal decomposition of such starting materials are helpful for the control of the gaseous concentration.

iv)   Some interesting phenomena are found in the present investigation from the point of structural chemistry. For example, the nonstoichiometry in the titanium carbide layers which are formed by the diffusion process of carbon atoms, causes unfamiliar X-ray behaviors (Chapter 3), and the cubic phase of W_2C and Mo_2C is obtained by discharge method (Chapter 4) which forces the quenching of the deposits. Instead, a well-known hexagonal WC or W_2C can be deposited in the C.V.D. described in Chapter 5.

v)   It is also found that the growth mechanism of one dimensional deposit can sometimes be represented by two steps, namely, the first is the axial growth of a crystal tip and the second is the lateral growth of the peripheral portion. In the case of single crystal needles or pillars (Chapter 2 & 5), the former step seems to be explained by the general whisker growth mechanism (V.L.S. mechanism or dislocation mechanism), while the latter by the movement of steps on the lateral face. In the

titanization of carbon filament, the titanium carbide double layers with two different chemical composition are also prepared by two steps (Chapter 3). The lateral growth of the fibre obtained by the discharge method is considered to occur during the quenching process of the grown tip.

List of the Papers Published

		Chapter in this thesis

** T.Takahashi, K.Sugiyama and H.Itoh,
"Single Crystal Growth of Titanium
Carbide by Chemical Vapor Deposi-   Chapter 2
tion"
    J. Electrochem. Soc.
        117[4] 541-5 (1970)

** T.Takahashi, K.Sugiyama and H.Itoh,
"Formation of Titanium Carbide Fil-   Chapter 3
ament by Titanization of Carbon
Filament"
    Kogyo Kagaku Zasshi
        74[4] 586-90 (1971)

** T.Takahashi, K.Sugiyama and H.Itoh,
"Fibrous Growth of Tungsten Carbide   Chapter 4
and Molybdenum Carbide by Discharge
Method"·
    Kogyo Kagaku Zasshi
        74[8] 1606-11 (1971)

** T.Takahashi and H.Itoh
"Chemical Vapor Deposition of Tung-
sten Carbide Dendrites"   Chapter 5
    J. Crystal Growth
        (to be published)